Open Ceramics 18 (2024) 100596

Contents lists available at ScienceDirect

Open Ceramics

journal homepage: www.sciencedirect.com/journal/open-ceramics

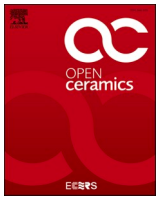

Exploring transformative and multifunctional potential of MXenes in 2D materials for next-generation technology

Raghvendra Kumar Mishra [a,*], Jayati Sarkar [b], Kartikey Verma [c], Iva Chianella [a], Saurav Goel [d,e], Hamed Yazdani Nezhad [f]

[a] School of Aerospace, Transport and Manufacturing, Cranfield University, MK430AL, United Kingdom
[b] Department of Chemical Engineering, Indian Institute of Technology Delhi, Hauz Khas, Delhi, 110016, India
[c] Department of Chemical Engineering, Indian Institute of Technology Kanpur, Kalyanpur, Kanpur, Uttar Pradesh, 208016, India
[d] School of Engineering, London South Bank University, London, SE10AA, United Kingdom
[e] University of Petroleum and Energy Studies, Dehradun, 248007, India
[f] School of Mechanical Engineering, Faculty of Engineering and Physical Sciences, University of Leeds, Leeds, United Kingdom

ARTICLE INFO

Handling editor: Dr P Colombo

Keywords:
MXenes
2D materials
Synthesis of MXenes
Characteristics of MXenes
Applications of MXenes

ABSTRACT

MXenes, a rapidly growing family of two-dimensional (2D) transition metal carbides, nitrides, or carbonitrides ($M_{n+1}X_nT_x$, where M is a transition metal, X is carbon, nitrogen, or both, and T represents surface functional groups), have captured the scientific community's interest due to their exceptional physicochemical properties and diverse technological applications. This comprehensive review explores the latest breakthroughs in MXene synthesis and characterisation, emphasising their multifaceted applications in energy storage, catalysis, sensing, and other cutting-edge domains. This review examines the most widely used MXene synthesis strategies, including selective etching and delamination, and highlight recent advancements in controlling surface terminations, composition, and morphology. The influence of these synthetic parameters on MXene properties is discussed in detail. Characterisation techniques, ranging from spectroscopic methods to electron microscopy, are essential for elucidating MXenes' structure-property relationships. Research into energy storage leverages MXenes' high electrical conductivity, large surface area, and chemical tunability. This has led to significant progress in the field. This paper presents research efforts focused on optimising MXenes for both battery and supercapacitor applications. Additionally, the catalytic prowess of MXenes, particularly in electrocatalysis and photocatalysis, is explored, emphasising their role in green energy technologies and environmental remediation. MXenes' remarkable sensitivity and selectivity make them promising candidates for sensing various gases, biomolecules, and ions, offering exciting possibilities in healthcare and environmental monitoring. Importantly, this review underscores the need for continued optimisation of MXene synthesis protocols to achieve large-scale production, enhanced stability, and precise control over properties across various fields.

Abbreviations:

Abbreviation	Meaning
AgNW	Silver nanowire
ANFs	Aramid nanofibers
CFf	Carbon fibre fabric
CFRP	Carbon fibre-reinforced polymer
CGG	Cationic guar gum
CNF	Cellulose nanofiber
CoC@CNF	Core–shell heterogeneous reduced graphene oxide/MXene films
CuNWs	Copper nanowires
EPOSS	Epoxied octamethyl-cyclotetrasiloxane
FMs	Face masks
GMA	Graphene oxide/MXene aerogel
GO	Graphene oxide
H–Ti3C2Tx	High-strength Ti3C2Tx MXenes
HA	Heterocyclic aramid
HFO	Hollow magnetic Fe3O4 nanospheres
MCW	MXene/cellulose nanocrystals/WPU composite films
MMX	Magnetic Ti3C2Tx Mxene
MPCF	Ti3C2Tx MXene/porous carbon foam composites

(*continued on next column*)

(*continued*)

(*continued on next page*)

* Corresponding author.
E-mail address: raghvendramishra4489@gmail.com (R.K. Mishra).

https://doi.org/10.1016/j.oceram.2024.100596
Received 26 December 2023; Received in revised form 13 April 2024; Accepted 15 April 2024
Available online 25 April 2024

(*continued*)

Abbreviation	Meaning
MX/HG	MXene/holey graphene composite films
Mxene	Two-dimensional carbide or nitride materials
MXrGO@PMMA	MXene/reduced graphene oxide in PMMA nanocomposites
MSCFs	MXene/sodium alginate composite fibres
PAM@fabric	Poly (dimethylsiloxane)/Ag NWs/MXene/fabric device
PET MPs	Polyethylene terephthalate microplastics
PNFs	Poly (*p*-phenylene-2,6-benzobisoxazole) nanofibers
PM-g-MA	Polypropylene grafted maleic anhydride
PMPCMs	MXene/delignified wood supported form-stable phase-change composites
PNWs	Positively charged polycarbonate microspheres with MXene flakes
rGO	Reduced graphene oxide
s-CPCs	Positively charged polycarbonate microspheres with MXene flakes
SHMA	Superhydrophobic Ti3C2Tx MXene/aramid nanofiber films
TOCN	TEMPO-oxidised cellulose nanofibers

1. Introduction

Modern scientific research focuses heavily on two-dimensional (2D) materials, particularly multilayers, because of their unique properties [1]. Graphene, a single layer of carbon atoms in a honeycomb lattice, boasts remarkable electrical conductivity, thermal conductance, and mechanical strength due to its sp^2 hybridisation [2]. Graphene's unique structure has motivated its exploration in various fields including electronics, optoelectronics, energy systems, and biomedical engineering. Research by Jayakumar et al., Kaul et al., and Wang et al. has made significant contributions to our understanding of synthesis techniques, material properties, and potential uses in these fields [1–3]. Graphene's conductivity and flexibility make it ideal for solar cells, touchscreens, and supercapacitors [4,5]. Graphene's unique properties — transparency, conductivity, high charge carrier mobility, and exceptional thermal conductivity — make it valuable in electronics for future devices [6,7]. Graphene's unique properties enable its exploration in the medical field, including as components in drug delivery systems and artificial tissues [8]. Fig. 1 illustrates graphene's remarkable impact across various fields. Inspired by its success, researchers are actively exploring other 2D materials, including borophene, germanene, silicene, stanene, phosphorene, and h-BN [9–13]. These materials exhibit a variety of stacking configurations, leading to a broad spectrum of potential uses. Notably, their categorisation as 2D materials doesn't necessarily require perfect atomic flatness. Borophene, for example, demonstrates unique properties despite its non-planar structure [9].MXenes (M_2X_3, M = transition metal, X = C, N, or both) are a prominent class of 2D materials due to their unique physical properties, making them a hotbed of research [14–16]. This review explores recent advancements in MXene synthesis, characterisation, fundamental properties, and applications.

2. MXenes: 2D materials with promising applications

MXenes, discovered in 2011, are a fascinating class of 2D materials produced by selectively etching aluminium layers from MAX phases [17]. This process unlocks remarkable properties, including high conductivity and hydrophilic surfaces, distinct from their MAX phase precursors [18,19]. The versatile $M_{n+1}X_nT_x$ formula allows for a broad range of MXene compositions (e.g., Ti_3C_2Tx, V_2CTx, Mo_2CTx), enabling their exploration in energy storage, catalysis, shielding, purification, and sensing [20]. MXenes' unique properties stem from their layered structure composed of transition metals and functional groups (Fig. 2a) [21]. These properties are highly tuneable. The choice of the MAX phase precursor, particularly the transition metal (e.g., Ti, V, Nb) and the A-element (like Al), significantly influences the MXene's composition and resulting functionalities [22]. Additionally, etching conditions, such as temperature and duration, affect A-element removal and surface functional group formation, further tailoring MXene properties [23–25]. Intercalation, the controlled insertion of ions, molecules, or functional groups between MXene layers, significantly alters properties like mechanical strength, surface area, and electrical conductivity. For example, intercalation with N-methyl formamide enhances stability and conductivity in humid environments, while water intercalation may slightly decrease conductivity due to lattice expansion [26,27]. Post-processing techniques, such as integrating various interlayers, can dramatically enhance mechanical strength, as demonstrated by ultra strong hydroxylated carbon nanotube (HCNT) intercalated $Ti_3C_2T_x$ films [27]. Precise control of synthesis and processing empowers researchers to engineer MXene properties, opening possibilities for a wide range of scientific and industrial uses [23]. Fig. 2b demonstrates MXenes' remarkable tunability through the interplay of synthesis, intercalation, and post-processing [28]. This adaptability enables researchers to design MXenes for a wide range of specific applications [29].

2.1. Synthesis and characterisation methods of MXenes

MXenes, derived from 3D MAX phases by selective etching of "A" elements, exhibit remarkable mechanical properties [17]. Studies have revealed exceptional strength and flexibility in MXenes. For instance, a single $Ti_3C_2T_x$ MXene nanosheet boasts a superior Young's modulus compared to graphene oxide, reduced graphene oxide, and MoS_2. Additionally, continuous $Ti_3C_2T_x$ MXene films can outperform aluminum foils in tensile strength [31]. The measured effective Young's modulus of a monolayer Ti_3C_2T was found to be 0.33 ± 0.03 TPa, exceeding the highest reported values from nanoindentation of other solution-processed 2D materials like graphene oxide [31,32]. This exceptional mechanical strength, combined with properties like high electrical conductivity, hydrophilic surface functionalities, and flexibility, suggests potential uses for MXenes in energy storage, sensing, catalysis, and mechanically reinforced composites. Layer thickness, functional groups, point defects, and the choice of transition metal significantly influence MXene mechanics [21]. Synthesis conditions, intercalation, and post-processing techniques can substantially affect

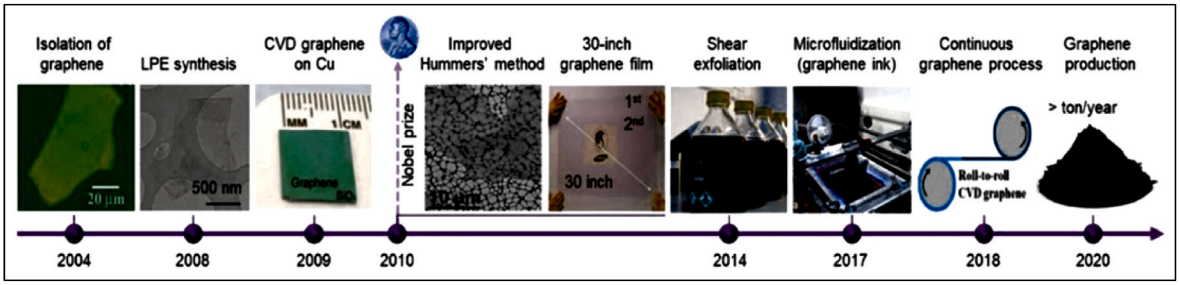

Fig. 1. Charting Graphene's evolution: Milestones in research and development since its isolation in 2004 [8].

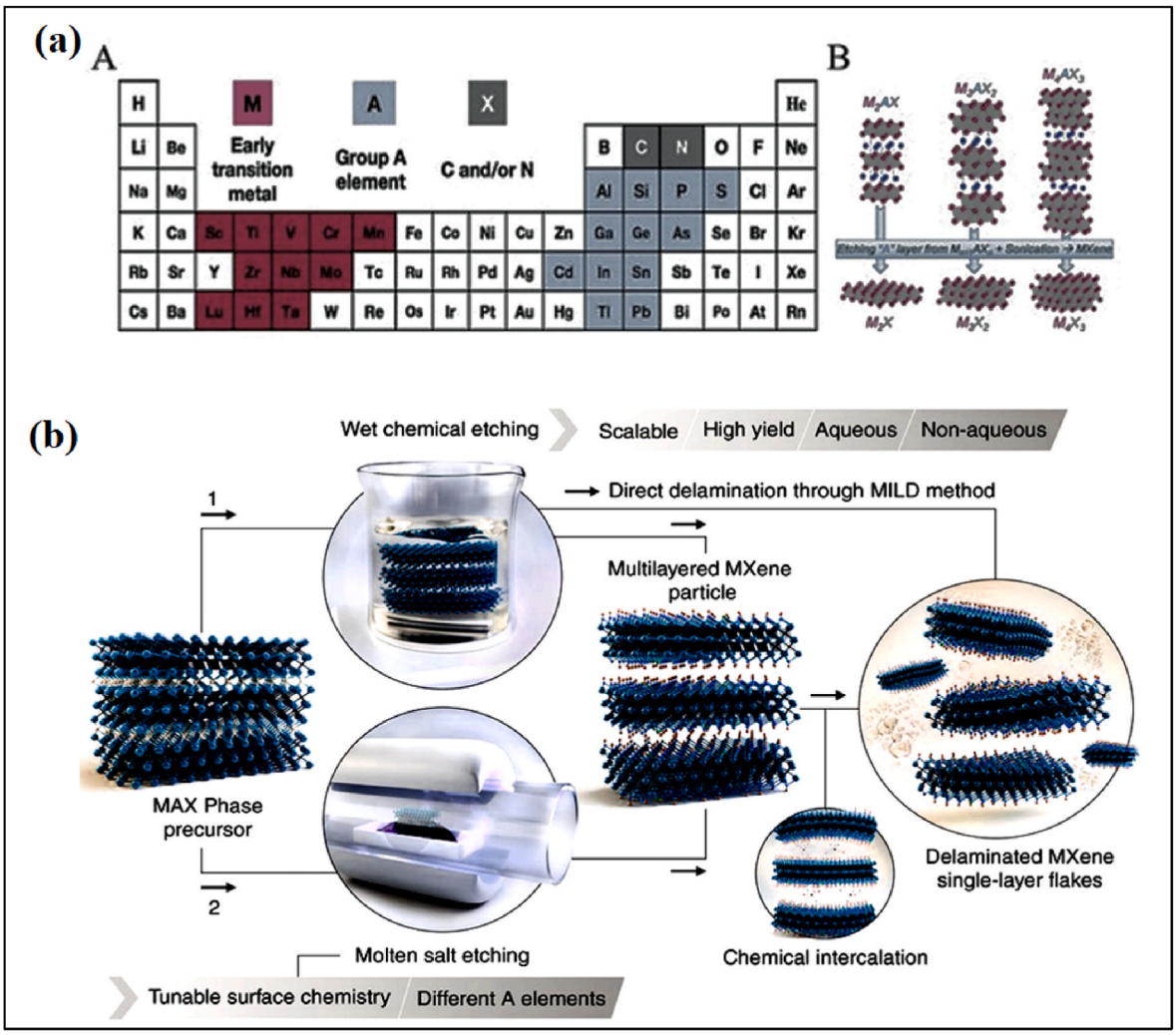

Fig. 2. (a) A representative of Elements involved in the formation of MAX phase and B representative of MXenes derived from different MAX phases [30], (b) Typical intercalation process in MXenes, emphasising the significance of this technique in tuning properties through synthesis conditions, intercalation, and post-processing [28].

mechanical properties [33,34]. Techniques like annealing can further refine electronic, optical, and catalytic characteristics [34]. While hydrofluoric acid (HF) was initially used for MXene synthesis (e.g., $Ti_3C_2T_x$ in 2011), advancements have led to alternative methods offering greater control and enhanced MXene characteristics [35,36]. These techniques include Ammonium bifluoride (NH_4HF_2) etching, LiF/HCl etching, and NaOH-based hydrothermal synthesis. The choice of etchant and precise temperature control remain crucial for MXene stability [25,37]. Traditional HF-based etching, although effective, can introduce surface defects that compromise stability by increasing susceptibility to oxidation [38]. Beyond etchant selection, achieving optimal MXene stability requires a holistic approach. Careful quality control of the MAX phase precursor, precise control of etching conditions, defect passivation techniques, selection of the dispersion medium, and optimised storage conditions all contribute significantly [37]. Different synthesis methods, such as arc discharge and chemical vapor deposition (CVD), can impact flake size, quality, and surface terminations. Fig. 3 illustrates the *P*63/mmc crystal structure of MAX phases, depicting the atomic arrangement within the lattice [39].

Research focuses on developing safer and more controllable etching methods than traditional hydrofluoric acid (HF). Innovations using ammonium bifluoride (NH_4HF_2) provide alternatives with greater safety and offer improvements in MXene characteristics [40]. Etching powdered Ti_3AlC_2 with LiF/HCl can produce larger, high-quality $Ti_3C_2T_x$ MXene flakes, ideal for flexible films with high volumetric capacitance. A safe and cost-effective LiF/HCl etching method combined with freeze-drying enables control over MXene morphology. This process transitions MXene structures from stacked to accordion-like and finally to ultra-thin dispersed sheets with increased etching time [41]. This approach offers advantages like easier delamination through sonication and the production of higher quality MXenes with fewer defects compared to traditional HF methods [42]. This is particularly beneficial for producing high-quality MXenes, which are essential in fields like electronics and optoelectronics. Higher etching temperatures can facilitate both the etching process and the exfoliation of MXene layers [43]. A thorough understanding of MXene properties relies on the application of various analytical techniques. These methods offer insights into different aspects of MXenes, including crystal structure and phase composition analysed through X-ray Diffraction (XRD) [44], vibrational modes studied via Raman Spectroscopy, and chemical bonding and molecular structure elucidated with Fourier Transform Infrared Spectroscopy (FTIR) [45]. Additionally, thermal stability is assessed through Thermogravimetric Analysis (TGA) and Differential Scanning Calorimetry (DSC) [46], while elemental composition and electronic states are determined using X-ray Photoelectron Spectroscopy (XPS) and Energy-Dispersive X-ray Spectroscopy (EDX) [47]. By employing these techniques collectively, researchers can comprehensively characterise MXenes. This understanding allows them to customise synthesis

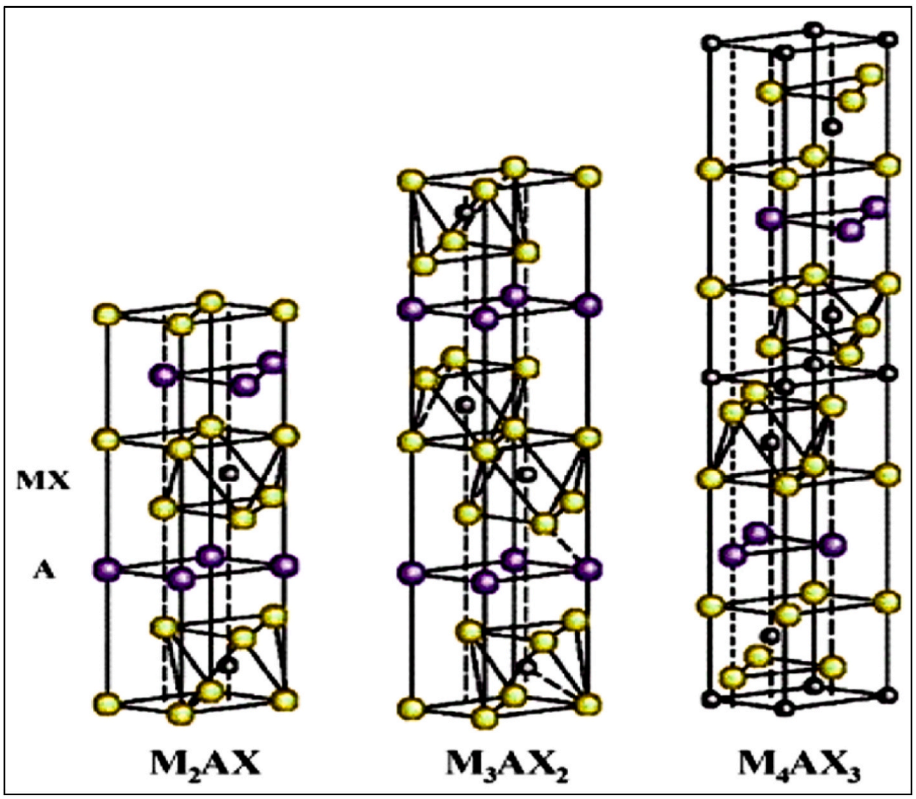

Fig. 3. MAX phase *P*63/mmc symmetry. Blue balls denote the A layer atoms, red balls denote the M layer atoms, and gray balls occupying the octahedral site denote the X atoms [39].

methods to achieve specific properties suitable for various uses [48]. MXenes' unique combination of properties and broad catalytic activity make them applicable in various fields. Their high electrical conductivity positions them well for use as electrodes in batteries and supercapacitors [49]. MXenes' hydrophilicity facilitates efficient water desalination via membrane filtration [50]. MXenes serve as catalysts in various reactions such as hydrogen evolution, oxygen evolution and reduction, nitrogen fixation, and carbon-carbon coupling, owing to their extensive surface area and flexibility. MXenes' biocompatibility and distinctive properties hold promise for biomedical research and potential development [49,50].

2.2. Selection of synthesis method for MXenes production

MXene production utilises various methods, each offering distinct advantages and considerations [51]. Etching involves the selective removal of the "A" element from the MAX phase using etchants. Common etchants include hydrofluoric acid (HF), although safer alternatives like a lithium fluoride (LiF) and hydrochloric acid (HCl) mixture are increasingly explored due to safety concerns with HF [51,52]. Top-Down Synthesis method involves exfoliating the MAX phase into MXenes through intercalation, the insertion of ions or molecules between layers, to facilitate separation. Bottom-Up Synthesis approach directly synthesises MXenes from elemental or binary precursors. The optimal synthesis method depends on the desired MXene properties, resource availability, and safety considerations [53]. Modern protocols emphasise efficiency and feasibility, incorporating techniques such as low-boiling solvents, physical synthesis methods, low-temperature MAX phase preparation, and the exploration of biological materials for synthesis. Synthesis conditions, including precursor selection, etchant choice, temperature, and reaction time, significantly impact MXene properties [45,51,52]. MXene synthesis typically involves wet chemical etching of MAX phases at room temperature. Strong interlayer bonds within the MAX phase necessitate robust etchants. While the "A" element (often aluminium) may corrode under specific conditions, the resulting $M_{n+1}X_n$ layers exhibit good chemical stability. Synthesis methods beyond traditional wet-chemical etching, such as arc discharge or chemical vapor deposition (CVD), can also influence MXene properties like flake size, quality, and surface terminations, as exemplified by $Ti_3C_2T_x$ [54].

2.2.1. HF-based synthesis methods and HF etching protocol for MXenes

Hydrofluoric acid (HF) has played a pivotal role in MXene synthesis, particularly for the pioneering discovery of $Ti_3C_2T_x$ [25,55]. This room-temperature etching method paved the way for the production of other carbide MXenes (Mo_2CT_x, V_2CT_x) [56]. However, due to the significant safety hazards associated with HF, researchers actively explore alternative etching processes [51,57]. While higher HF concentrations expedite etching, they also elevate risks [51]. A key research focus area is achieving efficient MXene synthesis using lower HF concentrations. Beyond HF concentration, various parameters influence wet-chemical etching, including temperature, pressure, and etching time. Techniques like hydrothermal and electrochemical etching offer greater control over these parameters, allowing for further optimisation of the synthesis process [25]. The corrosive nature of HF necessitates the development of safer alternatives. The LiF/HCl mixture is a promising example [25,55]. Several factors influence MXene synthesis efficiency. Etching time, particle size, and the concentration of the etching agent (e.g., HF) significantly impact the conversion of MAX phases to MXenes [58–60]. The choice of carbide precursor also plays a role. For instance, Ti_3AlC_2 can be readily converted within 2 h, while Ta_4AlC_3 and Nb_4AlC_3 require longer etching times and exhibit lower yields [35,61,62]. Conversely, Mo_2TiAlC_2 and $Mo_2Ti_2AlC_3$ demonstrate faster etching and higher yields [61]. Safety is paramount when handling hazardous materials like HF, particularly during aluminium etching [63]. A thorough risk assessment is crucial before initiating any etching process. Protocols

employing lower concentrations of hydrofluoric acid (HF), such as 5 % for 5 h, offer a safer alternative for MXene synthesis while maintaining acceptable yields. This approach mitigates the risks associated with handling HF, a highly corrosive and dangerous chemical [23]. Despite the use of lower HF concentrations, MXene synthesis can still involve environmentally harmful and toxic substances [64]. Researchers are actively exploring alternative synthetic routes that utilise in-situ forming HF agents. For example, a mixture of hydrochloric acid (HCl) and lithium fluoride (LiF) can be utilised to produce $Ti_3C_2T_x$ MXene [65]. Additionally, studies have shown that MXene obtained using the HBF_4 etching agent under mild conditions exhibits comparable structural and functional properties to MXene produced using 5 % HF [52]. Material purity is crucial for MXenes, following etching, centrifugation with deionised water is often employed to remove impurities [66]. Techniques like X-ray diffraction (XRD) and energy-dispersive X-ray spectroscopy (EDX) can then be used to validate the selective etching process and obtain structural information about the resulting MXene [67]. Contemporary MXene synthesis trends favor lower HF concentrations (around 5 %) to minimise safety hazards and environmental impact. This shift reflects a growing emphasis on responsible research practices. The search for safer and more sustainable etching methods extends beyond simply lowering HF concentration. Molten fluoride salt etching presents a promising alternative, particularly for MAX phases that do not contain aluminium [68–71]. Researchers are actively investigating various etching techniques, each offering unique advantages depending on the desired MXene properties and intended use [72].

2.2.2. Bifluoride-based etchants for MXenes

Fluoride-based etchants, particularly bifluorides, remain the dominant method for MXene synthesis due to their effectiveness in selectively removing the “A" element from MAX phases [73,74]. Fluoride salts, such as lithium fluoride (LiF) and ammonium fluoride (NH_4F), are strategically used, with their concentrations and etching temperatures optimised for specific MAX phases to ensure high-quality MXene production [75]. Compared to conventional HF etching, these salts offer a safer and more environmentally friendly alternative, making them attractive for large-scale synthesis [73,74]. Researchers actively explore alternative synthesis methods that prioritise safety and sustainability. These methods, including molten salts, alkaline solutions, and hydrothermal treatments, offer a range of synthesis pathways, enabling the production of MXenes with various properties [76]. Notably, the development of fluorine-free etching methods is particularly significant for creating biocompatible MXenes [74]. The NH_4– $Ti_3C_2T_x$ process exemplifies a significant advancement in MXene synthesis, emphasising both safety and sustainability. This method involves a controlled reaction between Ti_3AlC_2 powder and 2 M NH_4HF_2 for 24 h at room temperature, followed by thorough purification and precise drying. This approach offers several advantages. It avoids highly hazardous chemicals commonly used in other etching methods while ensuring complete removal of the “A" layer without compromising MXene integrity. Rigorous purification and drying procedures result in high-quality MXene materials. The NH_4–$Ti_3C_2T_x$ process highlights advances in process safety, efficiency, and MXene quality. This broader focus paves the way for promising research directions and demonstrates the potential for expanding MXene research and development [77].

2.2.3. Fluoride-based salt etchants for MXenes

Fluoride-based salts, particularly lithium fluoride (LiF) and ammonium fluoride (NH_4F), remain prevalent etchants in MXene synthesis due to their selectivity in removing the “A" element from MAX phases. Optimisation of salt concentration and etching temperature is crucial for achieving high-quality MXenes for specific MAX phases [75]. An alternative approach involves in-situ generated HF from fluoride salts, leveraging the essential role of the F^- anion in the etching process [55,78]. Notably, such alternatives hold promise for large-scale production due to their enhanced safety profiles and reduced environmental impact. The Minimally Intense Layer Delamination (MILD) method offers a controlled approach to MXene synthesis Variants, like the “Evaporated-Nitrogen” MILD (EN-MILD), enable the production of higher-quality MXenes with larger flake sizes and improved electrical conductivity [79]. MXene, emphasising selective etching of MAX phases followed by liquid exfoliation [79,80]. Properties can be precisely tailored by modifying the etchant composition and etching conditions. In the MILD method, manipulating the molar ratios of LiF:Ti_3AlC_2 and HCl concentrations during in-situ HF generation allows for fine control over flake size and defect reduction [49,81,82]. This control is critical for achieving desired electrical conductivity and enabling the fabrication of self-standing MXene films. The MILD method, initially using 12 M LiF and 9 M HCl at room temperature, significantly improved the production of high-quality single-layer $Ti_3C_2T_x$ [49]. This gentle approach with controlled stirring facilitates effective delamination. Optimisations involve careful washing cycles with deionised water at pH 4–5, doubling the $Ti_3C_2T_x$ sediment, and characteristic changes like a persistent dark-green supernatant, all contributing to enhanced quality and efficiency [83,84]. Notably, MILD’s distinctive swelling during washing, in contrast to the traditional “clay” method, is attributed to Li^+ ions and optimised HCl concentrations. MILD and its variants enable the production of high-quality, single-layer MXene flakes. These flakes hold promise for potential uses in energy storage (electrochemical devices like supercapacitors), electromagnetic interference shielding, water purification, and sensor technologies [79]. The unique 2D structure, high conductivity, and versatile surface groups of MXenes, particularly $Ti_3C_2T_x$, make them promising materials for exploration across a wide range of research fields [85,86]. They are being explored for supercapacitors, gas sensors, electrocatalysts for HER (hydrogen evolution reaction) due to their structure and favorable hydrogen adsorption, and photocatalysts for CO_2 reduction reactions (CO_2RR) due to surface defects. However, material stability remains a challenge for broader implementation, necessitating research efforts to optimise synthesis routes for enhanced stability [87]. The NH_4– $Ti_3C_2T_x$ process highlights advances in safer and more efficient MXene synthesis. Its success is evident in the development of a highly responsive ammonia sensor using Ti_3C_2Tx, which operates effectively at room temperature [88]. Continued research using the NH_4– $Ti_3C_2T_x$ process holds promise for deepening our understanding of MXenes and paving the way for advancements and innovations in existing technologies.

2.2.4. Functional groups exploration in MXenes

MXenes possess a unique characteristic: surface functional groups that significantly influence their properties [89,90]. These groups, typically oxygen, hydroxyl (-OH), fluorine (-F), and sometimes chlorine (-Cl), arise from the etching process, exposing metal atoms on the MXene surface [91]. They play a critical role in determining electronic, magnetic, mechanical, optical characteristics, and hydrophilicity/hydrophobicity of MXenes. Chemical modifications, such as surface-initiated polymerisation and single heteroatom doping, offer precise control over these functionalities [89]. Notably, intercalation and surface modification strategies conducted under safe conditions can yield MXenes with exceptional optical, electrical, and magnetic properties. The adaptability of MXenes allows for the introduction of various functional groups (O, NH_2, S, Cl, Se, Br, Te) or the creation of bare MXene [91]. Surface terminations on MXenes, like $Ti_3C_2T_x$, are crucial for synthesis and profoundly influence their properties [92]. While initial research focused on –OH terminations, studies by Liu et al. revealed the prevalence of –F and –O terminations in $Ti_3C_2T_x$, highlighting the dependence of surface chemistry on the chosen synthesis route [93]. For instance, fluorine-terminated $Ti_3C_2T_f$ exhibits superior thermal conductivity compared to its oxygen-terminated counterpart [92]. Synthesis parameters, such as centrifuge speed, significantly influence MXene properties. During MXene preparation, high-speed centrifugation and long-time ultrasonication are often used to intercalate cations into layers of MXene nanosheets (MNSs). The size of the

Table 1
Impact of synthesis conditions on the properties of MXenes.

Methods	Key Findings	Additional Notes	Ref.
MXene precursor phases	Varied chemical compositions allow for a range of MXene structures.	Harnessing chemical diversity of transition metal carbides and nitrides.	[116,117]
Computational prediction of exfoliation	Bond strength guides precursor selection for successful MXene synthesis.	Successful isolation depends on bond strength and choice of etchants.	[116]
Top-down synthesis from bulk precursors	Range of structures and compositions enables MXenes with varied properties.	Stability with vacancies in M and X sites for applications in catalysis, extreme environments.	[118,119]
A-elements react with HF for accordion-like	Easier preparation through wet acid etching compared to other precursors.	Wet acid etching common and effective for high-quality MXene products.	[120]
Ti_3C_2Tx synthesis with selective wet etching	Stable structure and properties in large-scale synthesis.	Consistent properties support commercialisation.	[121]
Selective etching methods, Weaker M-A metallic bond for extraction, Delamination via selective etching	Relatively easy, low-cost, high-yield synthesis. Essential for mono or few-layer MXenes. Achieved with fluoride salts, acids, or organics.	Selective extraction of Al layers; common method for MXene synthesis. Interlayer interactions in MXene multilayers stronger than graphite and MoS_2.	[61, 122–125]
TiVC synthesis with LiF/HCl, Delamination via LiF/HCl in TBAOH	Higher concentration of =O, suitable for energy storage. First systematic study on synthesis impact on TiVC MXenes' surface chemistry. 2.18 nm interlayer spacing facilitates ion transport.	Defects impact properties, degrade MXenes in the presence of water or oxygen. Influenced surface groups by synthesis conditions. DFT calculations and XPS measurements for surface chemistry investigation.	[126,127]
Surface dangling bonds react with solution	Hydrophilic nature attributed to surface terminations.	Aggressive etching may lead to destruction and carbide-derived carbon formation.	[125,128]
High surface area, conductivity, and active sites for various reactions	MXenes in catalysis and electrocatalysis	Catalytic activity influenced by metal interactions and surface terminations.	[129]
High-entropy MXenes from MAX phases	Characterisation, configurational entropy crucial for stability.	A range of single-phase high-entropy MXenes have been synthesised, offering exciting possibilities for material research.	[130]
Large-scale synthesis and antioxidation	Crucial for practical MXene applications.	Efficient synthesis with appropriate conditions and antioxidation strategies.	[63]
Thermal-assisted electrochemical etching	Benign synthesis: cobalt ion doping enhances multifunctionality.	Efficient retention and excellent electrical output for energy-related applications.	[131]
In situ chemical transformations	Hybrid structures; improved electrical conductivity through ammonisation.	Transition metal nitrides obtained through ammonisation of carbides.	[132,133]
Plasma etching for MXene synthesis	Large-scale Ti_2C film synthesis using plasma etching.	Plasma etching and solution-based nanolamination processes for MXene production.	[134]
Molten salt etching at high temperatures	Synthesis at 650–750 °C; lattice distortion due to salt templates.	Successful synthesis of Ti_4N_3; strict conditions for nitride MXenes.	[61,135, 136]
Chemical Vapor Deposition (CVD)	High-quality 2D crystal synthesis; applicable to various transition metal carbides.	Atomic construction control achieved, including vertical heterostructures.	[137–139]
Electrochemical etching and molten salt	Safer alternatives to traditional acid-based methods.	Fluoride-free MXenes are explored for biomedical applications due to safety concerns.	[132,133]

MXene flakes, affected by centrifuge speed, plays a crucial role in capacitance, electrical conductivity, and rate performance of free-standing film electrodes. Processing conditions also impact surface terminations and thermal stability, resulting in MXenes with tailored properties. Therefore, meticulous control of synthesis parameters, including centrifuge speed, is essential for achieving desired functionalities in MXenes [34,94]. Various techniques are employed to characterise surface terminations. Nuclear magnetic resonance (NMR) spectroscopy offers insights into internal terminations, while X-ray photoelectron spectroscopy (XPS) and energy-dispersive X-ray spectroscopy (EDS) reveal subtle chemical variations on MXene surfaces [95]. NMR studies, like those by Griffith et al. [96], investigate partially blocked surface functionalities in $Ti_3C_2T_x$ caused by water and etching byproducts. For V_2CT_x, solid-state NMR (H-1, F-19, and C-13) provides detailed analysis of surface termination groups [97]. Combined H-1 and F-19 NMR analysis revealed intricate interactions involving water, hydroxide layers, and fluoride attachment on V_2CT_x. Research investigates that different surface functionalization methods tailor MXene properties. For example, Lai et al. significantly enhanced piezoelectricity in $Ti_3C_2T_x$ by using organo-silane headgroup modifications [98].

2.2.5. *Surface functional groups and chemical modifications of MXenes*

MXenes ($(M_{n+1}X_nT_x)$, where T_x represents surface functional groups) derive their functionality in part from their surface groups [99]. These groups, typically oxygen, hydroxyl (-OH), fluorine (-F), and sometimes chlorine (-Cl), can be strategically modified to achieve tailored properties [89,100]. The etching process exposes metal atoms on the MXene surface, giving rise to these functional groups [101]. Researchers have a well-equipped toolbox for manipulating MXene surfaces. Techniques like surface-initiated polymerisation enable the controlled growth of polymers directly on the MXene surface, effectively expanding its functionalities [102]. Similarly, single heteroatom doping introduces foreign atoms, significantly modifying electronic, catalytic, and other properties [102,103]. Covalent grafting, using coupling agents, enables the attachment of various functional groups, offering the potential to tailor MXene properties for specific purposes [99]. Plasma annealing with Ar + O_2 plasma modifies surface properties and reactivity by increasing the presence of = O functional groups [102]. Defunctionalisation and re-functionalisation involve the selective removal of existing groups, followed by the targeted introduction of new ones using techniques like iodine or bromine vaporisation [53,104]. These versatile strategies demonstrate the adaptability of MXenes.

2.2.6. *Chemical modifications of MXene for enhanced electrochemical behaviour*

Building upon the established role of surface functionalisation in MXenes, targeted chemical modifications offer a powerful approach to enhance their electrochemical behaviour. Doping MXenes with specific elements, like nickel (Ni), can significantly improve their capacitive performance. Studies on Nb_2C MXene demonstrate this effect, with increased capacitance observed upon Ni doping [105]. Similarly, doping with erbium (Er) and lanthanum (La) tailors MXenes for specific functionalities, such as electrochemical hydrazine sensing and magnetic behaviour, respectively [106]. Surface functionalisation offers another avenue for optimising MXenes for energy storage. Techniques like surface-initiated polymerisation and single heteroatom doping significantly influence various MXene properties, including electronic conductivity and hydrophilicity, which directly impact their

electrochemical behaviour [105]. Designing open structures for MXene nanosheets increases their electrochemically accessible surface area. This facilitates improved ion transport to active redox sites within the material, ultimately enhancing performance [107]. The creation of hybrid structures, such as the MXene/Ni chain hybrid, exemplifies this concept, demonstrating outstanding electromagnetic wave absorption due to its unique morphology [106]. These targeted chemical modifications hold significant promise for optimising MXenes in various energy storage technologies, including supercapacitors, sensors, and batteries [108]. MXenes' exceptional performance in energy storage stems from the significant influence of their surface chemistry on electrochemical behaviour [109]. Strategic functionalisation methods like diazonium grafting and hydrazine intercalation can be utilised to customise surface groups and enhance the capacitance in MXenes [22,89]. Diazonium grafting involves the covalent attachment of functional groups onto the MXene surface, modifying its surface chemistry. For instance, a study demonstrated that grafting $C_6H_4SO_3H$ groups onto Ti_3C_2 improved its electrical properties [89]. Hydrazine intercalation, commonly used in other 2D materials, involves the insertion of hydrazine molecules between MXene layers and alters its properties [22]. These methods offer flexibility in tailoring MXene surface groups, thereby enhancing capacitance and other desired properties. However, the precise effects may vary depending on the specific MXene material and the functionalisation conditions employed [22,89]. MXenes's layered structure facilitates ion intercalation, enabling efficient electrolyte interaction. Additionally, their hydrophilicity ensures effective electrolyte interaction, while their metallic conductivity guarantees rapid electron transport. Moreover, MXenes boast high charge carrier mobility, promoting swift charge/discharge processes. Their tuneable bandgap allows for material optimisation, while their versatile surface chemistry enables targeted modifications. These combined properties, coupled with the capability to customise surface terminations and elemental compositions, offer a vast array of tailorable physical, chemical, and electrochemical characteristics [109]. Researchers employ various techniques to modify MXene surfaces and enhance their electrochemical performance. Pre-intercalation of Na^+ ions followed by grafting aryl diazonium salts onto the MXene surface [110]. This approach covalently bonds functional groups, altering reactivity and increasing interlayer spacing. Introduces ions between MXene sheets using sound waves (Low-energy sonication) in deionised water. This technique enhances performance by separating stacked MXene sheets and increasing the contact surface area with electrolytes [111,112]. Electrochemical modifications reveal that oxygen-rich surface groups enhance MXene capacitance. Modifying the surface chemistry, such as introducing hydrazine intercalation, can reduce OH groups and improve electrode cycling stability [113,114]. MXenes find application in various energy storage devices beyond supercapacitors. These include rechargeable lithium-ion, potassium-ion, and sodium-ion batteries, and even hydrogen storage [115]. Researchers are actively integrating MXenes into energy storage as electrode materials, conductive additives, surface modifiers, and more, capitalising on their unique properties for optimisation [109,115]. Table 1 offers an insightful overview of different synthesis conditions impacting various properties of MXenes, encompassing factors such as electrical conductivity, mechanical strength, and specific surface area. These properties are intricately linked to the choice of precursor materials, synthesis temperature, and reaction time employed during the synthesis process.

2.2.7. *Characterisation techniques for unveiling MXene properties*

Understanding the properties of MXenes necessitates employing various characterisation techniques, each offering unique insights into the material's composition and structure [140,141]. X-ray Diffraction (XRD) is pivotal in discerning the crystal structure and phase of MXenes, providing crucial information for comprehending their fundamental properties. Complementing XRD, X-ray Photoelectron Spectroscopy (XPS) furnishes detailed analysis of the elemental composition and electronic states within MXenes, contributing to a holistic understanding of their chemical makeup [142]. Additionally, Raman Spectroscopy plays a crucial role in elucidating the vibrational and rotational modes within MXenes, shedding light on their molecular structure, phase, and crystallinity. Moreover, techniques such as Scanning Electron Microscopy (SEM), Scanning Transmission Electron Microscopy (STEM), and Energy-Dispersive X-ray Spectroscopy (EDX) offer valuable insights into the morphology and atomic structure of MXenes, allowing visualisation of their physical characteristics at the nano-scale [141]. Furthermore, Particle Size Analysis aids in determining the size distribution of MXene particles, a critical factor influencing their properties and performance. Lastly, optical characterisation techniques provide essential information on MXenes' light absorption and emission characteristics. This knowledge enriches our understanding of their optical properties, contributing to the development of optoelectronic and photocatalytic technologies [141,142]. MXenes' ability to endure high temperatures is influenced by various factors, including synthesis conditions, chemical composition, transition metal type, and surface chemistry. Research on $Ti_3C_2T_x$, Nb_2CT_x, and Mo_2CT_x MXenes has shown stability up to temperatures of 800 °C, but carbon monoxide release begins at 830 °C. The hydrophilicity of MXenes fluctuates depending on etching and delamination methods. Surface terminations encompass various groups like hydroxyl, oxy, fluoride, and intercalated species such as salts and structural water. Thermal gravimetric analysis coupled with mass spectrometry has provided detailed insights into MXenes' surface terminations, even at temperatures as high as 1500 °C in a helium atmosphere. MXenes' thermal stability is influenced by synthesis conditions, chemical composition, transition metal type, and surface chemistry. The specific transition metal and surface terminations play crucial roles in determining thermal properties. Additionally, a comprehensive understanding of thermal analysis data and sample history can offer valuable insights for tuning MXene properties through specific thermal treatment conditions [143]. MXenes' distinctive thermal properties stem from their layered structure and composition, resulting in unique thermal stability and thermophysical characteristics [144]. The thermal and crystallisation behaviour of MXene-based polymer nanocomposites is influenced by factors such as surface-terminating groups, storage method, preparation technique, and treatment procedures like annealing. Evaluation methods for MXene thermal properties have been explored, emphasising the influence of MXene on polymer nanocomposite crystallisation [145]. Among investigated MXenes, $Ti_3C_2T_x$ and Ti_2CT_x demonstrated the highest and lowest thermal stability, respectively. This discrepancy suggests that factors like transition metal type, synthesis method, and MXene flake atomic layer count play pivotal roles in determining thermal stability. In situ spectroscopic ellipsometry (SE) analysed the optical properties of three MXene types, unveiling variations in MXene extinction and optical conductivity correlated with the quantity of intercalated water and hydroxyl termination groups [146]. Thermal evolution of $Ti_3C_2T_x$ MXene unfolds in two processes: process I (25–500 °C) and process II (500–777 °C), involving reduction of terminal groups and release of fluorine (-F) terminal groups. Four different pathways were identified, with probable final products involving C–Ti–O and C–C bonds. These studies provide insights into $Ti_3C_2T_x$ MXene thermal decomposition, facilitating design of functional materials [147]. Photoexcitation dynamics explore MXenes' thermal properties (Ti_3C_2, $Mo_2Ti_2C_3$, Nb_2C) via pump-probe techniques. These studies identified pronounced plasmonic effects in visible and near-infrared spectra, leading to rapid lattice temperature increase upon light excitation, observed as plasmon bleach in transient absorption measurements. Slow cooling kinetics suggest inherently low thermal conductivities in MXenes. Free carriers, particularly abundant in Ti_3C_2, limit thermal conductivity through phonon scattering. Light interaction with free electrons creates plasmons enhancing light absorption or scattering. Slow cooling kinetics imply MXenes take longer to return to original temperature after light exposure. Low thermal conductivity indicates slow heat transfer [148]. Thermal properties of $Ti_3C_2T_x$ MXene

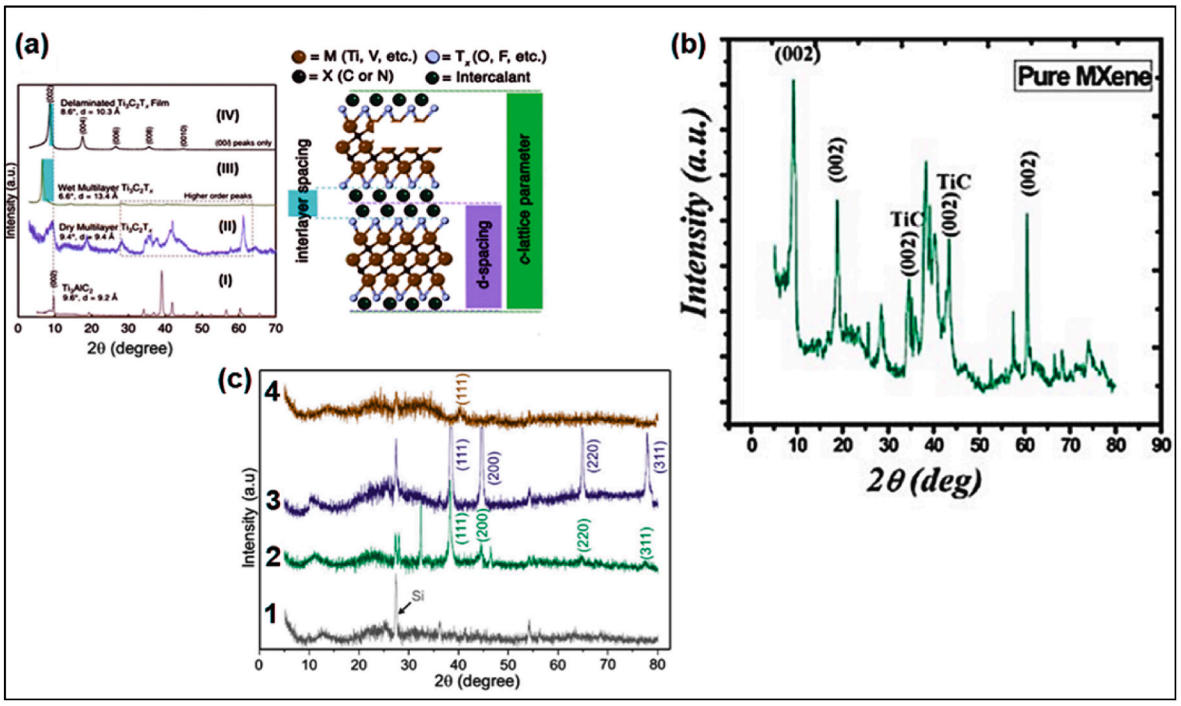

Fig. 4. (a)X-ray diffraction (XRD) spectrum of (I) Ti_3AlC_2 MAX phase, (II) dry multilayer MXene, (III) wet multilayers $Ti_3C_2T_x$ MXene, and (IV) LiCl delaminated Ti_3C_2Tx Mxene, the difference between interlayer spacing, d-spacing, and c-LP (lattice parameter) with two layers of intercalant (e.g., H_2O, Li^+ is presented in the schematics on the right side, adopted with permission [167], (b) X-ray diffraction (XRD) spectra of MXene (Ti_3C_2Tx) obtained from etched MAX powder, the peak positions and peak intensity after the etching process [170], (c) X-ray diffraction (XRD) spectra of MXene (Ti_3C_2Tx) (1) delaminated MXene nanosheets, and after hybridisation with (2) Ag, (3) Au and (4) Pd nanoparticles [168].

thin films were comprehensively analysed, including thermal diffusivity and conductivity using transient electro-thermal technique. A notable 16 % enhancement in thermal conductivity with increased temperature was observed, with phonon transport contributing significantly compared to electron transport. Molecular dynamic simulation investigated phonon thermal transport in Ti_3C_2 layer. Additionally, a room-temperature annealing process utilising electrical pulses and compressive mechanical loading significantly increased electrical conductivity while reducing void size and density [149]. MXenes exhibit high electrical conductivity, hydrophilicity, thermal stability, large interlayer spacing, tuneable structure, high surface area, and microporous structure, promising for sustainable energy technologies. To address aqueous MXene suspension limitations, Ti_3C_2-type MXene thin films are prepared from non-aqueous suspensions using a solvent exchange method, showing higher electrical conductivity from DMF-MXene layers than those from NMP, promising for hybrid photovoltaic devices as charge-transporting layers [150]. Conductive porous MXene/polyacrylamide structures were prepared via polymerising the continuous phase in oil/water high internal phase emulsions. These structures demonstrate stable electrical conductivity, suggesting suitability for research into electromagnetic interference shielding, sensing, energy storage, and catalysis. Their rapid microwave heating capabilities offer another area for practical exploration [151]. Tough, conductive, and electrochemically active fibres were fabricated using a sequential bridging strategy involving calcium cation (Ca^{2+}) infiltration of cellulose nanocrystal (CNC)-bridged MXene, resulting in fibres with record toughness and high volumetric capacitance. The fibres exhibited higher conductivity than pristine MXene counterparts, promising for wearable electronics and energy storage devices [152]. An anhydrous etching solution for $Ti_3C_2T_x$ MXene synthesis enhanced production yield and quality, achieving high electrical conductivity and exceptional mechanical strength. A novel nanosheet/organic superlattice construction method significantly improved MXene's electrical conductivity and thermoelectric performance. These advancements open possibilities for developing flexible thermoelectric modules [153]. An ultra stretchable, high-conductivity MXene-based organohydrogel (M − OH) for wearable electronics exhibited remarkable stretchability and conductivity. Its demonstrated use in high-sensitivity human health monitoring and object recognition suggests potential exploration in personal healthcare, human-machine interfaces, and artificial intelligence [154]. MXene transparent conductive films, fabricated through a transfer process, exhibited significantly higher electrical conductivity than conventionally spray-coated samples, with control over transparency and conductivity achieved by adjusting MXene material amount [155]. X-ray diffraction (XRD) is fundamental for MXene characterisation, offering insights into crystal structure, phase purity, and modifications [156]. Shifts in XRD (002) peak indicate alterations in interlayer spacing, crucial for understanding MXene processing [157–159]. Time-resolved operando X-ray reflectivity during cyclic voltammetry provided dynamic structural responses of Ti_3C_2 MXene, offering insights into electrochemical ion intercalation mechanisms [160]. Treatments using NaOH render MXenes ion-exchangeable, facilitating delamination. Structural analysis confirms Na ion intercalation, reducing van der Waals interaction between flakes [161]. First-principles calculations unveil MAX, MXA2, MXTx, and MXTxAx' structures, offering insights into charge storage mechanisms [162]. X-ray atomic pair distribution function and synchrotron radiation X-ray diffraction techniques examine MXenes' structural changes, revealing phase transformations and interlayer expansion upon solvent immersion or ion intercalation [163,164]. Small-Angle Neutron Scattering (SANS) characterises Ti_3C_2 MXene nanosheets, determining thickness and interstacking layer gaps, crucial for understanding MXene morphology [165]. X-ray techniques serve as potent tools for studying atomic and elemental information within MXenes. This capability enables researchers to examine and understand the material's structure and composition. X-ray diffraction, for instance, elucidates structural transformations during delamination and intercalation, which are essential processes for MXene synthesis [166]. X-ray diffraction spectra reveal structural alterations during

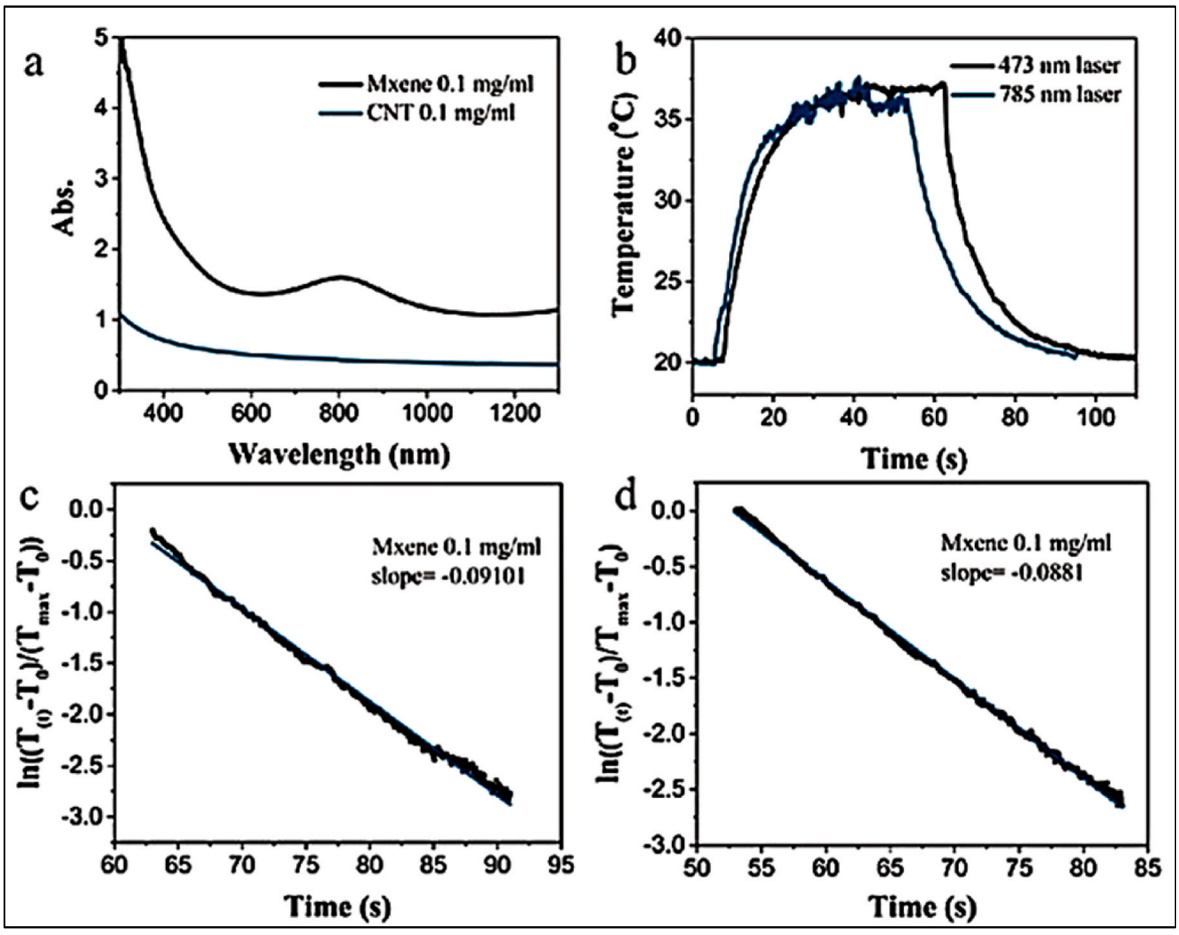

Fig. 5. The light-to-heat conversion performance of MXene and CNT solutions. Panel (a) UV–vis–NIR absorption spectra of both solutions at a mass concentration of 0.1 mg/mL. The broad absorption spectrum of MXene in the visible and NIR regions is evident, while CNTs exhibit a narrow absorption peak in the NIR region, (b) to (d) Time-dependent temperature profile of a droplet containing 0.1 mg/mL MXene during light-to-heat conversion experiments with two separate laser irradiations [179].

MXene processing, hybridisation, and modification, providing critical insights for material design and engineering [167,168]. Fig. 4a illustrates that XRD spectra reveal structural transformations during delamination and intercalation of MXene [169]. Additionally, Fig. 4b demonstrates the shift in peak position after the removal of aluminium, which signifies changes in MXene's interplanar distance and crystallinity [167]. Fig. 4c shows X-ray diffraction (XRD) spectra after hybridisation with silver (Ag), gold (Au), and palladium (Pd). This confirms successful hybridisation and offers insights into the process [168].

Absorption spectroscopy, particularly in the UV–Vis range, provides valuable insights into the electronic structure and optical properties of MXenes [171]. Within the UV/Visible spectrum (210–900 nm), light absorption prompts transitions between electronic energy levels, revealing critical details about MXene's electronic structure [37,172]. UV–Visible absorption spectra serve as a window into MXenes' optical properties, shedding light on their light absorption and emission characteristics, while also aiding in monitoring changes in their oxidation state, crucial for stability assessment [38]. For example, a study conducted UV–Vis analysis of $Ti_3C_2T_x$ MXene under various conditions, uncovering insights into its stability and concentration. The normalised absorbance of $Ti_3C_2T_x$ at 760 nm correlated with the relative concentration of MXene flakes [37]. This technique enables real-time monitoring of redox processes, offering insights into distinct charge storage mechanisms in MXenes [173]. Observable changes during oxidation include a decrease in MXene flake size and concentration in solution, along with a narrowing of the prominent UV absorption peak and a decrease in intensity in the NIR region. Furthermore, UV–Visible spectroscopy detects oxidation state changes by observing the MXene solution's colour transition from dark green or black to white TiO_2 solution, facilitating the monitoring of conductivity changes in MXene films [174]. MXenes exhibit strong UV absorption due to the presence of transition metal atoms, with specific absorption peaks indicating the bandgap of oxidised MXene [37,175]. Notably, specific absorption peaks in the visible region of MXene spectra may suggest defects or impurities within the material. For instance, a study on a fractal metamaterial solar absorber reported dual-band absorption over 80 % (400–1500 nm) and a narrow 100 % absorption peak in the visible range. These properties can lead to further investigations into their usefulness for sensing [176]. UV–Vis characterisation further elucidates MXenes' energy levels. This understanding is crucial for predicting their behaviour in various settings. For instance, Ti_2N MXene quantum dots displayed efficient photoluminescence (maximum quantum yield of 7.5 %) when excited by deep UV light (400-230 nm), suggesting potential avenues for exploration [177]. Additionally, MXenes demonstrate remarkable light-to-heat conversion efficiency, as illustrated in Fig. 5 [178]. Fig. 5 (a) displays UV–vis–NIR absorption spectra of both solutions at a mass concentration of 0.1 mg/mL. The broad absorption spectrum of MXene in the visible and NIR regions is evident, while CNTs exhibit a narrow absorption peak in the NIR region. Fig. 5 (b)–(d) depict the time-dependent temperature profile of a droplet containing 0.1 mg/mL MXene during light-to-heat conversion experiments with two separate laser irradiations [179].

Fourier-transform infrared (FTIR) spectroscopy stands out as a powerful analytical tool for characterising functional groups on MXene

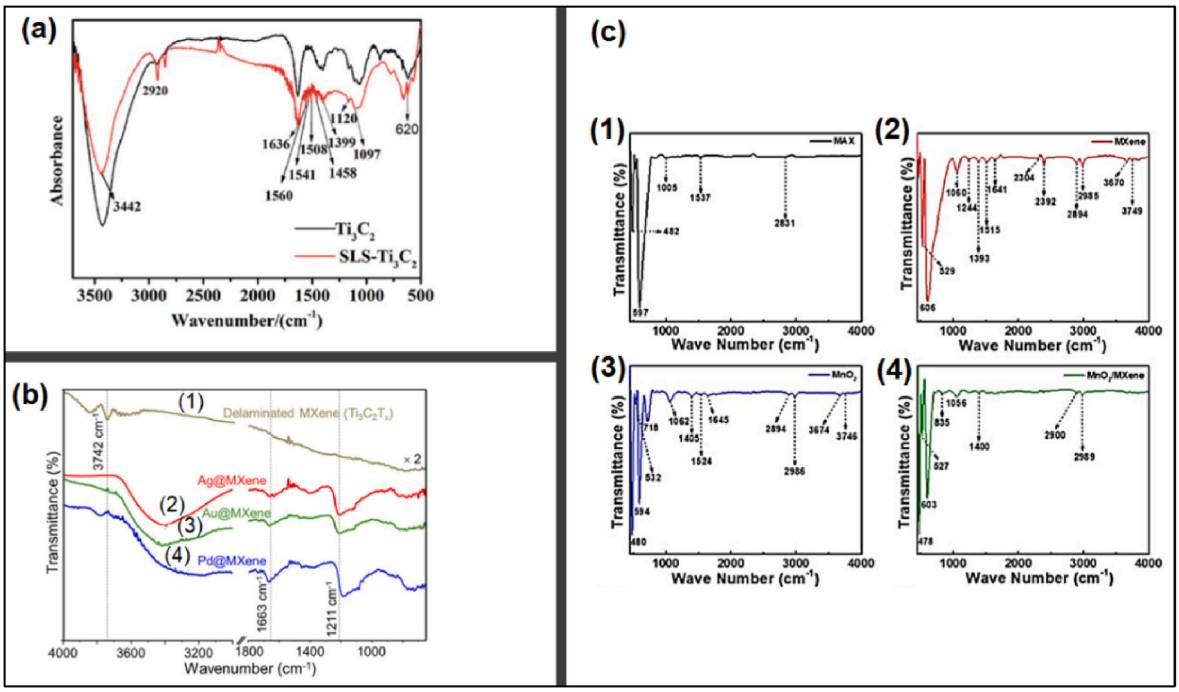

Fig. 6. (a) The FTIR spectra of $Ti_3C_2T_x$ with and without sodium lignin sulfonate (SLS) functionalisation [188], (b) The ATR-FTIR spectroscopy (1) delaminated MXene nanosheets (Ti_3C_2Tx), as well as (2) Ag@, (3) Au@, and (4) Pd@MXene hybrids [181], (c) The Fourier-transform infrared (FTIR) spectra of (1) MAX powder, (2) exfoliated MXene, (3) MnO_2 nanowires (NWRs), and (4) MnO_2/MXene composite [187].

surfaces. It identifies characteristic vibrations of chemical bonds within the infrared spectrum, corresponding to specific functional groups such as –OH, –O, and –F. Each functional group exhibits distinct absorption frequencies, enabling precise identification and quantification. Additionally, FTIR spectroscopy plays a crucial role in analysing MXene's surface chemistry, often terminated with functional groups like –O, –OH, and –F, providing invaluable insights into their surface properties. Moreover, it aids in monitoring chemical modifications, such as intercalation processes, with changes in spectra signalling successful intercalation events [104,180]. Analysing FTIR spectra differentiates groups like –OH, –O, and –F in various MXene samples [181]. For example, in $Ti_3C_2T_x$ MXene, peaks near 3430 cm^{-1}, 1620 cm^{-1}, and 1070 cm^{-1} indicate O–H stretching, H–*O*–H bending, and C–O stretching, respectively [104]. Hydroxyl groups (OH) typically exhibit a broad peak around 3400 cm^{-1} due to O–H stretching, while Ti–*O*–Ti bending manifests as a peak near 600 cm^{-1}. FTIR spectroscopy further aids in determining the presence of functional groups based on their characteristic absorption frequencies. For instance, alcohols, carboxylic acids, and primary amines exhibit O–H stretching within a broad range around 3400–3750 cm^{-1}, with alcohols displaying a stronger and broader peak compared to carboxylic acids. Alkanes, alkenes, and aldehydes exhibit C–H stretching, with slight variations in frequency. Ketones show a strong C=O stretching band around 1640–1680 cm^{-1}, affected by conjugation. Carboxylic acids also exhibit C=O stretching in a similar range, influenced by O–H stretches. Moreover, ethers, esters, amines, and nitro compounds demonstrate characteristic stretching bands within distinct frequency ranges [104,182–184]. FTIR spectroscopy not only elucidates MXene's composition but also reveals surface functional groups influencing electronic, optical, and chemical properties, aiding in identifying contaminants or substances interacting with MXene [177, 182,184]. Particularly useful for studying nanoparticles @MXene hybrids, FTIR analysis offers insights into hybrid functional groups formed [185,186]. Fig. 6a illustrates FTIR spectra of (1) delaminated MXene (Ti_3C_2Tx), along with (2) Ag@MXene, (3) Au@MXene, and (4) Pd@MXene hybrids, highlighting functional groups and modifications resulting from hybridisation. Fig. 6b provides a comprehensive FTIR analysis of MXene composition, encompassing surface functionalities and adsorbed substances. Fig. 6c displays FTIR spectra of (1) MAX powder, (2) exfoliated MXene, (3) MnO_2 nanowires (NWRs), and (4) MnO_2/MXene composite, illustrating FTIR's ability to distinguish materials and composite formation [181,187].

MXene materials possess a variety of morphological and structural features. Microscopy techniques like scanning electron microscopy (SEM) and transmission electron microscopy (TEM) are instrumental in exploring these features in detail [189,190]. Fig. 7 illustrates these properties and demonstrates how synthesis conditions can impact MXene characteristics [191]. Fig. 7a depicts that increasing the LiF and HCl molar ratio during synthesis promotes larger $Ti_3C_2T_x$ MXene flakes. In Fig. 7b and c, SEM (cross-sectional view in 7b) and TEM (12c) images reveal well-stacked flakes in various Ti3C2Tx-based films, including both pure MXene and SA composite films. Moreover, SEM and EDX analysis confirm the successful delamination of the Al layer from the V_4AlC_3 MAX phase and the formation of multilayered 2D V_4C_3Tx MXene, as shown in Fig. 7d. TEM plays a vital role in understanding the microstructure and crystallography of MAX phases. Fig. 7e highlights the application of TEM imaging and diffraction techniques (CBED and SAED) in characterising the Ti_3AlC_2 MAX phase [190]. Low-resolution TEM reveals distinct features, while high-resolution imaging demonstrates layering along [0001]. Diffraction patterns aid in determining point groups and crystal structures.

Raman spectroscopy plays a crucial role in confirming the successful conversion of a MAX phase (such as Ti_3AlC_2) to MXene (Ti_3C_2Tx). Specific spectral changes indicate the removal of Al layers and shifts in vibrational modes due to increased interplanar distance [193]. Moreover, Raman analysis ensures the retention of MXene's hexagonal structure post-synthesis and aids in monitoring impurities. It provides valuable insights into the functional groups present on MXene surfaces. This information is essential for understanding MXene properties and ensuring the quality of the synthesis process [194,195]. In Fig. 8a, Raman spectra for $Ti_3C_2T_x$ and the MAX phase depict changes following aluminium removal. The range of 230–475 cm^{-1} signifies the presence of functional surface species (Tx), while the 530–750 cm^{-1} range

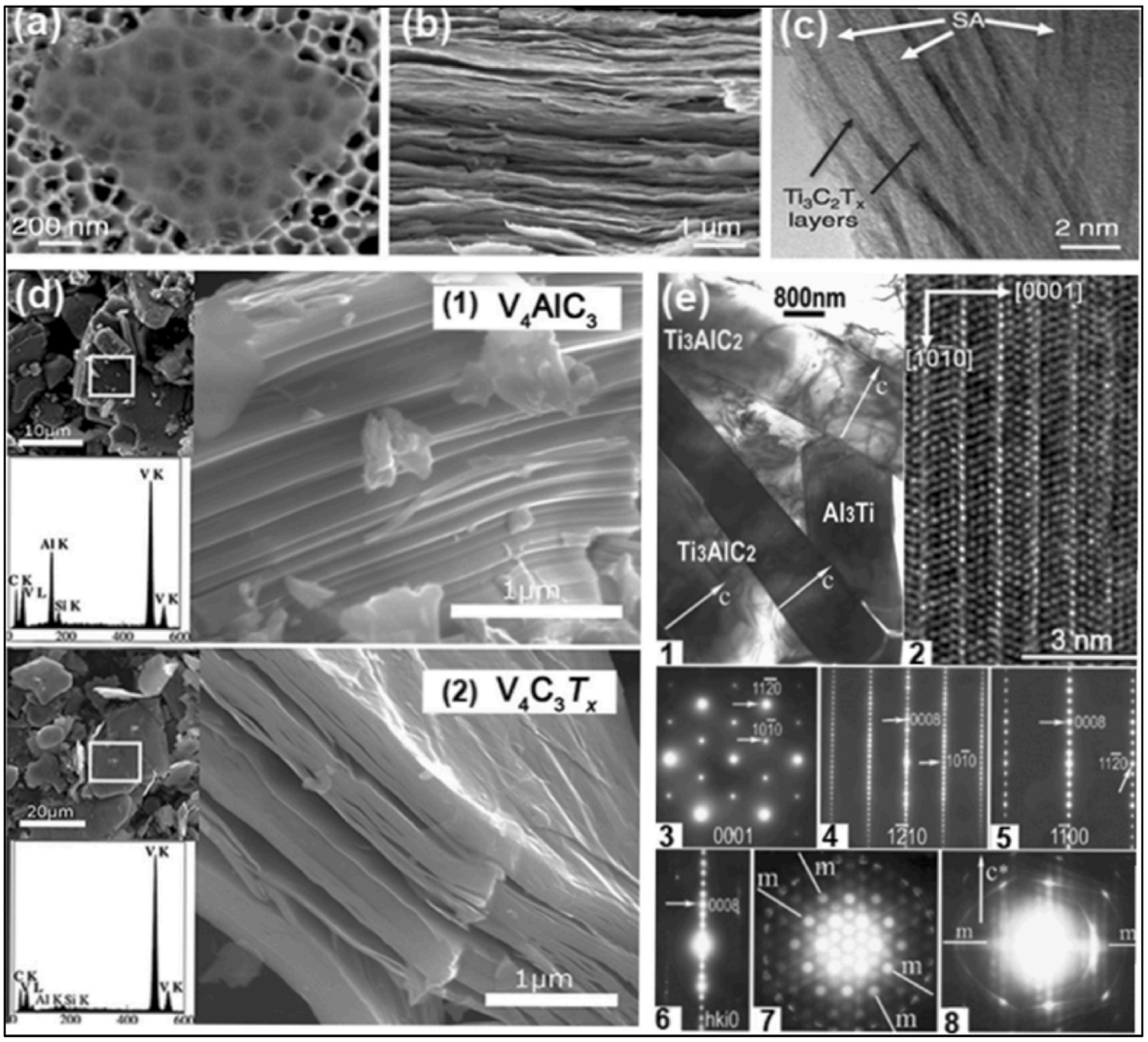

Fig. 7. Microscopy images of exfoliated MXene and its composite films, (a) SEM images of the exfoliated MXene flake, (b-c) show cross-sectional SEM and TEM images of the Ti_3C_2Tx MXene film and $Ti_3C_2T_x$ eSA composite film [192], (d) SEM imaging and EDX confirm the layered structure of MAX phase (V_4AlC_3) and successful Al layer removal, forming multilayered 2D MXene (V_4C_3Tx), insets in panels (1) and (2) indicate the location of EDX analyses [190], (e) TEM images of the polycrystalline Ti_3AlC_2 MAX phase and HRTEM images of the Zr_3AlC_2 MAX phase. SAED patterns (3–5) and CBED patterns (6–8) provide structural details [190].

corresponds to carbon vibrations [196]. Peaks in this region indicate the existence of functional groups attached to a graphene oxide layer. Through Raman analysis, insights into material behaviour, including its effects on GNO, rGNO, and carbon fabric, can be gained. Transitioning to Fig. 8(b–c), it illustrates the GN coating on MC and elucidates how MXene, graphene-flake (GN), and polymers interact in MGNC and MGNOC composites. The fabric coatings GN, GNO, and rGNO are denoted as GNMC, GNOMC, and rGNOMC, respectively. Conversely, the MXene-graphene-coated fabric, MXene-graphene composite, and MXene-graphene oxide composite are represented as MGNMC, MGNC, and MGNOC, respectively [197].

Extensive research has delved into the optical properties of MXenes, exploring their transparency, absorption, and wavelength-dependent behaviours. Studies have scrutinised the reflectivity, absorption spectra, and energy loss functions of MXenes such as Ti_2C, Ti_3C_2, Ti_2N, and Ti_3N_2. Notably, these materials exhibit strong plasmon resonances, with plasmon energies spanning from 10.00 eV to 11.62 eV (e.g., Ti_2C: 10.00 eV, Ti_3C_2: 10.81 eV, Ti_2N: 11.62 eV, Ti_3N_2: 11.38 eV) [171]. Additionally, MXenes manifest high reflectivity (~100 %) at energies below 1 eV [198–200]. Particularly, MXenes, notably $Ti_3C_2T_x$, demonstrate remarkable transparency in the visible spectrum when fabricated into thin films. Transmission rates per nanometre thickness approach those of single-layer graphene, especially for V_2CT_x [201,202]. The absorbance capacities of MXenes can vary depending on the wavelength and through intercalation with organic molecules or cations [198,201,203]. Intriguingly, MXene films etched with NH_4HF_2 exhibit enhanced transparency compared to HF-etched films [198]. Furthermore, inorganic molecules, such as Tetramethylammonium hydroxide (TMAOH), can enhance the transmission of $Ti_3C_2T_x$ thin films [201]. MXenes' distinctive combination of high electrical conductivity, extensive surface area, and optical properties suggests their value in various research fields. Their two-dimensional morphology facilitates rapid ion diffusion, enhancing their electrochemical activity. Additionally, their large surface areas make MXenes promising materials for research into catalysis. MXenes' selective and sensitive responses to adsorbed molecules highlight their exploration in the field of sensing [204,205]. Research into the dielectric, optical, and magnetic properties of MXenes seeks to optimise their composition and structure, driving advancements in synthesis and processing techniques [206].

3. MXene-based 2D heterostructures: design by stacking

The discovery of graphene ignited rapid advancements in the field of two-dimensional (2D) materials, providing a blueprint for exploring a

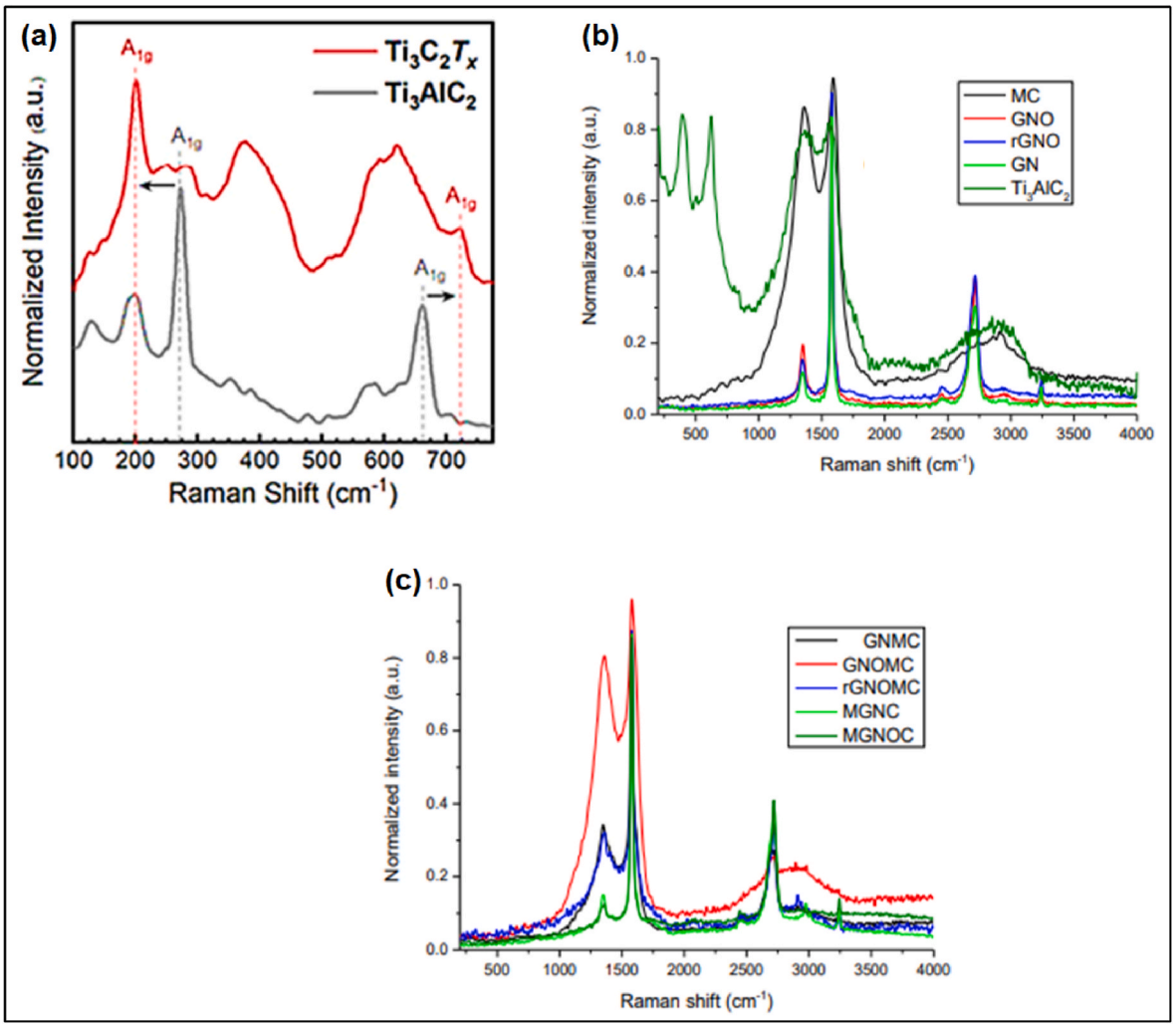

Fig. 8. (a) The Raman spectra of Ti_3C_2Tx MXene and Ti_3AlC_2 MAX phases, excited at 633 nm and 532 nm, respectively [196], (b) Normalised Raman spectra of MXene, MC, GN, GNO, rGNO, and (c) Normalised Raman spectra of MXene composites [197].

wide range of novel 2D materials [207]. Notable among these are transition metal dichalcogenides (TMDCs). These materials exhibit remarkable electron mobility, making them a subject of extensive research for their ability to form heterostructures with interesting properties [208]. Heterostructures, composed of multiple 2D materials layered together, are often fabricated using techniques such as mechanical exfoliation to produce thin films, ribbons, flakes, or sheets on substrates [209]. Substantial progress has been achieved in large-scale graphene synthesis by combining mechanical exfoliation with vapor deposition or epitaxial growth. Additionally, van der Waals epitaxy allows for the controlled growth of one 2D material on top of another, enabling precise stacking [210]. Two-dimensional (2D) heterostructures offer desirable properties such as malleability, translucency, and high surface area, making them valuable for electronics and catalysis. However, a key challenge lies in developing low-temperature growth methods to enable the creation of high-density field-effect transistor

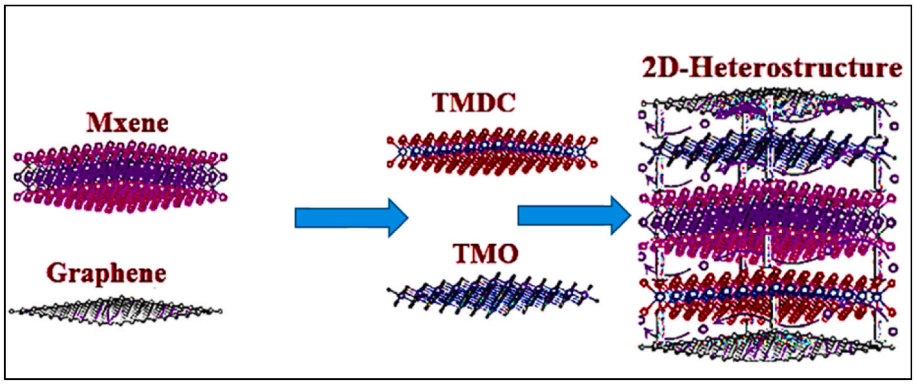

Fig. 9. Graphical representation of unique heterostructures involving Graphene, TMDC, TMO, and MXene.

(FET) circuits. Integrating these materials with silicon, implementing clean transfer techniques, dielectric film deposition, and uniform metal contacts are crucial for circuit fabrication. Scalable synthesis techniques are particularly important for Back-End-of-Line (BEOL) processes, essential for commercialising these 2D heterostructures [211]. Field-effect optoelectronics (FEO) is a rapidly developing area where van der Waals (vdW) 2D heterostructures play a central role. Understanding 2D heterostructures fields requires delving into synthesis methods like mechanical exfoliation, chemical vapor deposition, and van der Waals epitaxy, each with its unique strengths and limitations [212]. Additionally, 2D heterostructures play a pivotal role in the development of photodetectors [213]. For instance, research into MoS_2-WS_2 heterostructures focuses on optimising light-matter interactions for optoelectronics [214]. Integrating 2D heterostructures into ultrathin devices expands photodetection possibilities. For example, a lateral Gr-WS_2-Gr photodetector uses monolayer WS_2 as a semiconductor and graphene as electrodes, allowing for tuneable photoresponsivity and insights into contact engineering for 2D optoelectronics [215]. MoS_2/graphene photodetectors exhibit exceptional broadband performance across the visible spectrum [216]. Beyond photodetection, 2D heterostructures are explored for their potential in memory, sensing, and flexible electronics. Rewritable optoelectronic switches using graphene-on-MoS_2 heterostructures demonstrate both optoelectronic functionality and charge retention [217]. In biosensing, graphene/MoS_2 heterostructures enable DNA detection, while graphene/WS_2/hBN and BP/$MoSe_2$ structures provide sensitive and dynamic gas detection for pollutants like NO_2 and NH_3 [218]. Flexible electronics advance with the incorporation of 2D materials grown via chemical vapor deposition and exfoliation techniques. Although understanding the mechanical behaviour of 2D heterostructures under strain remains a challenge, the opportunity for scalable production and exploration of novel phenomena drives continuing research in this field [219]. MXene-based 2D heterostructures are engineered by stacking individual monolayer 2D materials layer-by-layer, leveraging strong intralayer covalent bonds and relatively weak interlayer van der Waals (vdW) interactions. This stacking approach circumvents the lattice matching constraints of the materials. Two primary methods for assembling these heterostructures are direct growth and mechanical transfer [220]. For example, MXene/graphene heterostructures have been fabricated by alternately stacking $Ti_3C_2T_x$ MXene and reduced graphene oxide (rGO) nanosheets via spray-assisted layer-by-layer assembly [221]. In another instance, Cr_2C and Cr_2N MXenes were stacked to create 2D heterostructures. Two stacking configurations were explored: Cr_2C atop Cr_2N, and vice versa. These heterostructures combine the advantages of each constituent, potentially yielding performance enhancements surpassing those of individual MXenes [220]. While promising, unintentionally induced strain during growth becomes significant in vertical superlattices. Hence, comprehending the structure, common fabrication methods, and potential uses of MXene-based heterostructures is crucial for their effective development [221]. Optimising MXene-based heterostructures involves several key strategies. Carefully selecting complementary materials to combine with MXenes is essential for tailoring the properties of the resulting heterostructure [222]. The choice of synthesis method significantly impacts the properties of the heterostructure. Techniques like layer-by-layer assembly enable the creation of MXene/graphene heterostructures with enhanced performance [221]. Modifying MXene properties through intercalation and delamination processes, involving the insertion or separation of layers, respectively, can be effective [223]. Chemical modification of MXene surfaces can improve their properties. Strategies such as surface-initiated polymerisation and single heteroatom doping are frequently explored for this purpose. Tailoring the design of the heterostructure, such as employing core-shell architectures, can further optimise performance. This optimisation has particular relevance in capacitor development [221]. Additional treatments post-synthesis, like annealing or chemical processes, can further enhance the properties of MXene-based heterostructures [224]. By strategically applying these methods, researchers tailor MXene-based heterostructures for various fields, including gas sensing, energy storage, and catalysis. This tailoring is made possible by the exceptional electrochemical, electronic, optical, and mechanical properties achieved in these materials [222,223]. MXene/Graphene heterostructures, created by stacking $Ti_3C_2T_x$ MXene and reduced graphene oxide (rGO) nanosheets, show significant potential for gas sensing research and development. The alternating layers provide unique properties that can enhance sensing performance [221]. In MXene heterostructures, researchers have explored novel 2D configurations. These structures combine the properties of both materials, suggesting potential research avenues in fields ranging from electronics to catalysis [220]. In Porphyrin-Based Covalent Organic Framework (Por-COF)/MXene Heterostructures, vertically grown porphyrin-based covalent organic framework nanosheets on modified MXene surfaces demonstrate enhanced capabilities for efficient electrocatalytic CO_2 reduction reactions. This research suggests a promising approach within the field of sustainable energy technology [225]. MXene-based heterostructures exhibit high conductivity and large surface area, making them promising candidates for energy storage in supercapacitors. These heterostructures are utilised in sensor development, particularly in gas sensors, due to their high sensitivity and selectivity [222]. MXene-based heterostructures are employed in battery technology as electrode materials, benefiting from their excellent electrochemical properties [221]. MXene heterostructures are actively explored for their potential in photocatalysis, such as water splitting and pollutant degradation, due to their

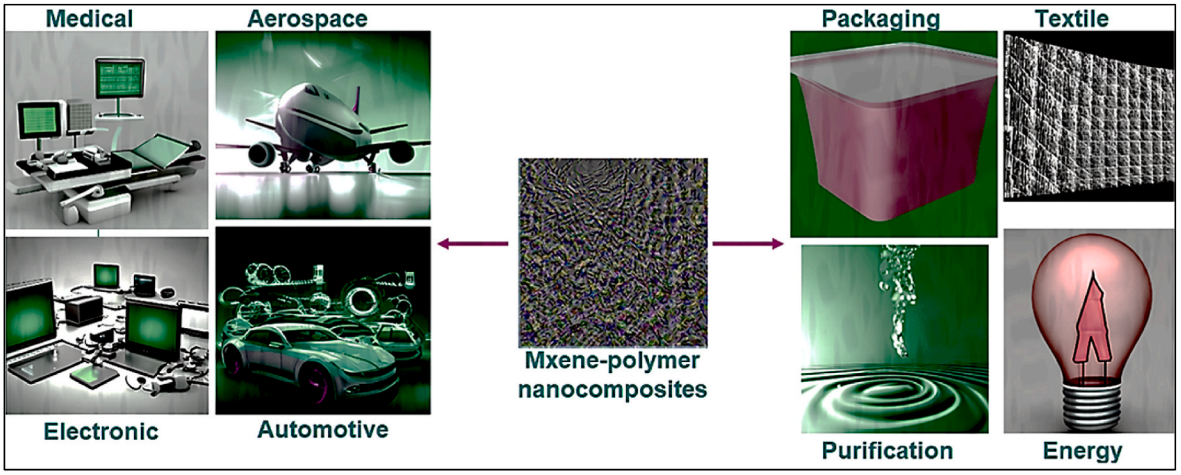

Fig. 10. Application of MXene and MXene-based composite materials.

Table 2
The combination of Mxene -combination with polymers.

Materials and Methods (Nanocomposites)	Key Findings	Explanation & References
Epoxy/ $Ti_3C_2T_x$	Enhanced thermal conductivity, glass transition temperatures, and stability	$Ti_3C_2T_x$ offers improved heat transfer, increased glass transition temperature, and enhanced material stability [237].
PVC/Mxene	Enhances thermal stability; Hinders volatile product evolution at high temperatures	Mxene improves PVC's resistance to thermal degradation, preventing volatile product release even at high temperatures [238].
MXene/PVA multilayered films	23-fold increase in thermal conductivity	Multilayered structure with MXene provides numerous thermal pathways, resulting in a significant increase in thermal conductivity [239].
MXene/PDMS	Threefold increase in thermal conductivity	MXene dispersion within PDMS forms conductive pathways, leading to a substantial enhancement in thermal conductivity [240].
MXene/PEO	Improved thermal stability	$Ti_3C_2T_x$ strengthens the PEO matrix, increasing its resistance to thermal degradation [241].
$Ti_3C_2T_x$ in epoxy nanocomposites	Reduced nylon-6 permeability by 94 %; Enhanced CO_2/N_2 selectivity	Functionalisation of $Ti_3C_2T_x$ reduces nylon-6 permeability and enhances CO_2/N_2 selectivity in membranes [242–245].
$Ti_3C_2T_x$ grafted to PIPD fibres	Improved barrier properties; Enhanced interfacial shear strength	Grafting $Ti_3C_2T_x$ onto PIPD fibres enhances barrier properties and interfacial shear strength [246,247].
MA-grafted PP $Ti_3C_2T_x$ Nanocomposites	Increased storage modulus and tensile strain to failure	MA grafting improves interfacial adhesion, enhancing mechanical properties [248].
Melt processing	MXene sheets evenly dispersed; Highest improvement for elastomeric MXene nanocomposites	Melt processing ensures uniform dispersion of MXene sheets, leading to the highest reported improvement in mechanical properties [238,249].
Solvent-based approach	Remarkable gain in composite moduli; Best results reported for elastomeric MXene nanocomposites	Solvent-based approach facilitates thorough mixing of MXene with elastomers, resulting in remarkable improvement in mechanical properties [249].
MXene-filled elastomers	Pronounced mechanical reinforcement	MXene reinforces elastomers, improving their mechanical strength and stiffness [250].
Neat Ti3C2 MXene	Young's modulus measured at 333 ± 30 GPa; Lower experimental values due to surface functionalisation and defects	Neat Ti_3C_2 MXene exhibits high Young's modulus, though lower than theoretical values due to surface functionalisation and defects [31].
PAM/MXene nanocomposites	Improved electrical conductivity; Temperature dependence observed	Adding MXene to a PAM matrix increases electrical conductivity, though resistance measurements show some temperature dependence [251].
PDMS/MXene nanocomposites	Enhanced EMI shielding performance; Improved electrical conductivity and mechanical properties	Adding MXene to a PDMS matrix offers improved EMI shielding, increased electrical conductivity, and stronger mechanical properties [252].
PP/MXene nanocomposites	Improved EMI shielding effectiveness	Adding MXene to a PP matrix improves its EMI shielding effectiveness [253].
PEI/MXene nanocomposites	Enhanced thermal stability and conductivity	MXene modifies a PEI matrix, improving its thermal stability and conductivity [254].
$Ti_3C_2T_x$ in epoxy resin	Increased electrical conductivity; Formation of conductive network in epoxy matrix	$Ti_3C_2T_x$ addition promotes the formation of a conductive network within the epoxy matrix, leading to increased electrical conductivity [255].
$Ti_3C_2T_x$ in PVDF matrix	Enhanced electrical conductivity; MXene incorporation enhances conductivity in various polymer matrices	MXene increases electrical conductivity in PVDF, demonstrating its potential for enhancing conductivity in other polymer matrices [256].
$Ti_3C_2T_x$ in annealed epoxy resin	Improved electrical conductivity and EMI shielding effectiveness; Removal of polar functional groups through annealing enhances conductivity	Annealing removes polar functional groups from $Ti_3C_2T_x$, improving electrical conductivity and EMI shielding effectiveness in epoxy resin [257].
3D $Ti_3C_2T_x$ aerogel/epoxy nanocomposites	Enhanced electrical conductivity and EMI shielding effectiveness; Successful preparation of three-dimensional MXene/epoxy composites via crosslinking	Three-dimensional structure enhances electrical conductivity and EMI shielding effectiveness, achieved through successful crosslinking of MXene/epoxy composites [258].
Ti3C2Tx as additive in PVDF-based composites	Increased dielectric constant with low dielectric loss; Enhanced dielectric properties attributed to MXene sheets' contribution to dipole-dipole interaction and interfacial polarisation	MXene addition increases dielectric constant while maintaining low dielectric loss in PVDF-based composites, attributed to MXene's role in dipole-dipole interaction and interfacial polarisation [259,260].
Ti3C2Tx in PVA matrices	Improved dielectric properties; Good dispersion state and nacre-like structure of polymer nanocomposites	Adding MXene to PVA matrices enhances their dielectric properties, thanks to good dispersion and a nacre-like structure [261].
PVA/V2C MXene composites	Enhanced dielectric properties with excellent interfacial compatibility; Improved permittivity values and low interfacial leakage current	MXene's excellent interfacial compatibility with PVA improves dielectric properties, increasing permittivity and reducing interfacial leakage current [262].
(PVDF)/V2C–TiO2 composites	Improved dielectric response with hybrid filler; Mechanisms induced by Fermi-level overlapping and dipole enhancement contribute to enhanced dielectric response	Hybrid filler of V_2C–TiO_2 improves dielectric response in PVDF, attributed to mechanisms involving Fermi-level overlapping and dipole enhancement [263].
MXenes in SPEEK polymer materials	Enhanced proton transport capabilities; Shortened proton hopping distance due to H-bonding network	Sulfonated Poly (ether ether ketone) with MXenes exhibits enhanced proton transport due to a shortened hopping distance facilitated by a hydrogen-bonding network [264].
Sulfonated $Ti_3C_2T_x$ MXene in Sulfonated-PEEK	Increased proton transport capabilities; Enhanced transport under anhydrous conditions	Sulfonated $Ti_3C_2T_x$ MXene incorporation into Sulfonated-PEEK enhances proton transport capabilities, particularly under anhydrous conditions [265].

established photocatalytic properties [222,223]. Achieving optimal sensitivity and selectivity towards specific gas analytes while dealing with complex gas mixtures in real-world environments poses a challenge [226]. MXenes encounter issues such as low sensitivity, poor selectivity, base-resistance drift, and poor environmental stability. Addressing these challenges is crucial for enhancing their overall performance [227]. The stacking phenomenon in MXenes hampers carrier diffusion in the vertical direction, potentially leading to reduced specific capacity under high current densities. Poor oxidation resistance of MXenes can affect their conductivity and cycling stability, posing challenges for their use in various settings, particularly flexible batteries dependent on water-based electrolytes [221]. Ensuring stability in physiological environments, controlled release of drugs, and biodegradability are critical challenges researchers must address when developing MXene-based materials for biomedical use [228]. Addressing these challenges requires focused strategies and interdisciplinary approaches. Researchers are actively investigating solutions to fully realise the capabilities of MXene-based heterostructures. Improving stability is essential for

enhancing their performance and longevity across various fields of research. Using high-quality starting materials, particularly the parent MAX phase, is crucial for obtaining stable MXenes and MXene-based heterostructures. Careful control of impurities and defects during synthesis significantly impacts their stability [37]. Fine-tuning the chemical etching process is essential for controlling the oxidation kinetics of MXenes. By adjusting parameters such as etchant concentration, temperature, and duration, researchers can optimise stability. Addressing defects in MXenes through passivation techniques can improve their stability. Passivation involves introducing protective layers or modifying the surface chemistry to reduce reactivity and enhance chemical stability. Maintaining MXene-based heterostructures in controlled storage conditions is crucial for preserving their stability over time. Storage in inert atmospheres or specific dispersion media can help prevent degradation and maintain performance [226]. Through these strategies, researchers have made significant strides in overcoming stability challenges and expanding the applicability of MXene-based heterostructures. This continuous exploration paves the way for the design of customised heterostructures, such as combinations of graphene-transition metal dichalcogenides (e.g., graphene-WS_2) and MXenes-transition metal oxides (Fig. 9). These tailored designs hold significant promise for advancements in various fields.

4. Applications of mxene and mxene based composites: from energy storage to catalysis and beyond

MXenes and their composites have become prominent materials due to their unique combination of physical and chemical properties. Their two-dimensional structure, rich surface chemistry, and tunability make them readily functionalisable and compatible with various materials, including polymers, metal oxides, and two-dimensional chalcogenides. These characteristics open up a wide range of research and development opportunities [229]. In various devices such as supercapacitors, batteries, and solar cells, MXenes enhance electrodes, demonstrating their value for energy storage research and development [229,230]. MXenes show promise in environmental fields like electro/photocatalytic water splitting and carbon dioxide reduction. Moreover, their hydrophilicity and selective permeability make them valuable for research into membrane-based water purification processes. The conductivity, reducibility, and biocompatibility of MXenes suggest potential for biosensing and other sensing research [230]. Furthermore, MXenes and their hybrids/composites provide effective electromagnetic interference (EMI) shielding and show promise in various biomedical research areas. Their properties contribute to the development of flexible and wearable devices [231]. MXenes possess several properties that make them valuable for various research pursuits. For instance, they surpass reduced graphene oxide in conductivity [232] and offer anisotropic conductivity, which could prove useful where directional current is required [233]. Moreover, MXenes combine conductivity and hydrophilicity, valuable for research into biosensors and energy storage [231]. Unlike graphene oxide, MXenes demonstrate stability in water and polar solvents, suggesting potential for water-related research [234]. MXene-polymer nanocomposites are actively investigated for their potential across a wide range of fields, as depicted in Fig. 10.

Titanium carbide MXene-polymer composites demonstrate enhanced stability, electrochemical activity, and sensitivity as sensing matrices [235]. Additionally, MXene/TiO_2/MoS_2 nanosheets enable the production of flexible dielectric materials with outstanding dielectric properties. Integration of Zr-MXene into thermoplastic polyurethane results in reduced flammability and enhanced mechanical properties [236]. Similar enhancements have been achieved for epoxy resins [235]. Table 2 likely provides additional examples and a comprehensive overview of these promising MXene-based composites.

4.1. Energy storage

MXenes and MXene-based composites have garnered significant attention in recent years due to their intriguing physical, chemical, mechanical, and electrochemical characteristics. They represent a novel and expansive family of 2D transition metal carbonitrides, carbides, and nitrides [266]. MXene properties are directly linked to their surface terminations and elemental compositions, resulting in a broad spectrum of characteristics. The ability to modify surface chemistry facilitates MXene composites with diverse materials (oxides, polymers, carbon nanotubes), enabling targeted properties and new research directions [109]. In the realm of energy storage, MXenes and MXene-based composites demonstrate significant capabilities. Their superior electrochemical performance and high conductivity make them compelling electrode materials [109,230]. Particularly, MXenes are being explored in sodium-ion batteries, lithium-sulphur batteries, and supercapacitors, owing to their excellent conductivity and specific surface area [229]. The exceptional characteristics of 2D MXenes, including their high

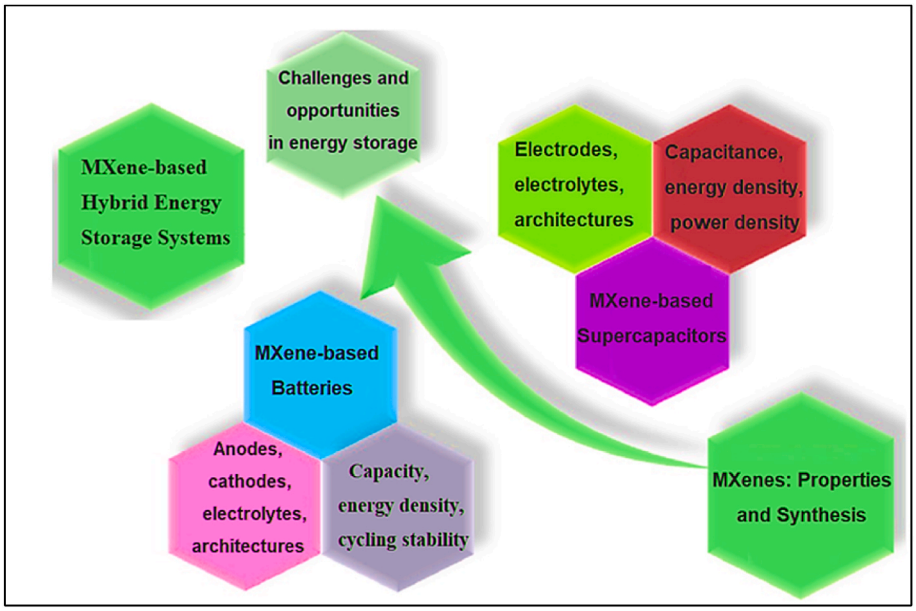

Fig. 11. Prospects of Mxene based energy storage system.

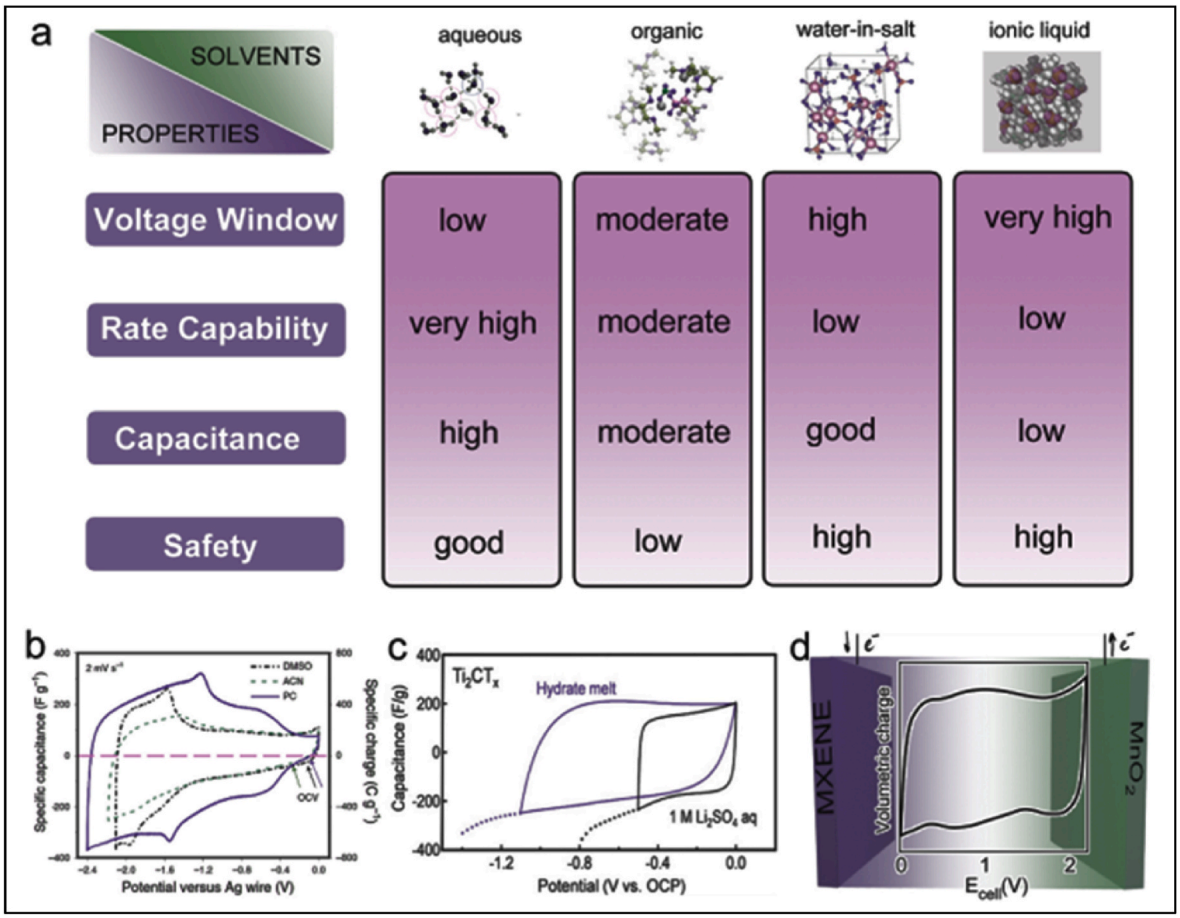

Fig. 12. The impact of solvents on MXene supercapacitors: (a) effects on performance and safety, (b) Cyclic voltammetry (CV) curves illustrating variations in chemical reactions and ion intercalation using different solvents, (c) CV curves demonstrating the effect of increasing electrolyte concentration in water, affecting voltage window and rate capability, and (d) a schematic of an MXene//α-MnO_2 asymmetric supercapacitor with an improved voltage window [274].

conductivity, large surface area, and enhanced hydrophilicity, have fuelled their adoption in energy storage devices, particularly in supercapacitors and batteries [267,268]. Supercapacitors, known for their high-power density and rapid charge-discharge rates, have seen significant advancements with the integration of MXene-based materials [269]. MXenes play versatile roles in battery technology, serving as electrodes, cathodes, or electrolytes in various battery systems, including lithium-ion, sodium-ion, and aluminium-ion batteries [270]. Hybrid energy storage systems, such as supercapacitor-battery hybrids or redox flow batteries, benefit greatly from MXenes, offering improved energy and power density, as well as cycling stability [271]. Furthermore, MXene-based energy storage solutions enhance the functionality of portable electronics and wearable devices by enabling longer battery life and faster charging for smartphones, laptops, and fitness trackers. The adaptability of MXene technology, as demonstrated by its application in aerospace, military, and medical devices, suggests significant promise for energy storage [272]. Fig. 11 illustrates various avenues of research into MXene-based energy storage systems, highlighting their potential role in shaping sustainable energy solutions.

Electrolyte strategies, such as water-in-salt and hydrate melts, are being explored to address the limitations of traditional electrolytes [273]. These unconventional electrolytes significantly broaden the electrochemical stability window, enhancing the energy density in MXene-based supercapacitors. Additionally, planar micro-supercapacitors (M-MSCs), with their interdigital architecture, offer advantages in rapid ion transport, thin device profiles, and seamless integration with on-chip electronics, aligning well with the 2D structure of MXenes [274]. The choice of solvent plays a crucial role in device performance, influencing chemical reactions and ion intercalation within MXenes. Fig. 12 provides a comprehensive overview of these effects on the overall energy density. Fig. 12a outlines the properties and trade-offs of various electrolytes and solvents, comparing different types of electrolytes (conventional, water-in-salt, etc.) based on properties such as potential window, conductivity, and viscosity. Meanwhile, Fig. 12b illustrates how the choice of solvent affects MXene interlayer intercalation and, consequently, charge storage. Different solvents used with MXene layers result in varying interlayer spacing and ion intercalation. Electrolytes like water-in-salt or hydrate melts demonstrate a wider potential window for MXene-based supercapacitors (up to nearly 1.2 V, Fig. 12c) compared to traditional electrolytes (0.6 V), potentially doubling energy density (e.g., from 20 to 45 mAh g^{-1}). Cyclic voltammetry curves compare MXene's potential window in different electrolytes. Electrolyte enables the design of asymmetric supercapacitors, where MXene serves as the negative electrode, paired with complementary positive electrode materials such as α-MnO_2. This strategy helps balance the voltage window and capacitance of the device (Fig. 12d), asymmetric supercapacitor (MXene//α-MnO_2) with electrolyte [274].

MXene-based micro-supercapacitors (M-MSCs) are gaining attention, particularly due to the adoption of the planar interdigital architecture [274]. These micro-supercapacitors demonstrate remarkable rate capability, as shown by the areal capacitance versus current density plot. Integrating 3D printing technology further enhances their specific areal capacitance. Fig. 13 shows a rigid 3D-printed M-MSC with impressive performance, as reflected in the areal capacitance plot. Specifically, Fig. 13a–(c) highlights the advantages of planar M-MSCs, such as rapid ion transport, reduced thickness, alignment with the 2D structure of

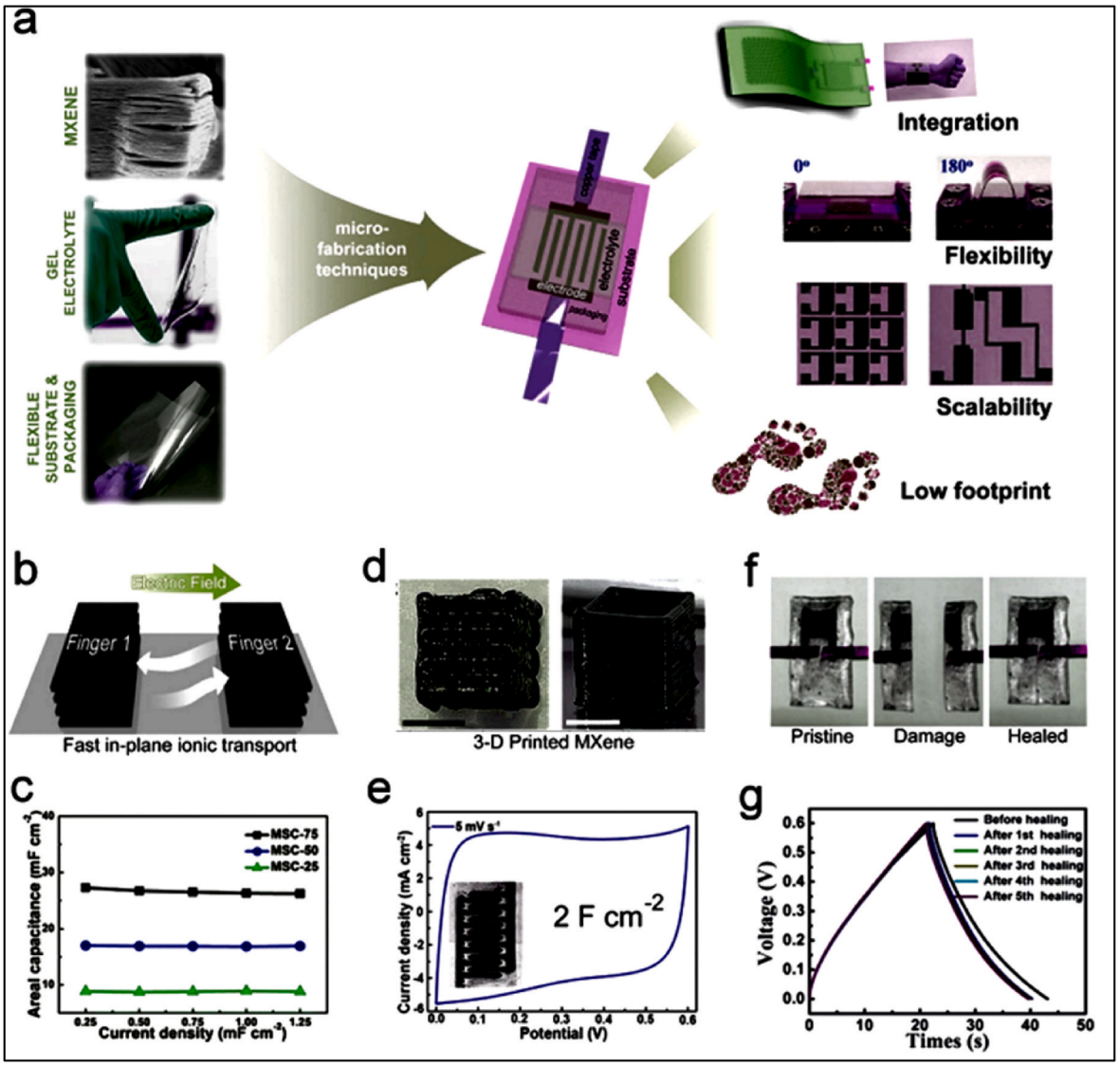

Fig. 13. (a) A schematic of the advantages of M-MSCs using the planar interdigital architecture, (b) quick ionic transport between adjacent fingers, (c) the plot of areal capacitance vs. current density highlighting the incredible rate capability of planar M-MSCs, (d-e) Thick M-MSCs made by 3D printing can offer a high capacitance of 2 F cm^{-2}, (f) self-healable MXene-graphene MSCs have been demonstrated with excellent healing efficiency, (g) Corresponding galvanostatic charge-discharge (GCD) profiles obtained at different healing cycles [274].

MXenes, and on-chip integration. These factors contribute to their exceptional performance. Fig. 13(d) and (e) illustrate the combination of MXenes with 3D printing, achieving a specific areal capacitance of 2 F cm^{-2} at 1.7 mA cm^{-2}. While challenges like breakage exist, precise alignment allows for partial electrical restoration, retaining 81 % capacitance (Fig. 13f and (g)). This highlights the need for intrinsically self-healable MXene-based electrodes to address the increase in internal resistance observed over multiple healing cycles [274].

MXene-based energy storage devices demonstrate significant capabilities, characterised by their high specific capacitance, cycling stability, and cost-effectiveness. However, certain challenges need addressing to fully realise their capabilities. Conventional electrolytes pose a limitation due to their low voltage window, and safety concerns arise with organic solvent-based electrolytes. Table 3 provides an overview of the current status, challenges, and active research directions for MXene-based energy storage devices such as supercapacitors, batteries, and hybrid systems.

4.2. EMI shielding

The increasing demand for lightweight, flexible, and multifunctional materials has fuelled the exploration of MXene-based electromagnetic interference (EMI) shielding solutions. MXenes, with their exceptional electrical conductivity, mechanical strength, and thermal management properties [289–291], have emerged as frontrunners in EMI shielding field. Researchers have developed a range of MXene composites to cater to various EMI shielding needs. Duan et al. [292] combined MXene, conductive PPy polymer, and recycled carbon felts to create porous conductive networks with high EMI shielding (60 dB) and electro-thermal capabilities, which are promising for wearables and sustainable materials. Yang et al. [293] significantly enhanced the EMI shielding of carbon fibre-reinforced poly (ether-ketone-ketone) (65.2 dB) by incorporating MXene, emphasising the importance of ohmic losses and multiple reflections in shielding mechanisms. Huang et al. [294] developed WPU/PCMC/MXene@PTA films that integrate phase change microcapsules for exceptional thermal management and EMI shielding, making them ideal for aerospace and electronics applications. Key characteristics for EMI shielding materials include high electrical

Table 3
MXene-based energy storage devices - status, challenges, and remarks.

Device Type	Status and Challenges	Remarks	Ref.
MXene in various applications	High-volumetric capacitance.	MXene's redox-active surface facilitates reversible chemical reactions, essential for energy storage and catalysis applications.	[273]
MXene-based materials	Low volumetric energy density and low-rate capability.	MXene combined with silicon offers high capacity and high-rate capability by exploiting pseudo capacitance, addressing low-rate capability challenge.	[275]
$Ti_3C_2T_x$ MXenes	Thickness-independent capacitance achieved through mechanical shearing.	Ti3C2Tx MXenes exhibit excellent rate capability and nearly thickness-independent performance up to 200 μm, highly attractive for next-gen energy storage applications.	[276]
MXene-based materials	Explored for non-Li batteries through various strategies.	Modification of MXene structures is crucial for improving specific capacity in non-Li batteries.	[276,277]
$Ti_3C_2T_x$ MXenes with cyclic voltammetry	Dynamic structure significantly influences functionality.	Two distinct charging regimes involving capacitive and non-capacitive (redox) characteristics are observed during electrochemical ion intercalation in Ti3C2Tx MXenes.	[278]
MXene-based materials	Explored for various metal-ion batteries.	Proper electrode design is critical for enhancing ion transport and electrochemical performance in various metal-ion batteries.	[279–281]
Supercapacitors	High capacitance, rate capability, low cost. Challenges: poor cycling stability, limited energy density.	Efforts focus on improving MXene stability, integrating new electrodes, and developing electrolytes.	[282]
$Ti_3C_2T_x$ in supercapacitors	Electrolytes: H2SO4 and KOH. Energy Density (Wh/kg): 27–70, Power Density (W/kg): 8000–10000.	MXene demonstrates high energy/power densities with different electrolytes.	[283,284]
Batteries	High theoretical capacity, good cycling stability. Challenges: limited rate capability, MXene conductivity.	Enhancing MXene conductivity, optimising morphology, and novel electrolytes aim to improve performance.	[285]
$Ti_3C_2T_x$ in Battery	LiTFSI in propylene carbonate. Energy Density (Wh/kg): 100–150, Power Density (W/kg): 1000-3000	MXene in battery applications offers energy density ranging from 100 to 150 Wh/kg and power density from 1000 to 3000 W/kg.	[286]
Hybrid Devices	Synergistic combination of supercapacitors and batteries. Challenges: limited understanding of MXene-electrolyte interactions.	Focus on studying MXene-electrolyte interactions and developing novel electrolytes for better performance.	[287]
MXene, (Poly (3,4-ethylenedioxythiophene) polystyrene sulfonate) as active material	Ultra-flexible interdigital Micro supercapacitor.	Retention of mesopores, fast ion transportation, and surface redox mechanism are crucial for efficient energy storage devices.	[288]

conductivity, ease of film formation, mechanical strength, and thermal stability [290]. For instance, a 45-μm $Ti_3C_2T_x$ film outperforms thicker composites due to its conductivity and internal reflections [295]. The ability to form MXene films and coatings facilitates electromagnetic interference (EMI) shielding of complex shapes [296]. MXene/cellulose films with interconnected conductive networks offer potential for research into personalised therapy and health management [296–298]. MXene/CNT films exhibit efficient Joule heating and high electromagnetic interference (EMI) shielding effectiveness (32.62 dB) [299]. Breathable MXene/textile composites offer piezoresistive sensing and EMI shielding [300]. E-textiles utilising MXene films exhibit self-reinforcement and superior shielding (50.44 dB) [301]. Table 4 summarises these innovations, including composite compositions, fabrication methods, and key EMI shielding results.

4.3. MXene -based systems and devices for advanced environmental applications

MXene nanosheets, with their large surface area and established functionalisation capabilities, have attracted significant attention for water filtration membranes [322]. Surface modifications play a crucial role in enhancing the antifouling, antibacterial, and antiviral properties of MXene-based systems [16,323,324]. Tailored MXene nanosheet-stacked films effectively remove heavy metal ions [325], while membranes with vertically oriented nanosheets offer high water permeability and efficient rejection of contaminants [19]. This strategic arrangement enhances membrane performance, offering potential for water purification research. Research highlights the capability of MXene-based membranes to address multifaceted water purification challenges [322]. Known for their mechanical and chemical stability, MXene membranes can be fabricated using various techniques such as vacuum filtration and Langmuir-Blodgett deposition. This provides flexibility in their integration into water treatment systems [326,327]. For example, MXene membranes applied to AAO substrates demonstrate significantly increased water permeability and high rejection rates [328]. Moreover, MXene's properties suggest potential for addressing broader environmental remediation challenges, with research actively exploring areas like air, water, radiation, and solid contamination [329]. While pristine MXenes show promise, challenges such as restacking, limited flexibility, and susceptibility to degradation exist. Combining MXenes with polymers provides a flexible approach for tailoring membrane properties to address these limitations and meet specific environmental remediation needs [330,331]. Fig. 14a illustrates the growth of research in MXenes and MXene-polymer hybrid membranes for environmental remediation from 2011 to the present. MXene-polymer hybrid membranes, as demonstrated in Fig. 14b, can address various environmental challenges, such as filtering contaminated water, capturing air pollutants, and treating radioactive waste.

MXene-polymer hybrid membranes provide a powerful tool for environmental remediation. They facilitate remote monitoring of contamination levels, reducing the need for manual intervention [333]. These cost-effective and energy-efficient membranes offer the potential to reduce remediation expenses [334]. Fabrication techniques such as spray coating and spin coating provide flexibility, allowing for the customisation of film properties [21]. MXene films contribute to electrochemical remediation through adsorbing contaminants from polluted water or air [335]. Their demonstrated effectiveness in removing heavy metal ions, organic dyes, waste oil, and bacteria underscores their potential for broad use in water purification [21]. Moreover, they show promise in treating oily wastewater, catalysing pollutant decomposition, and selectively filtering solvents while inhibiting bacterial growth [336]. Studies reveal the complex thermal properties of MXene-polymer composites. For example, incorporating MXene into PVA can slightly lower thermal conductivity (Fig. 15a). The MXene/PVA composite structure highlights any differences compared to pristine MXene that might cause reduced conductivity [337]. Even small amounts of MXene (<0.1 wt%) can spontaneously enhance thermal conductivity in PVDF composites (Fig. 15b), leading to increases in thermal conductivity with

Table 4
Summary of key findings from various research related to electromagnetic interference (EMI) shielding using MXene-based materials.

Materials/Methods	Key Findings	Ref.
PP-g-MA, MXene, hybrid MXene/rGO nanolayers	Improved electromagnetic interference (EMI) shielding effectiveness in hybrid cellular system	[302]
CuNWs/MXene/ANFs hybrid film	High-flexibility, mechanical properties, and outstanding EMI shielding capacity	[303]
MXene/rGO coated glass fabrics	Multifunctional aerospace composites with sensing and EMI shielding abilities	[304]
Ti_3C_2Tx MXene/GO on CF fabric	Flexible composite with improved mechanical and EMI shielding properties	[305]
MXene/carbon nanofiber composites	Homogeneous structure, enhanced EMI shielding performance	[306]
PAM@fabric device	Wearable electronic textile with pressure sensing, EMI shielding, and thermal management	[307]
MXene-reinforced carbon fibre reinforced polymer (CFRP) composite	Enhanced mechanical properties, electrical conductivity, and EMI shielding effectiveness	[308]
Sandwich-type multilayered GO@MXene films	Excellent EMI shielding performance	[309]
MXene/sodium alginate (SA) composite fibres	Continuous composite fibres with high strength and EMI shielding effectiveness	[310]
MXene/reduced graphene oxide (rGO)@poly (methyl methacrylate) (PMMA)	Tuneable thermal conductivity and superior EMI shielding performance	[311]
Graphene oxide coated Ti_3C_2Tx MXene films	Stable EMI shielding performance in humid environments	[312]
Reduced graphene oxide (rGO)/MXene film on non-woven fabric	Electromagnetic shielding electric heating device with flame retardancy	[313]
Hydrothermally treated Ti_3C_2Tx MXene composite films	Excellent mechanical properties and EMI shielding effectiveness	[314]
MXene/hydroxyapatite (HA) nanocomposite films	Outstanding mechanical performance, EMI shielding effectiveness, and thermal conductivity	[315]
Waste fly ash (FM), polyethylene terephthalate (PET) microplastics (MPs), and MXene composites	Addressing recycling problem of MPs after removal from water	[316]
Ti_3C_2Tx MXene/wood phase change materials (PMPCMs)	Superior solar-thermal conversion efficiency and flame-retardancy	[317]
Epoxy resin oligomer assisted Ti_3C_2Tx MXene spraying strategy	High effectiveness, excellent abrasion resistance, and good flame retardancy	[318]
Core–shell structured carbon nanofiber (CoC@CNF)/MXene films	Maximum EMI shielding effectiveness, high absorption capacity, fast electro-thermal conversion, and flexibility	[319]
MXene/polyaniline nanofibers (PNFs) composite films	Excellent electrical conductivity, thermal stability, and EMI shielding effectiveness	[320]
MXene/hyperbranched graphene (HG) composite films	Outstanding EMI shielding, low-voltage-driven Joule heating, and efficient photothermal conversion	[321]

varying MXene loading in PVDF [338]. Factors such as surface area, hydrogen bonding, and interfacial thermal resistance influence these effects. Additionally, the loading of MXene in composite membranes affects degradation temperature, crystallisation behaviour, and glass transition temperature (Tg). Research with LLDPE, epoxy, and MXene composites demonstrates increased degradation temperatures and changes in Tg, often attributed to restricted polymer chain mobility (Fig. 15c and d). Fig. 15c shows DMA results comparing the glass transition temperature (Tg) of epoxy membranes with different loadings of MXene. Fig. 15d depicts the changes in glass transition temperature (Tg) for the epoxy/MXene system, as shown in the differential scanning calorimetry curves [338–340].

Research shows that incorporating MXene into epoxy membranes restricts polymer chain mobility, affecting various thermal properties [338]. Dynamic Mechanical Analysis (DMA) shows that the glass transition temperature (Tg) increases as the MXene loading increases [339]. Similarly, differential scanning calorimetry (DSC) indicates a gradual increase in glass transition temperature (Tg) with the addition of Ti_3C_2 [340]. MXene-based membranes also show promising capabilities in water purification and gas separation. Compared to graphene oxide (GO) membranes, Ti_3C_2/PVDF membranes exhibit significantly higher water flux and reduced ion penetration, particularly for multiply charged ions with radii less than 4.5 Å [341,342]. Research by Ding et al. [341] highlights the exceptional gas separation properties of 2D Ti_3C_2Tx laminates, surpassing 2200 Barrer for H_2 gas permeance with an H_2/CO_2 selectivity exceeding. Notably, these laminates-maintained stability over 700 h of continuous H_2/CO_2 separation. Shen et al. [342] demonstrated similar potential, with 20 nm thick MXene nanofilms offering promising H_2/CO_2 selectivity and H_2 gas separation capabilities. This research demonstrates the efficacy of MXene membranes for hydrogen purification and CO_2 capture [343]. Fig. 16 illustrates that MXene membranes can achieve water/ion separation and/or gas separation. Fig. 16b illustrates the relationship between water flux and MXene membrane thickness. Fig. 16c shows a cross-sectional schematic of the Ti_3C_2Tx laminate used by Ding et al. [341]. Fig. 16d compares the H_2/CO_2 selectivity and H_2 gas permeance of MXene nanofilms to benchmarks in H_2 purification.

MXene-polymer hybrid membranes, with high adaptability and integration with advanced technologies, offer effective solutions for contemporary environmental challenges. Table 5 summarises active research and the significant capabilities of MXene-based membranes in environmental remediation applications.

4.4. Electrocatalysts for water splitting

Electrochemical water splitting, driven by renewable energy sources, offers a sustainable pathway for hydrogen production [362]. Driven by renewable sources like solar or wind, it represents a pathway towards environmentally friendly hydrogen generation. Both Electrolytic Cells and Electrochemical cell types involve chemical reactions (redox reactions) and the transfer of electrons, but there's a key difference. Electrolytic cells use external electrical energy to drive non-spontaneous chemical reactions. These reactions will not happen on their own and require an input of electricity to proceed. Electrochemical cells convert chemical energy into electrical energy through a spontaneous chemical reaction. These cells are used in batteries. The following reactions describe the process of water splitting, where electricity is used to break water (H_2O) into hydrogen (H_2) and oxygen (O_2). In the process of water splitting, the anode releases 4 electrons according to the equation $2H_2O \rightarrow O_2 + 4H^+ + 4e^-$, while the cathode absorbs 2 electrons as shown in $2H_2O + 2e^- \rightarrow H_2 + 2OH^-$. To ensure electron balance between the anode and cathode, the cathode reaction is multiplied by 2, resulting in $4H_2O + 4e^- \rightarrow 2H^2 + 4OH^-$. Now, both reactions involve the transfer of 4 electrons. Combining the balanced anode and cathode reactions yields the overall balanced equation for water splitting: $6H_2O \rightarrow 2H_2 + O_2 + 4H^+ + 4OH^-$. This demonstrates a fundamental principle in electrochemical reactions: the number of electrons lost in oxidation must equal the number gained in reduction to maintain charge balance. These equations represent the half-reactions that occur in the electrolysis of water. At the cathode, water gains electrons to form hydrogen gas and hydroxide ions, while at the anode, water loses electrons to form oxygen gas and hydrogen ions. Water splitting, a process pivotal in renewable energy conversion, hinges on non-spontaneous reactions necessitating an external energy source, typically electricity. This energy infusion drives the process within an electrolytic cell, where three key components orchestrate the transformation. First, electrodes, often composed of inert materials like platinum or graphite, serve as conduits for electron transfer. Second, an electrolyte solution, typically imbued with an

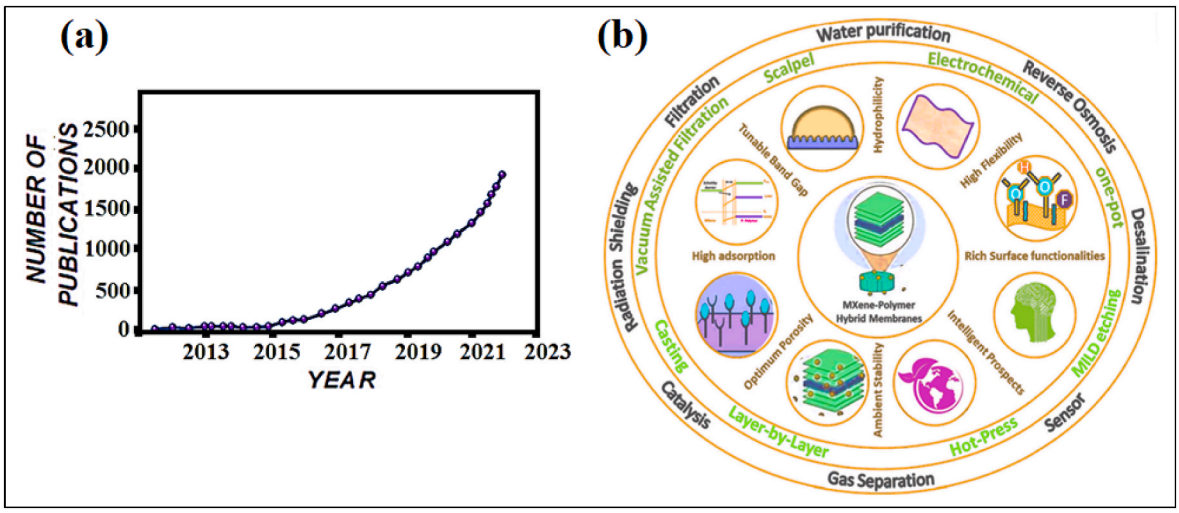

Fig. 14. (a) Research and development using keywords such as "MXene", "environmental remediation", and "MXene-polymer hybrid materials environmental contamination removal" over the past decade, source [Scopus, ACS, RSC], **(b)** The potential of MXene-polymer hybrid membranes as intelligent, adaptable solutions for environmental remediation. Integrated with advanced technologies, they contribute to a more sustainable and cleaner future [332].

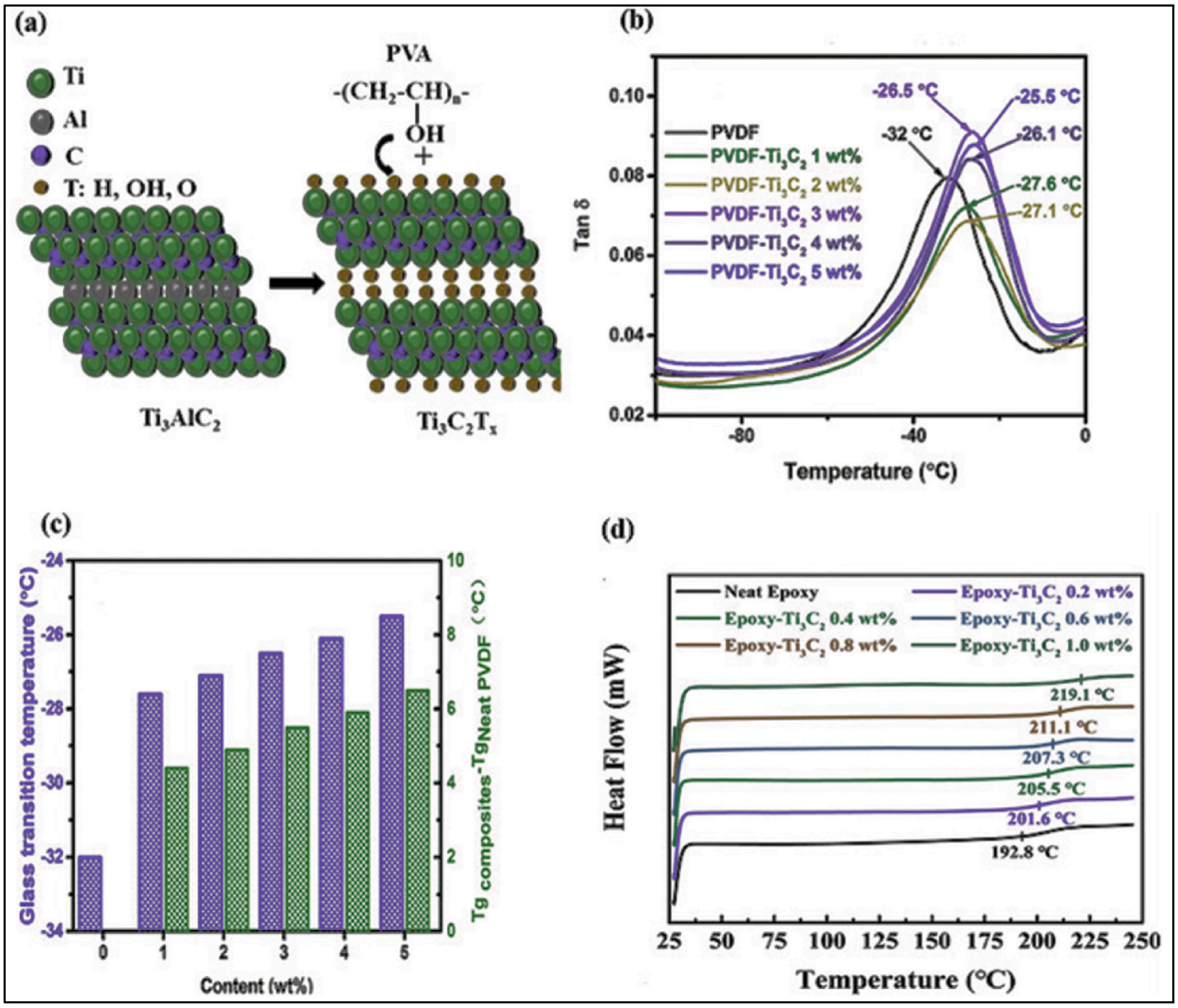

Fig. 15. a) MXene/PVA membrane structure [337], b) Graphical representation of thermal conductivity as a function of weight content for MXene with PVDF [339], c) Examination of the glass transition temperature (Tg) [339], d) Analysis of the glass transition temperature using Differential Scanning Calorimetry (DSC) [340].

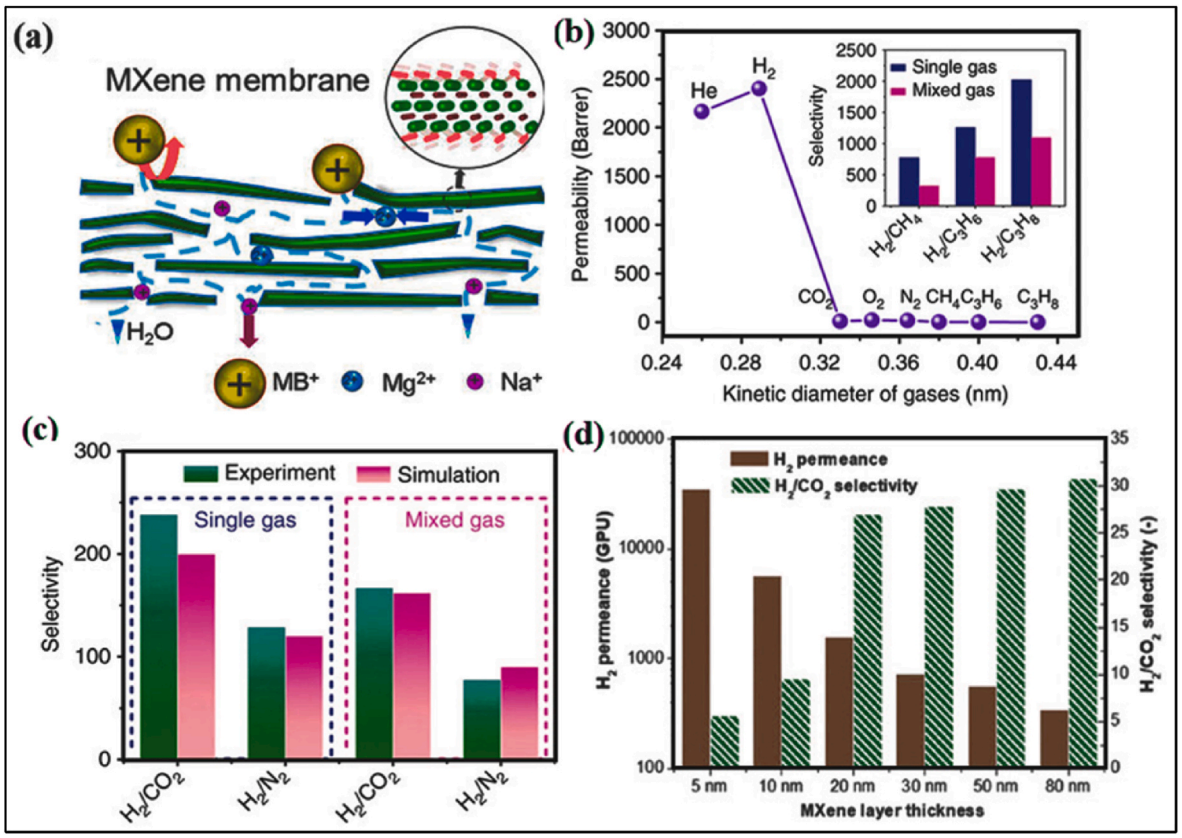

Fig. 16. a) MXene membrane operational mechanism [343,344], b) Investigation of water flux across $Ti_3C_2T_x$ membrane with different thicknesses, emphasising those used in ion permeation tests, marked by a red star [341], c) Comparative analysis of experimental and simulation studies on H_2/N_2 and H_2/CO_2 selectivity in lamellar membranes based on 20 nm thick MXene [341], d) Examination of gas permeation properties for H_2 gas and thickness impact on separation performance in H_2/CO_2 context [343].

acid or base, facilitates ion conduction essential for the reaction. Finally, an external power source, such as a battery or power supply, provides the requisite energy for the reactions to proceed. Water splitting finds applications in diverse realms, notably in hydrogen production, offering a clean fuel source, and energy storage, wherein excess renewable energy can be harnessed to generate hydrogen, thus stowing energy efficiently. Within this process, involving two pivotal half-cell reactions—hydrogen evolution at the cathode and oxygen evolution at the anode—MXenes and their hybrid architectures emerge as vital actors. These materials, coveted for their conductivity and tuneable surface chemistry, have found utility as electrocatalysts, effectively mediating both hydrogen and oxygen evolution reactions [363]. In electrolytic cells, the anode is positively charged (+), where oxidation takes place. Species at the anode lose electrons, which flow towards the positive terminal. Conversely, the cathode is negatively charged (−), where reduction occurs. Species at the cathode gain electrons drawn from the negative terminal. Unlike electrochemical cells like batteries, electrolytic cells require an external power source to drive non-spontaneous reactions. This power source pulls electrons away from the anode, making it positive, and pushes electrons towards the cathode, making it negative. This process occurs through two electrode reactions: the hydrogen evolution reaction (HER) at the cathode and the oxygen evolution reaction (OER) at the anode. While noble metals (e.g., Pt, Ru, Ir) are effective catalysts, their high cost and scarcity drive the search for alternatives. In electrochemical cells, such as batteries, the anode is negatively charged (−). Here, oxidation occurs spontaneously, releasing electrons that flow towards the positive terminal. The cathode is positively charged (+), where reduction takes place. Electrons are spontaneously drawn in from the negative terminal [364–366]. MXenes and other non-noble metal electrocatalysts show promise. However, further optimisation of their activity and stability is necessary for broader research into water splitting. MXenes, with their highly reactive edges, demonstrate unique catalytic properties that warrant further exploration [367]. Hybrid films incorporating Ti_3C_2 nanosheets with materials such as g-C_3N_4 exhibit enhanced electrochemical performance for water splitting [368]. Researchers synthesise MXene-based hybrid films through a well-defined process involving etching MAX phase precursors, dispersing the MXene material, and integrating it with a complementary material (e.g., g-C_3N_4) before deposition. This approach is actively explored with various combinations beyond g-C_3N_4, including Ti_3C_2 nanosheets combined with materials like Fe_2O_3, graphene, and carbon nanotubes. These MXene-hybrid materials exhibit versatility, suggesting their potential across various research fields including energy storage, catalysis, and sensing [369,370]. MXene hybrid films advance the development of efficient and affordable water-splitting electrocatalysts for clean energy solutions, [362,364]. Photocatalysis depends on the efficient utilisation of light energy to facilitate reactions such as HER, CO_2 reduction (CO_2RR), and pollutant degradation [371,372]. Nanomaterials, especially 2D materials, can offer improved photocatalytic properties due to their unique electronic structures [373]. MXenes, with their abundant surface functional groups, large surface area, and ability to promote charge carrier separation, are emerging as promising photocatalysts [374]. In water splitting, the hydrophilicity and capacity of Ti_3C_2TX to act as a co-catalyst enhance its HER performance [374–376]. A key obstacle is the oxidation of MXenes in aqueous environments, which impacts their long-term stability [377]. Research focuses on MXene modifications to enhance stability for environmental remediation. Studies investigate MXene's adsorptive capabilities for pollutants and CO_2, highlighting its potential in wastewater treatment and carbon capture [377,378]. MXenes suggest promise in a wide range of

Table 5
Fabrication of MXene Films and membranes systems and devices for Environmental contamination removal Applications.

Method	Description	Key Findings	Ref.
MXene and other precursors in hybrids/nanocomposites	High-performance environmental remediation due to synergetic effects.	Strategies require elevated temperature, tedious processing, toxicity, and low flexibility.	[345, 346]
MXene/polymer hybrids	Formation of hybrid/nanocomposites with optimum physicochemical characteristics.	Promising in diversified environmental remediation sectors, especially in adsorption-based technologies.	[346, 347]
Direct mixing of MXene and polymer materials	Fabrication of MXene-polymer hybrid membrane materials by direct mixing.	Improvement in mechanical strength due to hydrogen bonding.	[348]
MXene composite with PDA	Synthesis of composite microspheres.	Hydrogen bonding among composite materials, and environmental applications.	[349]
Surface modification of MXene and polymer	Related to hydrophilicity–hydrophobicity surfaces and chemical crosslinking.	N doping for nitrogen-based functional groups and Ti–N bond formation.	[350]
MXenes-polymer membranes	Efficient separation and long-term operation in liquid separation.	Significantly influenced by stability, dispersibility, and hydrophilicity of MXenes.	[351, 352]
$Ti_3C_2T_x$ membrane coated with MXene	Effective treatment of oily wastewater with reduced fouling.	Fabrication involves coating with MXene ink and vacuum filtration.	[353, 354]
Flexible $Ti_3C_2T_x$ membranes coated on paper	Excellent separation efficiency for oil/water emulsions.	Increasing MXene mass loading enhances oil removal ratio but decreases membrane flux.	[353, 354]
$Ti_3C_2T_x$ -Coated Membrane	Enhanced fouling resistance and reduced flux decreases compared to PVDF membranes.	Ti3C2Tx coating facilitates limited heating under visible light conditions and reduced organic fouling.	[355]
Hierarchical lamellar structured MXene-polymer hybrids	Hindered oxidation, enhanced effective surface area and porosity.	Increase interaction with environmental stimuli.	[356]
2D Lamellar MXene Membrane	Outstanding water permeance and promising removal of target compounds.	MXene nanofragments provide more water-transport pathways.	[357]
$Ti_3C_2T_x$ -graphene-oxide membranes	Synergistic effect for solute removal and high hydrophilicity.	Composite membranes fabricated via layer-by-layer stacking of MXene/graphene-oxide nanosheets.	[351]
$Ti_3C_2T_x$ -Graphene-Oxide Membrane	Membrane permeance varies depending on target compound with significant fouling by organic dyes.	–	[351, 352]
$Ti_3C_2T_x$-graphene-oxide composite membranes	Higher MXene content increased membrane permeability with high removal rates for organic dyes.	MXene-graphene-oxide membranes are water-stable and exhibit π-π attraction.	[351]
Graphene-Oxide-MXene-TiO_2 Membrane	High water permeability and removal rates of organic dyes.	Homogenous nano-channels for H2O molecule transport within the graphene-oxide membrane. MXene loading produces extra nano-channels for water transport.	[358]
Fabrication of mesoporous MXene-TiO_2 membranes	Uneven microstructures providing less transport resistance compared to pristine membranes.	High permeance and molecular weight cutoff properties achieved by eliminating pinhole defects associated with MXene-TiO_2 layer.	[359]
Performance evaluation of the MXene-TiO_2 membrane	High removal of dextran solution with various molecular weights.	Fabricated in a controlled manner to minimise defects.	[359]
Assessment of surface oxidation and TiO_2 formation	Higher growth inhibition of bacteria by aged membranes due to TiO_2 nanoparticles.	TiO_2 nanoparticles decrease bacterial growth.	[360]
Functionalised MXene-based thin-film nanocomposite	Varying permeate fluxes depending on functional groups and solvents.	Relatively high permeability for non-polar solvents and enhancement with specific functional groups.	[361]

environmental contexts, including toxic gas removal and radioactive waste management [230,341]. However, the long-term stability and recyclability of MXenes are hindered by the restacking and agglomeration of MXene flakes. This challenge has prompted research into combining MXenes with other materials to form hybrid architectures, offering the potential for enhanced electrocatalytic performance compared to pristine MXenes [363]. Despite these advancements, challenges remain and opportunities for further research exist. Strategies for enhancing the HER catalytic activity of MXenes include optimising active sites through termination modification and metal-atom doping, as well as increasing active sites by fabricating various nanostructures [379].

4.5. Sensors

MXenes, thin layers of transition metal carbides or nitrides with surface groups, boast exceptional properties that make them valuable for various sensor applications [226]. MXenes offer abundant active sites, metallic conductivity, tuneable surface chemistry, and outstanding stability, making them highly desirable for gas sensing applications. They have been effectively employed for detecting gases, volatile organic compounds (VOCs), and humidity [380]. MXenes have found applications in stress or force perception sensors. Their high flexibility, convenient solution processability, and ease of functionalisation enable the development of composites with other nanomaterials, opening new avenues for advanced sensor research [381]. MXenes are utilised in both optical and electrochemical biosensors, leveraging their high sensitivity and selectivity for detecting biological molecules. MXenes have been employed in environmental pollution sensors targeting VOCs and humidity. Their exceptional sensitivity and selectivity make them well-suited for this purpose [381]. The abundance of terminal groups on MXenes facilitates effective NH_3 detection, suggesting their potential for gas sensing research. In stress-sensing, MXenes exhibit exceptional performance, a feature made possible by their inherent electronic conductivity. MXenes also demonstrate potential in biosensing due to their biocompatibility and surface functional groups, which could enable precise and reliable detection [382,383]. Their hydrophilicity makes them well-suited for research into humidity sensing, potentially enabling accurate environmental monitoring and control [204,205]. MXenes contribute to gas sensing research by forming hydrogen bonds with NH_3 on O-terminated substrates. Surface defects can facilitate strong adsorption of gas molecules. For instance, the PEDOT:PSS/MXene sensor demonstrates enhanced gas sensing capabilities, exhibiting a 36.6 % response to 100 ppm of NH_3 [382]. MXene-based pressure sensors, such as the MXene@CS@TPU composite, exhibit high strain, reproducibility, and low detection limits. These characteristics suggest potential for research into wearable pressure sensors, paving the way for advancements in smart textiles for healthcare [384]. MXene research reveals their ability to effectively shield active proteins and facilitate direct electron transfer. This opens possibilities for creating biosensors with wide detection ranges for various analytes. Ideally, biosensors for the Internet of Things (IoT) era should be flexible, self-powered, and seamlessly integrated into wearable devices. MXene-based electrochemical sensors typically involve rigid or opaque components, but research on pristine $Ti_3C_2T_x$ electrodes suggests future possibilities for flexible and transparent sensors [383]. Researchers

investigated that material characteristics like flake size, orientation, film geometry, and uniformity influence the electrochemical activity of a specific molecule (ruthenium hexamine) using cyclic voltammetry. The optimised electrode, made of stacked large $Ti_3C_2T_x$ flakes, exhibited excellent reproducibility and resistance to bending, suggesting its suitability for reliable, robust, and flexible sensors. Furthermore, reducing the electrode thickness increased the faradaic-to-capacitance signal, a desirable feature for this application. This research led to the successful deposition of transparent thin $Ti_3C_2T_x$ films that maintained their best performance while achieving up to 73 % transparency [385]. During electrode fabrication, nanosheets often restack horizontally due to the highly anisotropic nature of MXene. This results in low porosity and limited utilisation of the MXene surface area. The electrochemical biosensing of antibody-antigen reactions has been demonstrated using a vertically aligned Ti_3C_2Tx MXene (VA-MXene) electrode. This electrode was prepared using freeze-drying-assisted electrophoretic deposition. The microporous structure of the VA-MXene electrode exhibited superior electrochemical response to the immunoreaction between the allergenic buckwheat protein (BWp16) and the antibody. This was in comparison to a non-porous, horizontally stacked MXene (HS-MXene) electrode and sensors reported previously. The sensor responsiveness, represented by the ratio of the obtained current density of the electrode to the antigen concentration, was significantly higher for the VA-MXene electrode (238 μA cm^{-2} (ng $mL^{-1})^{-1}$) than for the HS-MXene electrode. This technique is transferable to other exfoliated nanosheets and presents a novel approach for enhancing the sensing characteristics of electrochemical biosensors through the use of porous nanosheet electrodes [386].

5. Conclusion and future prospect

The study of MXenes reveals exciting advancements in materials science, with applications in energy storage, catalysis, and sensors. Careful attention is given to the crucial selective etching process, which shapes MXenes with tailored structures and properties. Researchers explore safer alternatives to hazardous etchants like HF, including NH_4HF_2, tetrabutylammonium fluoride [$(C_4H_9)_4NF$], NaF, KF, CsF, and CaF_2 with HCl or H_2SO_4. Optimal MXene synthesis depends on understanding the intended purpose, desired qualities, and necessary components. One detailed process involved using powdered Ti_3AlC_2, LiF, and HCl solutions to produce a specific MXene variant ($Ti_3C_2T_x$). This process yielded flakes with improved lateral dimensions and eliminated nanoscale flaws compared to materials etched with HF. Researchers are actively refining selective etching processes to further enhance the yield, purity, and properties of MXene materials. Recent research investigates MXenes in various fields, including flexible electronics, water purification, and biomedicine. Their exceptional electrical conductivity and mechanical strength position them as promising candidates for electronic and optoelectronic devices. Additionally, MXenes' high surface area and chemical stability make them well-suited for catalysis and water purification applications. Their biocompatibility and biodegradability also enable promising exploration in biomedical applications such as drug delivery and tissue engineering.

CRediT authorship contribution statement

Raghvendra Kumar Mishra: Writing – original draft, Writing – review & editing. **Jayati Sarkar:** Investigation. **Kartikey Verma:** Conceptualization. **Iva Chianella:** Visualization. **Saurav Goel:** Supervision. **Hamed Yazdani Nezhad:** Formal analysis.

Declaration of competing interest

The authors declare that they have no known competing financial interests or personal relationships that could have appeared to influence the work reported in this paper.

Acknowledgment

The authors gratefully acknowledge the support and funding received from the UK Engineering & Physical Sciences Research Council (EPSRC) under grant numbers EP/R016828/1 (Self-tuning Fibre-Reinforced Polymer Adaptive Nanocomposite, STRAIN comp) and EP/R513027/1 (Study of Microstructure of Dielectric Polymer Nanocomposites subjected to Electromagnetic Field for Development of Self-toughening Lightweight Composites).

References

[1] A. Jayakumar, A. Surendranath, M. Pv, 2D materials for next generation healthcare applications, Int. J. Pharm. 551 (2018) 309–321, https://doi.org/10.1016/j.ijpharm.2018.09.041.
[2] T. Bregar, D. An, S. Gharavian, M. Burda, I. Durazo-Cardenas, V.K. Thakur, D. Ayre, M. Słoma, M. Hardiman, C. McCarthy, H. Yazdani Nezhad, Carbon nanotube embedded adhesives for real-time monitoring of adhesion failure in high performance adhesively bonded joints, Sci. Rep. 10 (2020) 16833, https://doi.org/10.1038/s41598-020-74076-y.
[3] F. Wang, Z. Wang, T.A. Shifa, Y. Wen, F. Wang, X. Zhan, Q. Wang, K. Xu, Y. Huang, L. Yin, C. Jiang, J. He, Two-dimensional non-layered materials: synthesis, properties and applications, Adv. Funct. Mater. 27 (2017), https://doi.org/10.1002/adfm.201603254.
[4] M.S. Fuhrer, C.N. Lau, A.H. MacDonald, Graphene: materially better carbon, MRS Bull. 35 (2010) 289–295, https://doi.org/10.1557/mrs2010.551.
[5] R.K. Mishra, S. Goel, I. Chianella, H. Yazdani Nezhad, Graphene nanoplatelets/barium titanate polymer nanocomposite fibril: a remanufactured multifunctional material with unprecedented electrical, thermomechanical, and electromagnetic properties, Adv Sustain Syst 7 (2023), https://doi.org/10.1002/adsu.202300177.
[6] S. Deng, V. Berry, Wrinkled, rippled and crumpled graphene: an overview of formation mechanism, electronic properties, and applications, Mater. Today 19 (2016), https://doi.org/10.1016/j.mattod.2015.10.002.
[7] F. Catania, E. Marras, M. Giorcelli, P. Jagdale, L. Lavagna, A. Tagliaferro, M. Bartoli, A review on recent advancements of graphene and graphene-related materials in biological applications, Appl. Sci. 11 (2021), https://doi.org/10.3390/app11020614.
[8] N. Kumar, R. Salehiyan, V. Chauke, O. Joseph Botlhoko, K. Setshedi, M. Scriba, M. Masukume, S. Sinha Ray, Top-down synthesis of graphene: a comprehensive review, FlatChem 27 (2021) 100224, https://doi.org/10.1016/j.flatc.2021.100224.
[9] M. Ou, X. Wang, L. Yu, C. Liu, W. Tao, X. Ji, L. Mei, The emergence and evolution of borophene, Adv. Sci. 8 (2021), https://doi.org/10.1002/advs.202001801.
[10] A. Acun, L. Zhang, P. Bampoulis, M. Farmanbar, A. Van Houselt, A.N. Rudenko, M. Lingenfelder, G. Brocks, B. Poelsema, M.I. Katsnelson, H.J.W. Zandvliet, Germanene: the germanium analogue of graphene, J. Phys. Condens. Matter 27 (2015), https://doi.org/10.1088/0953-8984/27/44/443002.
[11] J. Zhao, H. Liu, Z. Yu, R. Quhe, S. Zhou, Y. Wang, C.C. Liu, H. Zhong, N. Han, J. Lu, Y. Yao, K. Wu, Rise of silicene: a competitive 2D material, Prog. Mater. Sci. 83 (2016) 24–151, https://doi.org/10.1016/j.pmatsci.2016.04.001.
[12] J. Pang, A. Bachmatiuk, Y. Yin, B. Trzebicka, L. Zhao, L. Fu, R.G. Mendes, T. Gemming, Z. Liu, M.H. Rummeli, Applications of phosphorene and black phosphorus in energy conversion and storage devices, Adv. Energy Mater. 8 (2018), https://doi.org/10.1002/aenm.201702093.
[13] A. Mehranfar, M. Khavani, M. Izadyar, A molecular dynamic study on the ability of phosphorene for designing new sensor for SARS-CoV-2 detection, J. Mol. Liq. 345 (2022), https://doi.org/10.1016/j.molliq.2021.117852.
[14] P. Afshari, M. Pavlyuk, C. Lira, K.B. Katnam, M. Bodaghi, H. Yazdani Nezhad, Mechanical strain tailoring via magnetic field assisted 3D printing of iron particles embedded polymer nanocomposites, Macromol. Mater. Eng. (2023), https://doi.org/10.1002/mame.202300194.
[15] M. Lalegani Dezaki, R. Sales, A. Zolfagharian, H. Yazdani Nezhad, M. Bodaghi, Soft pneumatic actuators with integrated resistive sensors enabled by multi-material 3D printing, Int. J. Adv. Manuf. Technol. 128 (2023), https://doi.org/10.1007/s00170-023-12181-8.
[16] R.K. Mishra, D. Li, I. Chianella, S. Goel, S. Lotfian, H. Yazdani Nezhad, Low electric field induction in BaTiO3-epoxy nanocomposites, Functional Composite Materials 4 (2023) 6, https://doi.org/10.1186/s42252-023-00043-1.
[17] S.S. Siwal, K. Sheoran, K. Mishra, H. Kaur, A.K. Saini, V. Saini, D.V.N. Vo, H. Y. Nezhad, V.K. Thakur, Novel synthesis methods and applications of MXene-based nanomaterials (MBNs) for hazardous pollutants degradation: future perspectives, Chemosphere 293 (2022), https://doi.org/10.1016/j.chemosphere.2022.133542.
[18] Z. Lin, H. Shao, K. Xu, P.L. Taberna, P. Simon, MXenes as high-rate electrodes for energy storage, Trends Chem 2 (2020), https://doi.org/10.1016/j.trechm.2020.04.010.
[19] K. Gong, K. Zhou, X. Qian, C. Shi, B. Yu, MXene as emerging nanofillers for high-performance polymer composites: a review, Compos. B Eng. 217 (2021) 108867, https://doi.org/10.1016/j.compositesb.2021.108867.
[20] M. Naguib, M.W. Barsoum, Y. Gogotsi, Ten years of progress in the synthesis and development of MXenes, Adv. Mater. 33 (2021), https://doi.org/10.1002/adma.202103393.

[21] I. Ali, M. Faraz Ud Din, Z.-G. Gu, MXenes thin films: from fabrication to their applications, Molecules 27 (2022) 4925, https://doi.org/10.3390/molecules27154925.

[22] H. Li, R. Fan, B. Zou, J. Yan, Q. Shi, G. Guo, Roles of MXenes in biomedical applications: recent developments and prospects, J. Nanobiotechnol. 21 (2023), https://doi.org/10.1186/s12951-023-01809-2.

[23] L. Zhang, W. Song, H. Liu, H. Ding, Y. Yan, R. Chen, Influencing factors on synthesis and properties of MXene: a review, Processes 10 (2022), https://doi.org/10.3390/pr10091744.

[24] M. Rahman, M.S. Al Mamun, Future prospects of MXenes: synthesis, functionalization, properties, and application in field effect transistors, Nanoscale Adv. 6 (2024) 367–385, https://doi.org/10.1039/D3NA00874F.

[25] S. Jin, Y. Guo, F. Wang, A. Zhou, The synthesis of MXenes, MRS Bull. 48 (2023) 245–252, https://doi.org/10.1557/s43577-023-00491-x.

[26] J. Xu, T. Peng, X. Qin, Q. Zhang, T. Liu, W. Dai, B. Chen, H. Yu, S. Shi, Recent advances in 2D MXenes: preparation, intercalation and applications in flexible devices, J Mater Chem A Mater 9 (2021), https://doi.org/10.1039/d1ta03070a.

[27] S. Anand, M.C. Vu, D. Mani, J.-B. Kim, T.-H. Jeong, W.-K. Choi, J.-C. Won, S.-R. Kim, A continuous interfacial bridging approach to fabricate ultrastrong hydroxylated carbon nanotubes intercalated MXene films with superior electromagnetic interference shielding and thermal dissipating properties, Adv. Compos. Hybrid Mater. 7 (2024) 33, https://doi.org/10.1007/s42114-024-00842-5.

[28] D. Ayodhya, A review of recent progress in 2D MXenes: synthesis, properties, and applications, Diam. Relat. Mater. 132 (2023) 109634, https://doi.org/10.1016/j.diamond.2022.109634.

[29] L. Damptey, B.N. Jaato, C.S. Ribeiro, S. Varagnolo, N.P. Power, V. Selvaraj, D. Dodoo-Arhin, R.V. Kumar, S.P. Sreenilayam, D. Brabazon, V. Kumar Thakur, S. Krishnamurthy, Surface functionalized MXenes for wastewater treatment—a comprehensive review, Global Challenges (2022), https://doi.org/10.1002/gch2.202100120.

[30] I. Ali, M. Faraz Ud Din, Z.-G. Gu, MXenes thin films: from fabrication to their applications, Molecules 27 (2022) 4925, https://doi.org/10.3390/molecules27154925.

[31] A. Lipatov, H. Lu, M. Alhabeb, B. Anasori, A. Gruverman, Y. Gogotsi, A. Sinitskii, Elastic properties of 2D Ti3C2Tx MXene monolayers and bilayers, Sci. Adv. 4 (2018), https://doi.org/10.1126/sciadv.aat0491.

[32] J. Zhang, N. Kong, S. Uzun, A. Levitt, S. Seyedin, P.A. Lynch, S. Qin, M. Han, W. Yang, J. Liu, X. Wang, Y. Gogotsi, J.M. Razal, Scalable manufacturing of free-standing, strong Ti3C2Tx MXene films with outstanding conductivity, Adv. Mater. 32 (2020), https://doi.org/10.1002/adma.202001093.

[33] A. Lipatov, A. Sinitskii, Electronic and mechanical properties of MXenes derived from single-flake measurements, in: 2D Metal Carbides and Nitrides (MXenes): Structure, Properties and Applications, 2019, https://doi.org/10.1007/978-3-030-19026-2_16.

[34] K.A. Papadopoulou, A. Chroneos, D. Parfitt, S.R.G. Christopoulos, A perspective on MXenes: their synthesis, properties, and recent applications, J. Appl. Phys. 128 (2020), https://doi.org/10.1063/5.0021485.

[35] M. Naguib, M. Kurtoglu, V. Presser, J. Lu, J. Niu, M. Heon, L. Hultman, Y. Gogotsi, M.W. Barsoum, Two-dimensional nanocrystals produced by exfoliation of Ti3ALC2, in: MXenes: from Discovery to Applications of Two-Dimensional Metal Carbides and Nitrides, 2023, https://doi.org/10.1201/9781003306511-4.

[36] S. Biswas, P.S. Alegaonkar, MXene: evolutions in chemical synthesis and recent advances in applications, Surfaces 5 (2022), https://doi.org/10.3390/surfaces5010001.

[37] A. Iqbal, J. Hong, T.Y. Ko, C.M. Koo, Improving oxidation stability of 2D MXenes: synthesis, storage media, and conditions, Nano Converg 8 (2021), https://doi.org/10.1186/s40580-021-00259-6.

[38] R.A. Soomro, P. Zhang, B. Fan, Y. Wei, B. Xu, Progression in the oxidation stability of MXenes, Nano-Micro Lett. 15 (2023), https://doi.org/10.1007/s40820-023-01069-7.

[39] P. Eklund, M. Beckers, U. Jansson, H. Högberg, L. Hultman, The M+1AX phases: materials science and thin-film processing, Thin Solid Films 518 (2010) 1851–1878, https://doi.org/10.1016/j.tsf.2009.07.184.

[40] M. Benchakar, L. Loupias, C. Garnero, T. Bilyk, C. Morais, C. Canaff, N. Guignard, S. Morisset, H. Pazniak, S. Hurand, P. Chartier, J. Pacaud, V. Mauchamp, M. W. Barsoum, A. Habrioux, S. Célérier, One MAX phase, different MXenes: a guideline to understand the crucial role of etching conditions on Ti3C2Tx surface chemistry, Appl. Surf. Sci. 530 (2020) 147209, https://doi.org/10.1016/j.apsusc.2020.147209.

[41] Z. Xu, R. Zhou, Q. Ma, X. Li, X. Cheng, Study on the electromagnetic wave absorption performance of Ti3C2 MXene with different etching states, J. Mater. Sci. 58 (2023), https://doi.org/10.1007/s10853-023-08337-2.

[42] T. Zhang, L. Pan, H. Tang, F. Du, Y. Guo, T. Qiu, J. Yang, Synthesis of two-dimensional Ti3C2TxMXene using HCl+LiF etchant: enhanced exfoliation and delamination, J. Alloys Compd. 695 (2017), https://doi.org/10.1016/j.jallcom.2016.10.127.

[43] A.J.Y. Wong, K.R.G. Lim, Z.W. Seh, Fluoride-free synthesis and long-term stabilization of MXenes, J. Mater. Res. 37 (2022), https://doi.org/10.1557/s43578-022-00680-5.

[44] S. Mourdikoudis, R.M. Pallares, N.T.K. Thanh, Characterization techniques for nanoparticles: comparison and complementarity upon studying nanoparticle properties, Nanoscale 10 (2018), https://doi.org/10.1039/c8nr02278j.

[45] H.H. Radamson, Raman Spectroscopy, Fourier Transform Infrared Spectroscopy (FTIR) and X-Ray Photoelectron Spectroscopy (XPS), 2023, pp. 87–114, https://doi.org/10.1007/978-3-031-26434-4_3.

[46] R.K. Mishra, J. Cherusseri, K. Joseph, Thermal and crystallization behavior of micro and nano fibrillar in-situ composites. https://doi.org/10.1016/B978-0-08-101991-7.00009-1, 2017.

[47] R.K. Mishra, S. Thomas, A.K. Zachariah, Energy-Dispersive X-Ray Spectroscopy Techniques for Nanomaterial, 2017, https://doi.org/10.1016/B978-0-323-46141-2.00012-2.

[48] T.B. Asafa, O. Adedokun, T.T. Dele-Afolabi, Characterization Techniques in Nanotechnology: the State of the Art, 2021, pp. 21–73, https://doi.org/10.1007/978-981-33-4777-9_2.

[49] H. Shi, P. Zhang, Z. Liu, S. Park, M.R. Lohe, Y. Wu, A. Shaygan Nia, S. Yang, X. Feng, Ambient-stable two-dimensional titanium carbide (MXene) enabled by iodine etching, Angew. Chem. 133 (2021), https://doi.org/10.1002/ange.202015627.

[50] Z. Wu, T. Shang, Y. Deng, Y. Tao, Q. Yang, The assembly of MXenes from 2D to 3D, Adv. Sci. 7 (2020), https://doi.org/10.1002/advs.201903077.

[51] K. Chaturvedi, V. Hada, S. Paul, B. Sarma, D. Malvi, M. Dhangar, H. Bajpai, A. Singhwane, A.K. Srivastava, S. Verma, The rise of MXene: a wonder 2D material, from its synthesis and properties to its versatile applications—a comprehensive review, Top. Curr. Chem. 381 (2023), https://doi.org/10.1007/s41061-023-00420-1.

[52] T. Amrillah, C.A.C. Abdullah, A. Hermawan, F.N.I. Sari, V.N. Alvani, Towards greener and more sustainable synthesis of MXenes: a review, Nanomaterials 12 (2022), https://doi.org/10.3390/nano12234280.

[53] U.U. Rahman, M. Humayun, U. Ghani, M. Usman, H. Ullah, A. Khan, N.M. El-Metwaly, A. Khan, MXenes as emerging materials: synthesis, properties, and applications, Molecules 27 (2022) 4909, https://doi.org/10.3390/molecules27154909.

[54] U. Yorulmaz, A. Özden, N.K. Perkgöz, F. Ay, C. Sevik, Vibrational and mechanical properties of single layer MXene structures: a first-principles investigation, Nanotechnology 27 (2016), https://doi.org/10.1088/0957-4484/27/33/335702.

[55] X. Li, F. Ran, F. Yang, J. Long, L. Shao, Advances in MXene Films: Synthesis, Assembly, and Applications, vol. 27, Transactions of Tianjin University, 2021, https://doi.org/10.1007/s12209-021-00282-y.

[56] T. Amrillah, A. Hermawan, V.N. Alviani, Z.W. Seh, S. Yin, MXenes and their derivatives as nitrogen reduction reaction catalysts: recent progress and perspectives, Mater. Today Energy 22 (2021), https://doi.org/10.1016/j.mtener.2021.100864.

[57] S. Venkateshalu, A.N. Grace, Synthesis and Processing Strategies, 2022, pp. 17–36, https://doi.org/10.1007/978-3-031-05006-0_2.

[58] X.H. Wang, Y.C. Zhou, Layered machinable and electrically conductive Ti2AlC and Ti3AlC2 ceramics: a review, J. Mater. Sci. Technol. 26 (2010), https://doi.org/10.1016/S1005-0302(10)60064-3.

[59] K. Zhu, Y. Jin, F. Du, S. Gao, Z. Gao, X. Meng, G. Chen, Y. Wei, Y. Gao, Synthesis of Ti2CT MXene as electrode materials for symmetric supercapacitor with capable volumetric capacitance, J. Energy Chem. 31 (2019) 11–18, https://doi.org/10.1016/j.jechem.2018.03.010.

[60] A. VahidMohammadi, A. Hadjikhani, S. Shahbazmohamadi, M. Beidaghi, Two-dimensional vanadium carbide (MXene) as a high-capacity cathode material for rechargeable aluminum batteries, ACS Nano 11 (2017) 11135–11144, https://doi.org/10.1021/acsnano.7b05350.

[61] B. Anasori, Y. Xie, M. Beidaghi, J. Lu, B.C. Hosler, L. Hultman, P.R.C. Kent, Y. Gogotsi, M.W. Barsoum, Two-dimensional, ordered, double transition metals carbides (MXenes), ACS Nano 9 (2015) 9507–9516, https://doi.org/10.1021/acsnano.5b03591.

[62] S. Zhao, X. Meng, K. Zhu, F. Du, G. Chen, Y. Wei, Y. Gogotsi, Y. Gao, Li-ion uptake and increase in interlayer spacing of Nb4C3 MXene, Energy Storage Mater. 8 (2017) 42–48, https://doi.org/10.1016/j.ensm.2017.03.012.

[63] Y. Wei, P. Zhang, R.A. Soomro, Q. Zhu, B. Xu, Advances in the synthesis of 2D MXenes, Adv. Mater. 33 (2021) 2103148, https://doi.org/10.1002/adma.202103148.

[64] C.E. Shuck, K. Ventura-Martinez, A. Goad, S. Uzun, M. Shekhirev, Y. Gogotsi, Safe synthesis of MAX and MXene: guidelines to reduce risk during synthesis, ACS Chemical Health and Safety 28 (2021), https://doi.org/10.1021/acs.chas.1c00051.

[65] K.R.G. Lim, M. Shekhirev, B.C. Wyatt, B. Anasori, Y. Gogotsi, Z.W. Seh, Fundamentals of MXene synthesis, Nature Synthesis 1 (2022), https://doi.org/10.1038/s44160-022-00104-6.

[66] R.A. Vaia, A. Jawaid, A. Hassan, G. Neher, D. Nepal, R. Pachter, W. Joshua Kennedy, S. Ramakrishnan, Halogen etch of Ti3AlC2 MAX phase for mxene fabrication, ACS Nano 15 (2021), https://doi.org/10.1021/acsnano.0c08630.

[67] M. Han, X. Yin, H. Wu, Z. Hou, C. Song, X. Li, L. Zhang, L. Cheng, Ti3C2 MXenes with modified surface for high-performance electromagnetic absorption and shielding in the X-band, ACS Appl. Mater. Interfaces 8 (2016), https://doi.org/10.1021/acsami.6b06455.

[68] M. Tahir, B. Tahir, In-situ growth of TiO2 imbedded Ti3C2TA nanosheets to construct PCN/Ti3C2TA MXenes 2D/3D heterojunction for efficient solar driven photocatalytic CO2 reduction towards CO and CH4 production, J. Colloid Interface Sci. 591 (2021), https://doi.org/10.1016/j.jcis.2021.01.099.

[69] T. Placke, J. Gonzalez-Julian, P. Bärmann, R. Nölle, V. Siozios, M. Ruttert, O. Guillon, M. Winter, Solvent co-intercalation into few-layered Ti3C2Tx mxenes in lithium ion batteries induced by acidic or basic post-treatment, ACS Nano 15 (2021), https://doi.org/10.1021/acsnano.0c10153.

[70] P. Urbankowski, B. Anasori, T. Makaryan, D. Er, S. Kota, P.L. Walsh, M. Zhao, V. B. Shenoy, M.W. Barsoum, Y. Gogotsi, Synthesis of two-dimensional titanium nitride Ti4N3 (MXene), Nanoscale 8 (2016), https://doi.org/10.1039/c6nr02253g.

[71] J. Zhou, X. Zha, F.Y. Chen, Q. Ye, P. Eklund, S. Du, Q. Huang, A two-dimensional zirconium carbide by selective etching of Al3C3 from nanolaminated Zr3Al3C5, Angew. Chem. Int. Ed. 55 (2016), https://doi.org/10.1002/anie.201510432.

[72] R. Meshkian, Q. Tao, M. Dahlqvist, J. Lu, L. Hultman, J. Rosen, Theoretical stability and materials synthesis of a chemically ordered MAX phase, Mo2ScAlC2, and its two-dimensional derivate Mo2ScC2 MXene, Acta Mater. 125 (2017), https://doi.org/10.1016/j.actamat.2016.12.008.

[73] Y.J. Lei, Z.C. Yan, W.H. Lai, S.L. Chou, Y.X. Wang, H.K. Liu, S.X. Dou, Tailoring MXene-based materials for sodium-ion storage: synthesis, mechanisms, and applications, Electrochem. Energy Rev. 3 (2020), https://doi.org/10.1007/s41918-020-00079-y.

[74] A. Zamhuri, G.P. Lim, N.L. Ma, K.S. Tee, C.F. Soon, MXene in the lens of biomedical engineering: synthesis, applications and future outlook, Biomed. Eng. Online 20 (2021) 33, https://doi.org/10.1186/s12938-021-00873-9.

[75] R.P.R. Dinesh, S. Dinesh, N.A.Z. Siti, The effect of fluoride based salt etching in the synthesis of MXene, in: Materials Research Proceedings, 2023, https://doi.org/10.21741/9781644902516-8.

[76] K. Maleski, M. Alhabeb, Top-down MXene synthesis (selective etching), in: 2D Metal Carbides and Nitrides (MXenes): Structure, Properties and Applications, 2019, https://doi.org/10.1007/978-3-030-19026-2_5.

[77] X. Wang, L. Wu, H. Gao, X. Zhang, Synthesis of Ti3AlC2 and electrochemical performance of Ti3C2Tx nanosheet electrode, Scientia Sinica Chimica 48 (2018), https://doi.org/10.1360/N032017-00183.

[78] K. Arole, J.W. Blivin, A.M. Bruce, S. Athavale, I.J. Echols, H. Cao, Z. Tan, M. Radovic, J.L. Lutkenhaus, M.J. Green, Exfoliation, delamination, and oxidation stability of molten salt etched Nb2CTz MXene nanosheets, Chem. Commun. 58 (2022), https://doi.org/10.1039/d2cc02237k.

[79] A. Shayesteh Zeraati, S.A. Mirkhani, P. Sun, M. Naguib, P.V. Braun, U. Sundararaj, Improved synthesis of Ti3C2T: XMXenes resulting in exceptional electrical conductivity, high synthesis yield, and enhanced capacitance, Nanoscale 13 (2021), https://doi.org/10.1039/d0nr06671k.

[80] A. VahidMohammadi, E. Kayali, J. Orangi, M. Beidaghi, Techniques for MXene delamination into single-layer flakes, in: 2D Metal Carbides and Nitrides (MXenes): Structure, Properties and Applications, 2019, https://doi.org/10.1007/978-3-030-19026-2_11.

[81] R.M. Ronchi, J.T. Arantes, S.F. Santos, Synthesis, structure, properties and applications of MXenes: current status and perspectives, Ceram. Int. 45 (2019) 18167–18188, https://doi.org/10.1016/j.ceramint.2019.06.114.

[82] C.J. Zhang, Y. Ma, X. Zhang, S. Abdolhosseinzadeh, H. Sheng, W. Lan, A. Pakdel, J. Heier, F. Nüesch, Two-dimensional transition metal carbides and nitrides (MXenes): synthesis, properties, and electrochemical energy storage applications, ENERGY & ENVIRONMENTAL MATERIALS 3 (2020) 29–55, https://doi.org/10.1002/eem2.12058.

[83] D.B. Lioi, G. Neher, J.E. Heckler, T. Back, F. Mehmood, D. Nepal, R. Pachter, R. Vaia, W.J. Kennedy, Electron-withdrawing effect of native terminal groups on the lattice structure of Ti3C2Tx MXenes studied by resonance Raman scattering: implications for embedding MXenes in electronic composites, ACS Appl. Nano Mater. 2 (2019), https://doi.org/10.1021/acsanm.9b01194.

[84] N. Tao, D. Zhang, X. Li, D. Lou, X. Sun, C. Wei, J. Li, J. Yang, Y.N. Liu, Near-infrared light-responsive hydrogels: via peroxide-decorated MXene-initiated polymerization, Chem. Sci. 10 (2019), https://doi.org/10.1039/c9sc03917a.

[85] J. Zhao, L. Zhang, X.Y. Xie, X. Li, Y. Ma, Q. Liu, W.H. Fang, X. Shi, G. Cui, X. Sun, Ti3C2Tx (T = F, OH) MXene nanosheets: conductive 2D catalysts for ambient electrohydrogenation of N2 to NH3, J Mater Chem A Mater 6 (2018), https://doi.org/10.1039/c8ta09840a.

[86] H. Yu, H. Jiang, S. Zhang, X. Feng, S. Yin, W. Zhao, Review of two-dimensional MXenes (Ti3C2Tx) materials in photocatalytic applications, Processes 11 (2023), https://doi.org/10.3390/pr11051413.

[87] X. Li, Y. Bai, X. Shi, N. Su, G. Nie, R. Zhang, H. Nie, L. Ye, Applications of MXene ($Ti_3C_2T_x$) in photocatalysis: a review, Mater Adv 2 (2021) 1570–1594, https://doi.org/10.1039/D0MA00938E.

[88] L. Yao, X. Tian, X. Cui, R. Zhao, X. Xiao, Y. Wang, Partially oxidized Ti3C2Tx MXene-sensitive material-based ammonia gas sensor with high-sensing performances for room temperature application, J. Mater. Sci. Mater. Electron. 32 (2021), https://doi.org/10.1007/s10854-021-07166-w.

[89] M. Mozafari, M. Soroush, Surface functionalization of MXenes, Mater Adv 2 (2021), https://doi.org/10.1039/d1ma00625h.

[90] R. Verma, A. Sharma, V. Dutta, A. Chauhan, D. Pathak, S. Ghotekar, Recent trends in synthesis of 2D MXene-based materials for sustainable environmental applications, Emergent Mater 7 (2024), https://doi.org/10.1007/s42247-023-00591-z.

[91] S. Palei, G. Murali, C.H. Kim, I. In, S.Y. Lee, S.J. Park, A review on interface engineering of MXenes for perovskite solar cells, Nano-Micro Lett. 15 (2023), https://doi.org/10.1007/s40820-023-01083-9.

[92] H. Gholivand, S. Fuladi, Z. Hemmat, A. Salehi-Khojin, F. Khalili-Araghi, Effect of surface termination on the lattice thermal conductivity of monolayer Ti3C2Tz MXenes, J. Appl. Phys. 126 (2019), https://doi.org/10.1063/1.5094294.

[93] C. Liu, X. Li, L. Hao, Y. Deng, Q. Yin, Y. Bao, Research progress of functional modification of MXene and its applications, Fuhe Cailiao Xuebao/Acta Materiae Compositae Sinica 38 (2021), https://doi.org/10.13801/j.cnki.fhclxb.20201218.003.

[94] S. Munir, A. Rasheed, T. Rasheed, I. Ayman, S. Ajmal, A. Rehman, I. Shakir, P. O. Agboola, M.F. Warsi, Exploring the influence of critical parameters for the effective synthesis of high-quality 2D MXene, ACS Omega 5 (2020), https://doi.org/10.1021/acsomega.0c03970.

[95] M.A. Hope, A.C. Forse, K.J. Griffith, M.R. Lukatskaya, M. Ghidiu, Y. Gogotsi, C. P. Grey, NMR reveals the surface functionalisation of Ti3C2 MXene, Phys. Chem. Chem. Phys. 18 (2016), https://doi.org/10.1039/c6cp00330c.

[96] K.J. Griffith, M.A. Hope, P.J. Reeves, M. Anayee, Y. Gogotsi, C.P. Grey, Bulk and surface chemistry of the niobium MAX and MXene phases from multinuclear solid-state NMR spectroscopy, J. Am. Chem. Soc. 142 (2020), https://doi.org/10.1021/jacs.0c09044.

[97] T. Kobayashi, Y. Sun, K. Prenger, D.E. Jiang, M. Naguib, M. Pruski, Nature of terminating hydroxyl groups and intercalating water in Ti3C2TxMXenes: a study by 1H solid-state NMR and DFT calculations, J. Phys. Chem. C 124 (2020), https://doi.org/10.1021/acs.jpcc.0c04744.

[98] S.-N. Lai, W.Y. Chen, C.-C. Yen, Y.-S. Liao, P.-H. Chen, L. Stanciu, J.M. Wu, An ultraefficient surface functionalized $Ti_3C_2T_x$ MXene piezocatalyst: synchronous hydrogen evolution and wastewater treatment, J Mater Chem A Mater 12 (2024) 3340–3351, https://doi.org/10.1039/D3TA06291K.

[99] N. Parra-Muñoz, M. Soler, A. Rosenkranz, Covalent functionalization of MXenes for tribological purposes - a critical review, Adv. Colloid Interface Sci. 309 (2022), https://doi.org/10.1016/j.cis.2022.102792.

[100] S. Jung, U. Zafar, L.S.K. Achary, C.M. Koo, Ligand Chemistry for Surface Functionalization in <scp>MXenes</scp> : A Review, vol. 5, EcoMat, 2023, https://doi.org/10.1002/eom2.12395.

[101] J. Zou, J. Wu, Y. Wang, F. Deng, J. Jiang, Y. Zhang, S. Liu, N. Li, H. Zhang, J. Yu, T. Zhai, H.N. Alshareef, Correction: additive-mediated intercalation and surface modification of MXenes, Chem. Soc. Rev. 51 (2022), https://doi.org/10.1039/d2cs90024f.

[102] J.L. Hart, K. Hantanasirisakul, Y. Gogotsi, M.L. Taheri, Termination-property coupling via reversible oxygen functionalization of MXenes, ACS Nanoscience Au 2 (2022), https://doi.org/10.1021/acsnanoscienceau.2c00024.

[103] T. Zhang, L. Chang, X. Xiao, Surface and interface regulation of MXenes: methods and properties, Small Methods 7 (2023), https://doi.org/10.1002/smtd.202201530.

[104] M. Hilal, W. Yang, Y. Hwang, W. Xie, Tailoring MXene thickness and functionalization for enhanced room-temperature trace NO2 sensing, Nano-Micro Lett. 16 (2024) 84, https://doi.org/10.1007/s40820-023-01316-x.

[105] L. Lorencova, P. Kasak, N. Kosutova, M. Jerigova, E. Noskovicova, A. Vikartovska, M. Barath, P. Farkas, J. Tkac, MXene-based electrochemical devices applied for healthcare applications, Microchim. Acta 191 (2024), https://doi.org/10.1007/s00604-023-06163-6.

[106] A. Zaheer, S.A. Zahra, M.Z. Iqbal, A. Mahmood, S.A. Khan, S. Rizwan, Nickel-adsorbed two-dimensional Nb2C MXene for enhanced energy storage applications, RSC Adv. 12 (2022), https://doi.org/10.1039/d2ra00014h.

[107] Z. Otgonbayar, S. Yang, I.J. Kim, W.C. Oh, Recent advances in two-dimensional MXene for supercapacitor applications: progress, challenges, and perspectives, Nanomaterials 13 (2023), https://doi.org/10.3390/nano13050919.

[108] M. Han, D. Zhang, C.E. Shuck, B. McBride, T. Zhang, R. John Wang, K. Shevchuk, Y. Gogotsi, Electrochemically modulated interaction of MXenes with microwaves, Nat. Nanotechnol. 18 (2023), https://doi.org/10.1038/s41565-022-01308-9.

[109] D.N. Ampong, E. Agyekum, F.O. Agyemang, K. Mensah-Darkwa, A. Andrews, A. Kumar, R.K. Gupta, MXene: fundamentals to applications in electrochemical energy storage, Discover Nano 18 (2023), https://doi.org/10.1186/s11671-023-03786-9.

[110] Y. Li, H. Shao, Z. Lin, J. Lu, L. Liu, B. Duployer, P.O.Å. Persson, P. Eklund, L. Hultman, M. Li, K. Chen, X.H. Zha, S. Du, P. Rozier, Z. Chai, E. Raymundo-Piñero, P.L. Taberna, P. Simon, Q. Huang, A general Lewis acidic etching route for preparing MXenes with enhanced electrochemical performance in non-aqueous electrolyte, Nat. Mater. 19 (2020), https://doi.org/10.1038/s41563-020-0657-0.

[111] M. Rajapakse, B. Karki, U.O. Abu, S. Pishgar, M.R.K. Musa, S.M.S. Riyadh, M. Yu, G. Sumanasekera, J.B. Jasinski, Intercalation as a versatile tool for fabrication, property tuning, and phase transitions in 2D materials, NPJ 2D Mater Appl 5 (2021), https://doi.org/10.1038/s41699-021-00211-6.

[112] F. Kong, X. He, Q. Liu, X. Qi, Y. Zheng, R. Wang, Y. Bai, Improving the electrochemical properties of MXene Ti3C2 multilayer for Li-ion batteries by vacuum calcination, Electrochim. Acta 265 (2018), https://doi.org/10.1016/j.electacta.2018.01.196.

[113] Y. Dall'Agnese, P. Rozier, P.L. Taberna, Y. Gogotsi, P. Simon, Capacitance of two-dimensional titanium carbide (MXene) and MXene/carbon nanotube composites in organic electrolytes, J. Power Sources 306 (2016), https://doi.org/10.1016/j.jpowsour.2015.12.036.

[114] M.R. Lukatskaya, O. Mashtalir, C.E. Ren, Y. Dall'Agnese, P. Rozier, P.L. Taberna, M. Naguib, P. Simon, M.W. Barsoum, Y. Gogotsi, Cation intercalation and high volumetric capacitance of two-dimensional titanium carbide, Science 341 (2013), https://doi.org/10.1126/science.1241488 (1979).

[115] M.S. Ashiq, A. Iqbal, J. Shoukat, Anila, S. Kausar, K. Rizwan, A.A. Altaf, Diverse applications of MXene composites for electrochemical, Energy Storage (2023), https://doi.org/10.1007/978-981-99-2038-9_11.

[116] K. Hantanasirisakul, B. Anasori, S. Nemsak, J.L. Hart, J. Wu, Y. Yang, R. V. Chopdekar, P. Shafer, A.F. May, E.J. Moon, J. Zhou, Q. Zhang, M.L. Taheri, S. J. May, Y. Gogotsi, Evidence of a magnetic transition in atomically thin $Cr_2TiC_2T_x$ MXene, Nanoscale Horiz 5 (2020) 1557–1565, https://doi.org/10.1039/D0NH00343C.

[117] M. Han, K. Maleski, C.E. Shuck, Y. Yang, J.T. Glazar, A.C. Foucher, K. Hantanasirisakul, A. Sarycheva, N.C. Frey, S.J. May, V.B. Shenoy, E.A. Stach,

Y. Gogotsi, Tailoring electronic and optical properties of MXenes through forming solid solutions, J. Am. Chem. Soc. 142 (2020) 19110–19118, https://doi.org/10.1021/jacs.0c07395.
[118] A. VahidMohammadi, J. Rosen, Y. Gogotsi, The world of two-dimensional carbides and nitrides (MXenes), Science 372 (2021), https://doi.org/10.1126/science.abf1581 (1979).
[119] Y. Fan, L. Li, Y. Zhang, X. Zhang, D. Geng, W. Hu, Recent advances in growth of transition metal carbides and nitrides (MXenes) crystals, Adv. Funct. Mater. 32 (2022) 2111357, https://doi.org/10.1002/adfm.202111357.
[120] M. Alhabeb, K. Maleski, B. Anasori, P. Lelyukh, L. Clark, S. Sin, Y. Gogotsi, Guidelines for synthesis and processing of two-dimensional titanium carbide ($Ti_3C_2T_x$ MXene), Chem. Mater. 29 (2017) 7633–7644, https://doi.org/10.1021/acs.chemmater.7b02847.
[121] C.E. Shuck, A. Sarycheva, M. Anayee, A. Levitt, Y. Zhu, S. Uzun, V. Balitskiy, V. Zahorodna, O. Gogotsi, Y. Gogotsi, Scalable synthesis of $Ti_3C_2T_x$ MXene, Adv. Eng. Mater. 22 (2020) 1901241, https://doi.org/10.1002/adem.201901241.
[122] K. Hantanasirisakul, Y. Gogotsi, Electronic and optical properties of 2D transition metal carbides and nitrides (MXenes), Adv. Mater. 30 (2018) 1804779, https://doi.org/10.1002/adma.201804779.
[123] B. Soundiraraju, B.K. George, Two-dimensional titanium nitride (Ti_2N) MXene: synthesis, characterization, and potential application as surface-enhanced Raman scattering substrate, ACS Nano 11 (2017) 8892–8900, https://doi.org/10.1021/acsnano.7b03129.
[124] M. Naguib, M. Kurtoglu, V. Presser, J. Lu, J. Niu, M. Heon, L. Hultman, Y. Gogotsi, M.W. Barsoum, Two-dimensional nanocrystals produced by exfoliation of Ti3AlC2, Adv. Mater. 23 (2011) 4248–4253, https://doi.org/10.1002/adma.201102306.
[125] B. Anasori, M.R. Lukatskaya, Y. Gogotsi, 2D metal carbides and nitrides (MXenes) for energy storage, Nat. Rev. Mater. 2 (2017) 16098, https://doi.org/10.1038/natrevmats.2016.98.
[126] S. Yazdanparast, S. Soltanmohammad, A. Fash-White, G.J. Tucker, G. L. Brennecka, Synthesis and surface chemistry of 2D TiVC solid-solution MXenes, ACS Appl. Mater. Interfaces 12 (2020) 20129–20137, https://doi.org/10.1021/acsami.0c03181.
[127] G. Wang, H. Wu, Y. Liu, Y. Pang, J. Hao, F. Cheng, A. Qian, H. Shi, Surface fluorine preservation dependence of $Ti_3C_2T_x$ MXene for high electrochemical properties in ionic liquid electrolytes, Chem. Commun. 59 (2023) 1369–1372, https://doi.org/10.1039/D2CC06009D.
[128] M. Naguib, V.N. Mochalin, M.W. Barsoum, Y. Gogotsi, 25th anniversary article: MXenes: a new family of two-dimensional materials, Adv. Mater. 26 (2014) 992–1005, https://doi.org/10.1002/adma.201304138.
[129] Á. Morales-García, F. Calle-Vallejo, F. Illas, MXenes: new horizons in catalysis, ACS Catal. 10 (2020) 13487–13503, https://doi.org/10.1021/acscatal.0c03106.
[130] S.K. Nemani, B. Zhang, B.C. Wyatt, Z.D. Hood, S. Manna, R. Khaledialidusti, W. Hong, M.G. Sternberg, S.K.R.S. Sankaranarayanan, B. Anasori, High-entropy 2D carbide MXenes: TiVNbMoC$_3$ and TiVCrMoC$_3$, ACS Nano 15 (2021) 12815–12825, https://doi.org/10.1021/acsnano.1c02775.
[131] M. Khazaei, A. Ranjbar, K. Esfarjani, D. Bogdanovski, R. Dronskowski, S. Yunoki, Insights into exfoliation possibility of MAX phases to MXenes, Phys. Chem. Chem. Phys. 20 (2018) 8579–8592, https://doi.org/10.1039/C7CP08645H.
[132] P. Urbankowski, B. Anasori, K. Hantanasirisakul, L. Yang, L. Zhang, B. Haines, S. J. May, S.J.L. Billinge, Y. Gogotsi, 2D molybdenum and vanadium nitrides synthesized by ammoniation of 2D transition metal carbides (MXenes), Nanoscale 9 (2017) 17722–17730, https://doi.org/10.1039/C7NR06721F.
[133] J. Jeon, Y. Park, S. Choi, J. Lee, S.S. Lim, B.H. Lee, Y.J. Song, J.H. Cho, Y.H. Jang, S. Lee, Epitaxial synthesis of molybdenum carbide and formation of a Mo_2C/MoS_2 hybrid structure *via* chemical conversion of molybdenum disulfide, ACS Nano 12 (2018) 338–346, https://doi.org/10.1021/acsnano.7b06417.
[134] Y. Yang, S. Umrao, S. Lai, S. Lee, Large-area highly conductive transparent two-dimensional Ti_2CT_x film, J. Phys. Chem. Lett. 8 (2017) 859–865, https://doi.org/10.1021/acs.jpclett.6b03064.
[135] P. Urbankowski, B. Anasori, T. Makaryan, D. Er, S. Kota, P.L. Walsh, M. Zhao, V. B. Shenoy, M.W. Barsoum, Y. Gogotsi, Synthesis of two-dimensional titanium nitride Ti_4N_3 (MXene), Nanoscale 8 (2016) 11385–11391, https://doi.org/10.1039/C6NR02253G.
[136] I.R. Shein, A.L. Ivanovskii, Graphene-like titanium carbides and nitrides Tin+1Cn, Tin+1Nn (n=1, 2, and 3) from de-intercalated MAX phases: first-principles probing of their structural, electronic properties and relative stability, Comput. Mater. Sci. 65 (2012) 104–114, https://doi.org/10.1016/j.commatsci.2012.07.011.
[137] X. Xiao, H. Yu, H. Jin, M. Wu, Y. Fang, J. Sun, Z. Hu, T. Li, J. Wu, L. Huang, Y. Gogotsi, J. Zhou, Salt-templated synthesis of 2D metallic Mon and other nitrides, ACS Nano 11 (2017) 2180–2186, https://doi.org/10.1021/acsnano.6b08534.
[138] X. Zhao, W. Sun, D. Geng, W. Fu, J. Dan, Y. Xie, P.R.C. Kent, W. Zhou, S. J. Pennycook, K.P. Loh, Edge segregated polymorphism in 2D molybdenum carbide, Adv. Mater. 31 (2019) 1808343, https://doi.org/10.1002/adma.201808343.
[139] C. Xu, L. Wang, Z. Liu, L. Chen, J. Guo, N. Kang, X.-L. Ma, H.-M. Cheng, W. Ren, Large-area high-quality 2D ultrathin Mo2C superconducting crystals, Nat. Mater. 14 (2015) 1135–1141, https://doi.org/10.1038/nmat4374.
[140] G. Zhu, Y. Zhang, Properties of MXenes, 2022, pp. 37–52, https://doi.org/10.1007/978-3-031-05006-0_3.
[141] M. Tang, J. Li, Y. Wang, W. Han, S. Xu, M. Lu, W. Zhang, H. Li, Surface terminations of MXene: synthesis, characterization, and properties, Symmetry 14 (2022), https://doi.org/10.3390/sym14112232.
[142] S. Kumar Singh, A. Kumar Tiwari, H.K. Paliwal, A holistic review of MXenes for solar device applications: synthesis, characterization, properties and stability, FlatChem 39 (2023), https://doi.org/10.1016/j.flatc.2023.100493.
[143] M. Seredych, C.E. Shuck, D. Pinto, M. Alhabeb, E. Precetti, G. Deysher, B. Anasori, N. Kurra, Y. Gogotsi, High-temperature behavior and surface chemistry of carbide MXenes studied by thermal analysis, Chem. Mater. 31 (2019), https://doi.org/10.1021/acs.chemmater.9b00397.
[144] L.P. Yu, L. Xu, L. Lu, Z. Alhalili, X.H. Zhou, Thermal properties of MXenes and relevant applications, ChemPhysChem 23 (2022), https://doi.org/10.1002/cphc.202200203.
[145] S. Bismark, B. Tawiah, Thermal and crystallization behavior of MXene/polymer nanocomposites, in: MXene-Filled Polymer Nanocomposites, 2022, https://doi.org/10.1201/9781003164975-7.
[146] A.A. Shamsabadi, H. Fang, D. Zhang, A. Thakur, C.Y. Chen, A. Zhang, H. Wang, B. Anasori, M. Soroush, Y. Gogotsi, Z. Fakhraai, The evolution of MXenes conductivity and optical properties upon heating in air, Small Methods 7 (2023), https://doi.org/10.1002/smtd.202300568.
[147] W. Eom, H. Shin, T.H. Han, Tracking the thermal dynamics of Ti3C2Tx MXene with XPS and two-dimensional correlation spectroscopy, Appl. Phys. Lett. 122 (2023), https://doi.org/10.1063/5.0143298.
[148] E. Colin-Ulloa, A. Fitzgerald, K. Montazeri, J. Mann, V. Natu, K. Ngo, J. Uzarski, M.W. Barsoum, L.V. Titova, Ultrafast spectroscopy of plasmons and free carriers in 2D MXenes, Adv. Mater. 35 (2023), https://doi.org/10.1002/adma.202208659.
[149] H. Wu, J. Gu, Z. Li, W. Liu, H. Bao, H. Lin, Y. Yue, Characterization of phonon thermal transport of Ti3C2TxMXene thin film, J. Phys. Condens. Matter 34 (2022), https://doi.org/10.1088/1361-648X/ac4f1c.
[150] O. Gutsul, O. Szabo, N. Kumar, R. Pfeifer, B. Dzurnak, K. Sasitharan, V. Slobodyan, A. Kromka, B. Rezek, Electrical properties of MXene thin films prepared from non-aqueous polar aprotic solvents, J. Mater. Res. 38 (2023), https://doi.org/10.1557/s43578-023-01033-6.
[151] H. Cao, Y. Wang, A. Sarmah, K.-W. Liu, Z. Tan, K.D. Arole, J.L. Lutkenhaus, M. Radovic, M.J. Green, E.B. Pentzer, Electrically conductive porous $Ti_3C_2T_x$ MXene-polymer composites from high internal phase emulsions (HIPEs), 2D Mater. 9 (2022) 044004, https://doi.org/10.1088/2053-1583/ac914c.
[152] K.A.S. Usman, J. Zhang, C.J.O. Bacal, S. Qin, P. Mota-Santiago, P.A. Lynch, M. Naebe, L.C. Henderson, D. Hegh, J.M. Razal, Tension-induced toughening and conductivity enhancement in sequentially bridged MXene fibers, 2D Mater. 9 (2022), https://doi.org/10.1088/2053-1583/ac8c51.
[153] Z. Wang, M. Chen, Z. Cao, J. Liang, Z. Liu, Y. Xuan, L. Pan, K.M. Razeeb, Y. Wang, C. Wan, P.A. Zong, MXene nanosheet/organics superlattice for flexible thermoelectrics, ACS Appl. Nano Mater. 5 (2022), https://doi.org/10.1021/acsanm.2c03813.
[154] Q. Li, X. Zhi, Y. Xia, S. Han, W. Guo, M. Li, X. Wang, Ultrastretchable high-conductivity MXene-based organohydrogels for human health monitoring and machine-learning-assisted recognition, ACS Appl. Mater. Interfaces 15 (2023), https://doi.org/10.1021/acsami.3c00432.
[155] Y. Shibata, R. Suizu, K. Awaga, J. Hirotani, H. Omachi, Fabrication of MXene transparent conductive films via transfer process, APEX 16 (2023), https://doi.org/10.35848/1882-0786/acbbb8.
[156] B. Anasori, Y. Gogotsi, Introduction to 2D transition metal carbides and nitrides (MXenes), in: 2D Metal Carbides and Nitrides (MXenes): Structure, Properties and Applications, 2019, https://doi.org/10.1007/978-3-030-19026-2_1.
[157] M. Ghidiu, M.W. Barsoum, The {110} reflection in X-ray diffraction of MXene films: misinterpretation and measurement via non-standard orientation, J. Am. Ceram. Soc. 100 (2017), https://doi.org/10.1111/jace.15124.
[158] S.-N. Lai, W.Y. Chen, C.-C. Yen, Y.-S. Liao, P.-H. Chen, L. Stanciu, J.M. Wu, An ultraefficient surface functionalized $Ti_3C_2T_x$ MXene piezocatalyst: synchronous hydrogen evolution and wastewater treatment, J Mater Chem A Mater 12 (2024) 3340–3351, https://doi.org/10.1039/D3TA06291K.
[159] G. Zhu, Y. Zhang, Properties of MXenes, 2022, pp. 37–52, https://doi.org/10.1007/978-3-031-05006-0_3.
[160] T.B. Sobyra, K. Matthews, T.S. Mathis, Y. Gogotsi, P. Fenter, *Operando* X-ray reflectivity reveals the dynamical response of Ti_3C_2 MXene film structure during electrochemical cycling, ACS Energy Lett. 7 (2022) 3612–3617, https://doi.org/10.1021/acsenergylett.2c01577.
[161] K. Montazeri, H. Badr, K. Ngo, K. Sudhakar, T. Elmelegy, J. Uzarski, V. Natu, M. W. Barsoum, Delamination of MXene flakes using simple inorganic bases, J. Phys. Chem. C 127 (2023), https://doi.org/10.1021/acs.jpcc.3c02318.
[162] J. Wen, X. Zhang, H. Gao, Structural formation and charge storage mechanisms for intercalated two-dimensional carbides MXenes, Phys. Chem. Chem. Phys. 19 (2017) 9509–9518, https://doi.org/10.1039/C7CP00670E.
[163] C. Shi, M. Beidaghi, M. Naguib, O. Mashtalir, Y. Gogotsi, S.J.L. Billinge, Structure of Nanocrystalline Ti_3C_2 MXene Using Atomic Pair Distribution Function, Phys. Rev. Lett. 112 (2014) 125501, https://doi.org/10.1103/PhysRevLett.112.125501.
[164] A. Iakunkov, A. Nordenström, N. Boulanger, C. Hennig, I. Baburin, A.V. Talyzin, Temperature-dependent swelling transitions in MXene Ti3C2Tx, Nanoscale 14 (2022), https://doi.org/10.1039/d2nr03075f.
[165] A.C.Y. Yuen, T.B.Y. Chen, B. Lin, W. Yang, I.I. Kabir, I.M. De Cachinho Cordeiro, A.E. Whitten, J. Mata, B. Yu, H.D. Lu, G.H. Yeoh, Study of structure morphology and layer thickness of Ti3C2 MXene with Small-Angle Neutron Scattering (SANS),

Composites Part C: Open Access 5 (2021), https://doi.org/10.1016/j.jcomc.2021.100155.
[166] J. Zhang, K.A.S. Usman, M.A.N. Judicpa, D. Hegh, P.A. Lynch, J.M. Razal, Applications of X-ray-based characterization in MXene research, Small Methods 7 (2023), https://doi.org/10.1002/smtd.202201527.
[167] M. Shekhirev, C.E. Shuck, A. Sarycheva, Y. Gogotsi, Characterization of MXenes at every step, from their precursors to single flakes and assembled films, Prog. Mater. Sci. 120 (2021) 100757, https://doi.org/10.1016/j.pmatsci.2020.100757.
[168] E. Satheeshkumar, T. Makaryan, A. Melikyan, H. Minassian, Y. Gogotsi, M. Yoshimura, One-step solution processing of Ag, Au and Pd@MXene hybrids for SERS, Sci. Rep. 6 (2016) 32049, https://doi.org/10.1038/srep32049.
[169] A. Tariq, S.I. Ali, D. Akinwande, S. Rizwan, Efficient visible-light photocatalysis of 2D-MXene nanohybrids with Gd3+- and Sn4+-codoped bismuth ferrite, ACS Omega 3 (2018), https://doi.org/10.1021/acsomega.8b01951.
[170] A. Tariq, S.I. Ali, D. Akinwande, S. Rizwan, Efficient visible-light photocatalysis of 2D-MXene nanohybrids with Gd $^{3+}$ - and Sn $^{4+}$ -codoped bismuth ferrite, ACS Omega 3 (2018) 13828–13836, https://doi.org/10.1021/acsomega.8b01951.
[171] Y. Wang, Y. Xu, M. Hu, H. Ling, X. Zhu, MXenes: focus on optical and electronic properties and corresponding applications, Nanophotonics 9 (2020), https://doi.org/10.1515/nanoph-2019-0556.
[172] K. Laqua, W.H. Melhuish, M. Zander, Molecular absorption spectroscopy , ultraviolet and visible (Uv/Vis), Pure Appl. Chem. 60 (1988).
[173] UV–vis spectroscopy for monitoring oxidation state changes during electrochemical energy storage, Nat. Energy 8 (2023), https://doi.org/10.1038/s41560-023-01258-z.
[174] G. Murali, J.K.R. Modigunta, Y.H. Park, S.Y. Park, I. In, Stability and degradation of MXene, in: Engineering Materials, 2022, https://doi.org/10.1007/978-3-031-05006-0_5.
[175] S.-N. Lai, W.Y. Chen, C.-C. Yen, Y.-S. Liao, P.-H. Chen, L. Stanciu, J.M. Wu, An ultraefficient surface functionalized Ti $_3$ C $_2$ T $_x$ MXene piezocatalyst: synchronous hydrogen evolution and wastewater treatment, J Mater Chem A Mater 12 (2024) 3340–3351, https://doi.org/10.1039/D3TA06291K.
[176] S. Nandakumar, Y. Trabelsi, B. Vasudevan, S. Gunasekaran, MXene fractal-based dual-band metamaterial absorber in the visible and near-infrared regime, Opt. Quant. Electron. 55 (2023), https://doi.org/10.1007/s11082-023-05227-4.
[177] A.S. Sharbirin, S. Roy, T.T. Tran, S. Akhtar, J. Singh, D.L. Duong, J. Kim, Light-emitting Ti2N (MXene) quantum dots: synthesis, characterization and theoretical calculations, J Mater Chem C Mater 10 (2022), https://doi.org/10.1039/d2tc00568a.
[178] R. Li, L. Zhang, L. Shi, P. Wang, MXene Ti3C2: an effective 2D light-to-heat conversion material, ACS Nano 11 (2017), https://doi.org/10.1021/acsnano.6b08415.
[179] R. Li, L. Zhang, L. Shi, P. Wang, MXene Ti $_3$ C $_2$: an effective 2D light-to-heat conversion material, ACS Nano 11 (2017) 3752–3759, https://doi.org/10.1021/acsnano.6b08415.
[180] M. Ahmaruzzaman, MXenes and MXene-supported nanocomposites: a novel materials for aqueous environmental remediation, RSC Adv. 12 (2022), https://doi.org/10.1039/d2ra05530a.
[181] E. Satheeshkumar, T. Makaryan, A. Melikyan, H. Minassian, Y. Gogotsi, M. Yoshimura, One-step solution processing of Ag, Au and Pd@MXene hybrids for SERS, Sci. Rep. 6 (2016) 32049, https://doi.org/10.1038/srep32049.
[182] K.H. Norris, Understanding and correcting the factors which affect diffuse transmittance spectra, NIR News 12 (2001), https://doi.org/10.1255/nirn.613.
[183] J. Lee, Analysis of the effects of interface reflections on FTIR transmission spectra of thin layer samples, Vib. Spectrosc. 123 (2022), https://doi.org/10.1016/j.vibspec.2022.103456.
[184] L. Zhang, W. Song, H. Liu, H. Ding, Y. Yan, R. Chen, Influencing factors on synthesis and properties of MXene: a review, Processes 10 (2022), https://doi.org/10.3390/pr10091744.
[185] S. Thurakkal, X. Zhang, Noncovalent functionalization of Ti3C2TX using cationic porphyrins with enhanced stability against oxidation, Mater. Chem. Front. 6 (2022), https://doi.org/10.1039/d1qm01326b.
[186] B.C. Smith, Fundamentals of Fourier Transform Infrared Spectroscopy, second ed., 2011.
[187] M. Mahmood, A. Rasheed, I. Ayman, T. Rasheed, S. Munir, S. Ajmal, P. O. Agboola, M.F. Warsi, M. Shahid, Synthesis of ultrathin MnO $_2$ nanowire-intercalated 2D-MXenes for high-performance hybrid supercapacitors, Energy Fuel. 35 (2021) 3469–3478, https://doi.org/10.1021/acs.energyfuels.0c03939.
[188] Y. Li, X. Zhou, J. Wang, Q. Deng, M. Li, S. Du, Y.-H. Han, J. Lee, Q. Huang, Facile preparation of in situ coated Ti $_3$ C $_2$ T $_x$/Ni $_{0.5}$ Zn $_{0.5}$ Fe $_2$ O $_4$ composites and their electromagnetic performance, RSC Adv. 7 (2017) 24698–24708, https://doi.org/10.1039/C7RA03402D.
[189] I.M. Chirica, A.G. Mirea, Ş. Neaţu, M. Florea, M.W. Barsoum, F. Neaţu, Applications of MAX phases and MXenes as catalysts, J Mater Chem A Mater 9 (2021), https://doi.org/10.1039/d1ta04097a.
[190] H. Alnoor, A. Elsukova, J. Palisaitis, I. Persson, E.N. Tseng, J. Lu, L. Hultman, P.O. Å. Persson, Exploring MXenes and their MAX phase precursors by electron microscopy, Mater Today Adv 9 (2021) 100123, https://doi.org/10.1016/j.mtadv.2020.100123.
[191] A. Iqbal, J. Kwon, M.-K. Kim, C.M. Koo, MXenes for electromagnetic interference shielding: experimental and theoretical perspectives, Mater Today Adv 9 (2021) 100124, https://doi.org/10.1016/j.mtadv.2020.100124.
[192] A. Iqbal, J. Kwon, M.-K. Kim, C.M. Koo, MXenes for electromagnetic interference shielding: experimental and theoretical perspectives, Mater Today Adv 9 (2021) 100124, https://doi.org/10.1016/j.mtadv.2020.100124.
[193] A. Rawat, N.K. Chourasia, S.K. Saini, G. Rajput, A. Yadav, R.K. Chourasia, G. Gupta, P.K. Kulriya, Investigation of charge carrier dynamics in a Ti $_3$ C $_2$ T $_x$ MXene for ultrafast photonics applications, Mater Adv 4 (2023) 6427–6438, https://doi.org/10.1039/D3MA00429E.
[194] P. Dixit, T. Maiti, A facile pot synthesis of (Ti3AlC2) MAX phase and its derived MXene (Ti3C2Tx), Ceram. Int. 48 (2022), https://doi.org/10.1016/j.ceramint.2022.08.172.
[195] A. Sarycheva, Y. Gogotsi, Raman spectroscopy analysis of the structure and surface chemistry of Ti3C2Tx MXene, in: MXenes: from Discovery to Applications of Two-Dimensional Metal Carbides and Nitrides, 2023, https://doi.org/10.1201/9781003306511-16.
[196] M. Mustakeem, J.K. El-Demellawi, M. Obaid, F. Ming, H.N. Alshareef, N. Ghaffour, MXene-coated membranes for autonomous solar-driven desalination, ACS Appl. Mater. Interfaces 14 (2022) 5265–5274, https://doi.org/10.1021/acsami.1c20653.
[197] K. Raagulan, R. Braveenth, H. Jang, Y. Seon Lee, C.-M. Yang, B. Mi Kim, J. Moon, K. Chai, Electromagnetic shielding by MXene-graphene-PVDF composite with hydrophobic, lightweight and flexible graphene coated fabric, Materials 11 (2018) 1803, https://doi.org/10.3390/ma11101803.
[198] G. Ying, A.D. Dillon, A.T. Fafarman, M.W. Barsoum, Transparent, conductive solution processed spincast 2D Ti2CTx (MXene) films, Mater Res Lett 5 (2017), https://doi.org/10.1080/21663831.2017.1296043.
[199] H. Lashgari, M.R. Abolhassani, A. Boochani, S.M. Elahi, J. Khodadadi, Electronic and optical properties of 2D graphene-like compounds titanium carbides and nitrides: DFT calculations, Solid State Commun. 195 (2014), https://doi.org/10.1016/j.ssc.2014.06.008.
[200] Y. Bai, K. Zhou, N. Srikanth, J.H.L. Pang, X. He, R. Wang, Dependence of elastic and optical properties on surface terminated groups in two-dimensional MXene monolayers: a first-principles study, RSC Adv. 6 (2016), https://doi.org/10.1039/c6ra03090d.
[201] A.D. Dillon, M.J. Ghidiu, A.L. Krick, J. Griggs, S.J. May, Y. Gogotsi, M. W. Barsoum, A.T. Fafarman, Highly conductive optical quality solution-processed films of 2D titanium carbide, Adv. Funct. Mater. 26 (2016), https://doi.org/10.1002/adfm.201600357.
[202] R.R. Nair, P. Blake, A.N. Grigorenko, K.S. Novoselov, T.J. Booth, T. Stauber, N.M. R. Peres, A.K. Geim, Fine structure constant defines visual transparency of graphene, Science 320 (2008), https://doi.org/10.1126/science.1156965 (1979).
[203] G. Ying, S. Kota, A.D. Dillon, A.T. Fafarman, M.W. Barsoum, Conductive transparent V2CTx (MXene) films, FlatChem 8 (2018), https://doi.org/10.1016/j.flatc.2018.03.001.
[204] J.D. Gouveia, Á. Morales-García, F. Viñes, F. Illas, J.R.B. Gomes, MXenes as promising catalysts for water dissociation, Appl. Catal., B 260 (2020), https://doi.org/10.1016/j.apcatb.2019.118191.
[205] R. Khan, S. Andreescu, Mxenes-based bioanalytical sensors: design, characterization, and applications, Sensors 20 (2020), https://doi.org/10.3390/s20185434.
[206] X. Jiang, A.V. Kuklin, A. Baev, Y. Ge, H. Ågren, H. Zhang, P.N. Prasad, Two-dimensional MXenes: from morphological to optical, electric, and magnetic properties and applications, Phys. Rep. 848 (2020), https://doi.org/10.1016/j.physrep.2019.12.006.
[207] S. Wang, S. Zhao, X. Guo, G. Wang, 2D material-based heterostructures for rechargeable batteries, Adv. Energy Mater. 12 (2022), https://doi.org/10.1002/aenm.202100864.
[208] S. Pei, Z. Wang, J. Xia, High pressure studies of 2D materials and heterostructures: a review, Mater. Des. 213 (2022), https://doi.org/10.1016/j.matdes.2021.110363.
[209] Z. Zhang, S. Wang, X. Liu, Y. Chen, C. Su, Z. Tang, Y. Li, G. Xing, Metal halide perovskite/2D material heterostructures: syntheses and applications, Small Methods 5 (2021), https://doi.org/10.1002/smtd.202000937.
[210] K.S. Novoselov, A. Mishchenko, A. Carvalho, A.H. Castro Neto, 2D materials and van der Waals heterostructures, Science 353 (2016), https://doi.org/10.1126/science.aac9439 (1979).
[211] P.V. Pham, S.C. Bodepudi, K. Shehzad, Y. Liu, Y. Xu, B. Yu, X. Duan, 2D heterostructures for ubiquitous electronics and optoelectronics: principles, opportunities, and challenges, Chem. Rev. 122 (2022) 6514–6613, https://doi.org/10.1021/acs.chemrev.1c00735.
[212] L.D. Varma Sangani, R.S. Surya Kanthi, P. Chandra Adak, S. Sinha, A. H. Marchawala, T. Taniguchi, K. Watanabe, M.M. Deshmukh, Facile deterministic cutting of 2D materials for twistronics using a tapered fibre scalpel, Nanotechnology 31 (2020), https://doi.org/10.1088/1361-6528/ab8b93.
[213] Q. Fu, J. Han, X. Wang, P. Xu, T. Yao, J. Zhong, W. Zhong, S. Liu, T. Gao, Z. Zhang, L. Xu, B. Song, 2D transition metal dichalcogenides: design, modulation, and challenges in electrocatalysis, Adv. Mater. 33 (2021), https://doi.org/10.1002/adma.201907818.
[214] L. Zhang, Y. Tang, A.R. Khan, M.M. Hasan, P. Wang, H. Yan, T. Yildirim, J. F. Torres, G.P. Neupane, Y. Zhang, Q. Li, Y. Lu, 2D materials and heterostructures at extreme pressure, Adv. Sci. 7 (2020), https://doi.org/10.1002/advs.202002697.
[215] H. Tan, Y. Fan, Y. Zhou, Q. Chen, W. Xu, J.H. Warner, Ultrathin 2D photodetectors utilizing chemical vapor deposition grown WS $_2$ with graphene electrodes, ACS Nano 10 (2016) 7866–7873, https://doi.org/10.1021/acsnano.6b03722.
[216] W. Zhang, C.-P. Chuu, J.-K. Huang, C.-H. Chen, M.-L. Tsai, Y.-H. Chang, C.-T. Liang, Y.-Z. Chen, Y.-L. Chueh, J.-H. He, M.-Y. Chou, L.-J. Li, Ultrahigh-gain photodetectors based on atomically thin graphene-MoS2 heterostructures, Sci. Rep. 4 (2014) 3826, https://doi.org/10.1038/srep03826.

[217] K. Roy, M. Padmanabhan, S. Goswami, T.P. Sai, G. Ramalingam, S. Raghavan, A. Ghosh, Graphene–MoS2 hybrid structures for multifunctional photoresponsive memory devices, Nat. Nanotechnol. 8 (2013) 826–830, https://doi.org/10.1038/nnano.2013.206.
[218] Z. Feng, B. Chen, S. Qian, L. Xu, L. Feng, Y. Yu, R. Zhang, J. Chen, Q. Li, Q. Li, C. Sun, H. Zhang, J. Liu, W. Pang, D. Zhang, Chemical sensing by band modulation of a black phosphorus/molybdenum diselenide van der Waals heterostructure, 2D Mater. 3 (2016) 035021, https://doi.org/10.1088/2053-1583/3/3/035021.
[219] N. Mounet, M. Gibertini, P. Schwaller, D. Campi, A. Merkys, A. Marrazzo, T. Sohier, I.E. Castelli, A. Cepellotti, G. Pizzi, N. Marzari, Two-dimensional materials from high-throughput computational exfoliation of experimentally known compounds, Nat. Nanotechnol. 13 (2018) 246–252, https://doi.org/10.1038/s41565-017-0035-5.
[220] S.J. Gutierrez-Ojeda, R. Ponce-Pérez, J. Guerrero-Sánchez, M.G. Moreno-Armenta, MXene heterostructures based on Cr2C and Cr2N: evidence of strong interfacial interactions that induce an antiferromagnetic alignment, Graphene 2D Mater. (2023), https://doi.org/10.1007/s41127-023-00068-0.
[221] R. Yang, X. Chen, W. Ke, X. Wu, Recent research progress in the structure, fabrication, and application of MXene-based heterostructures, Nanomaterials 12 (2022), https://doi.org/10.3390/nano12111907.
[222] S. Nahirniak, B. Saruhan, MXene heterostructures as perspective materials for gas sensing applications, Sensors 22 (2022), https://doi.org/10.3390/s22030972.
[223] S.T. Mahmud, M.M. Hasan, S. Bain, S.T. Rahman, M. Rhaman, M.M. Hossain, M. Ordu, Multilayer MXene heterostructures and nanohybrids for multifunctional applications: a review, ACS Mater. Lett. 4 (2022), https://doi.org/10.1021/acsmaterialslett.2c00175.
[224] S. Zhang, X. Xu, X. Liu, Q. Yang, N. Shang, X. Zhao, X. Zang, C. Wang, Z. Wang, J. G. Shapter, Y. Yamauchi, Heterointerface optimization in a covalent organic framework-on-MXene for high-performance capacitive deionization of oxygenated saline water, Mater. Horiz. 9 (2022) 1708–1716, https://doi.org/10.1039/D1MH01882E.
[225] L. Zhou, Q. Tian, X. Shang, Y. Zhao, W. Yao, H. Liu, Q. Xu, Heterostructure construction of covalent organic frameworks/Ti3C2-MXene for high-efficiency electrocatalytic CO2 reduction, Green Chem. 26 (2023), https://doi.org/10.1039/d3gc03778a.
[226] R.A.B. John, K. Vijayan, N.L.W. Septiani, A. Hardiansyah, A.R. Kumar, B. Yuliarto, A. Hermawan, Gas-sensing mechanisms and performances of MXenes and MXene-based heterostructures, Sensors 23 (2023), https://doi.org/10.3390/s23218674.
[227] H.F. Zhang, J.Y. Xuan, Q. Zhang, M.L. Sun, F.C. Jia, X.M. Wang, G.C. Yin, S.Y. Lu, Strategies and challenges for enhancing performance of MXene-based gas sensors: a review, Rare Met. 41 (2022), https://doi.org/10.1007/s12598-022-02087-x.
[228] S. Iravani, R.S. Varma, MXenes and MXene-based materials for tissue engineering and regenerative medicine: recent advances, Mater Adv 2 (2021), https://doi.org/10.1039/d1ma00189b.
[229] P. Krishnaiah, H.T.A. Awan, R. Walvekar, S. Manickam, MXene-Based Composites and Their Applications, 2022, pp. 53–86, https://doi.org/10.1007/978-3-031-05006-0_4.
[230] X. Zhan, C. Si, J. Zhou, Z. Sun, MXene and MXene-based composites: synthesis, properties and environment-related applications, Nanoscale Horiz 5 (2020), https://doi.org/10.1039/c9nh00571d.
[231] A.A.P.R. Perera, K.A.U. Madhushani, B.T. Punchihewa, A. Kumar, R.K. Gupta, MXene-based nanomaterials for multifunctional applications, Materials 16 (2023), https://doi.org/10.3390/ma16031138.
[232] E.C. Ahn, 2D materials for spintronic devices, NPJ 2D Mater Appl 4 (2020), https://doi.org/10.1038/s41699-020-0152-0.
[233] H. Zhang, Introduction: 2D materials chemistry, Chem. Rev. 118 (2018) 6089–6090, https://doi.org/10.1021/acs.chemrev.8b00278.
[234] E. Lee, D.-J. Kim, Review— recent exploration of two-dimensional MXenes for gas sensing: from a theoretical to an experimental view, J. Electrochem. Soc. 167 (2020), https://doi.org/10.1149/2.0152003jes.
[235] L. Liu, M. Zhu, Z. Ma, X. Xu, S. Mohesen Seraji, B. Yu, Z. Sun, H. Wang, P. Song, A reactive copper-organophosphate-MXene heterostructure enabled antibacterial, self-extinguishing and mechanically robust polymer nanocomposites, Chem. Eng. J. 430 (2022) 132712, https://doi.org/10.1016/j.cej.2021.132712.
[236] W. Ma, K. Yang, C. Zhou, H. Li, Enhanced dielectric constant and suppressed electrical conductivity in polymer nanocomposite films via loading MXene/TiO2/MoS2 nanosheets, Ceram. Int. 48 (2022) 10447–10457, https://doi.org/10.1016/j.ceramint.2021.12.253.
[237] S. Kilikevičius, S. Kvietkaitė, K. Žukienė, M. Omastová, A. Aniskevich, D. Zeleniakienė, Numerical investigation of the mechanical properties of a novel hybrid polymer composite reinforced with graphene and MXene nanosheets, Comput. Mater. Sci. 174 (2020), https://doi.org/10.1016/j.commatsci.2019.109497.
[238] S. Mazhar, A.A. Qarni, Y. Ul Haq, Z. Ul Haq, I. Murtaza, Promising PVC/MXene based flexible thin film nanocomposites with excellent dielectric, thermal and mechanical properties, Ceram. Int. 46 (2020), https://doi.org/10.1016/j.ceramint.2020.02.023.
[239] X. Jin, J. Wang, L. Dai, X. Liu, L. Li, Y. Yang, Y. Cao, W. Wang, H. Wu, S. Guo, Flame-retardant poly(vinyl alcohol)/MXene multilayered films with outstanding electromagnetic interference shielding and thermal conductive performances, Chem. Eng. J. 380 (2020), https://doi.org/10.1016/j.cej.2019.122475.
[240] D. Wang, Y. Lin, D. Hu, P. Jiang, X. Huang, Multifunctional 3D-MXene/PDMS nanocomposites for electrical, thermal and triboelectric applications, Composer Part A Appl Sci Manuf 130 (2020), https://doi.org/10.1016/j.compositesa.2019.105754.
[241] Z. Huang, S. Wang, S. Kota, Q. Pan, M.W. Barsoum, C.Y. Li, Structure and crystallization behavior of poly(ethylene oxide)/Ti3C2Tx MXene nanocomposites, Polymer 102 (2016), https://doi.org/10.1016/j.polymer.2016.09.011.
[242] A.A. Shamsabadi, A.P. Isfahani, S.K. Salestan, A. Rahimpour, B. Ghalei, E. Sivaniah, M. Soroush, Pushing rubbery polymer membranes to Be economic for CO2 separation: embedment with Ti3C2Tx MXene nanosheets, ACS Appl. Mater. Interfaces 12 (2020), https://doi.org/10.1021/acsami.9b19960.
[243] G. Liu, S. Liu, K. Ma, H. Wang, X. Wang, G. Liu, W. Jin, Polyelectrolyte functionalized ti2ct x mxene membranes for pervaporation dehydration of isopropanol/water mixtures, Ind. Eng. Chem. Res. 59 (2020), https://doi.org/10.1021/acs.iecr.9b06881.
[244] M.S. Carey, M. Sokol, G.R. Palmese, M.W. Barsoum, Water transport and thermomechanical properties of Ti3C2T z MXene epoxy nanocomposites, ACS Appl. Mater. Interfaces 11 (2019), https://doi.org/10.1021/acsami.9b11448.
[245] Q. Pan, Y. Zheng, S. Kota, W. Huang, S. Wang, H. Qi, S. Kim, Y. Tu, M. W. Barsoum, C.Y. Li, 2D MXene-containing polymer electrolytes for all-solid-state lithium metal batteries, Nanoscale Adv. 1 (2019), https://doi.org/10.1039/c8na00206a.
[246] G. Choudalakis, A.D. Gotsis, Permeability of polymer/clay nanocomposites: a review, Eur. Polym. J. 45 (2009), https://doi.org/10.1016/j.eurpolymj.2009.01.027.
[247] L.E. Nielsen, Models for the permeability of filled polymer systems, J. Macromol. Sci. Part A - Chemistry 1 (1967), https://doi.org/10.1080/10601326708053745.
[248] Y. Shi, C. Liu, L. Liu, L. Fu, B. Yu, Y. Lv, F. Yang, P. Song, Strengthening, toughing and thermally stable ultra-thin MXene nanosheets/polypropylene nanocomposites via nanoconfinement, Chem. Eng. J. 378 (2019), https://doi.org/10.1016/j.cej.2019.122267.
[249] X. Sheng, Y. Zhao, L. Zhang, X. Lu, Properties of two-dimensional Ti3C2 MXene/thermoplastic polyurethane nanocomposites with effective reinforcement via melt blending, Compos. Sci. Technol. 181 (2019), https://doi.org/10.1016/j.compscitech.2019.107710.
[250] Z. Jia, W. Zhang, B. Tang, S. Zhu, M. Liu, B. Zhong, Y. Luo, F. Liu, D. Jia, L. Kong, Rational design for enhancing mechanical and conductive properties of Ti3C2 MXene based elastomer composites, Compos. Commun. 25 (2021), https://doi.org/10.1016/j.coco.2021.100725.
[251] M. Naguib, T. Saito, S. Lai, M.S. Rager, T. Aytug, M. Parans Paranthaman, M. Q. Zhao, Y. Gogotsi, Ti3C2TX (MXene)-polyacrylamide nanocomposite films, RSC Adv. 6 (2016), https://doi.org/10.1039/c6ra10384g.
[252] R. Giménez, B. Serrano, V. San-Miguel, J.C. Cabanelas, Recent advances in MXene/epoxy composites: trends and prospects, Polymers 14 (2022), https://doi.org/10.3390/polym14061170.
[253] R. Sun, H. Bin Zhang, J. Liu, X. Xie, R. Yang, Y. Li, S. Hong, Z.Z. Yu, Highly conductive transition metal carbide/carbonitride(MXene)@polystyrene nanocomposites fabricated by electrostatic assembly for highly efficient electromagnetic interference shielding, Adv. Funct. Mater. 27 (2017), https://doi.org/10.1002/adfm.201702807.
[254] Y. Feng, H. Wang, J. Xu, X. Du, X. Cheng, Z. Du, H. Wang, Fabrication of MXene/PEI functionalized sodium alginate aerogel and its excellent adsorption behavior for Cr(VI) and Congo Red from aqueous solution, J. Hazard Mater. 416 (2021), https://doi.org/10.1016/j.jhazmat.2021.125777.
[255] A. Feng, T. Hou, Z. Jia, Y. Zhang, F. Zhang, G. Wu, Preparation and characterization of epoxy resin filled with Ti3C2Tx MXene nanosheets with excellent electric conductivity, Nanomaterials 10 (2020), https://doi.org/10.3390/nano10010162.
[256] K. Rajavel, S. Luo, Y. Wan, X. Yu, Y. Hu, P. Zhu, R. Sun, C. Wong, 2D Ti3C2Tx MXene/polyvinylidene fluoride (PVDF) nanocomposites for attenuation of electromagnetic radiation with excellent heat dissipation, Composer Part A Appl Sci Manuf 129 (2020), https://doi.org/10.1016/j.compositesa.2019.105693.
[257] L. Wang, H. Qiu, P. Song, Y. Zhang, Y. Lu, C. Liang, J. Kong, L. Chen, J. Gu, 3D Ti3C2Tx MXene/C hybrid foam/epoxy nanocomposites with superior electromagnetic interference shielding performances and robust mechanical properties, Composer Part A Appl Sci Manuf 123 (2019), https://doi.org/10.1016/j.compositesa.2019.05.030.
[258] L. Guo, Z. Zhang, M. Li, R. Kang, Y. Chen, G. Song, S.T. Han, C. Te Lin, N. Jiang, J. Yu, Extremely high thermal conductivity of carbon fiber/epoxy with synergistic effect of MXenes by freeze-drying, Compos. Commun. 19 (2020), https://doi.org/10.1016/j.coco.2020.03.009.
[259] S. Tu, Q. Jiang, X. Zhang, H.N. Alshareef, Large dielectric constant enhancement in MXene percolative polymer composites, ACS Nano 12 (2018), https://doi.org/10.1021/acsnano.7b08895.
[260] J. Shao, J.W. Wang, D.N. Liu, L. Wei, S.Q. Wu, H. Ren, A novel high permittivity percolative composite with modified MXene, Polymer 174 (2019), https://doi.org/10.1016/j.polymer.2019.04.057.
[261] S.A. Mirkhani, A. Shayesteh Zeraati, E. Aliabadian, M. Naguib, U. Sundararaj, High dielectric constant and low dielectric loss via poly(vinyl alcohol)/Ti3C2Tx MXene nanocomposites, ACS Appl. Mater. Interfaces 11 (2019), https://doi.org/10.1021/acsami.9b00393.
[262] Q. Deng, F. Zhou, B. Qin, Y. Feng, Z. Xu, Eco-friendly poly(vinyl alcohol)/delaminated V2C MXene high-k nanocomposites with low dielectric loss enabled by moderate polarization and charge density at the interface, Ceram. Int. 46 (2020), https://doi.org/10.1016/j.ceramint.2020.07.218.
[263] Y. Feng, F. Zhou, M. Bo, Y. Huang, Q. Deng, C. Peng, Enabling high dielectric response in PVDF/V2C MXene-TiO2 composites based on nontypical V-F-Ti

bonding and fermi-level overlapping mechanisms, J. Phys. Chem. C 124 (2020), https://doi.org/10.1021/acs.jpcc.0c08444.
[264] J. Gu, Q. Zhang, J. Dang, C. Xie, Thermal conductivity epoxy resin composites filled with boron nitride, Polym. Adv. Technol. 23 (2012), https://doi.org/10.1002/pat.2063.
[265] J. Zhang, Y. Liu, Z. Lv, T. Zhao, P. Li, Y. Sun, J. Wang, Sulfonated Ti3C2Tx to construct proton transfer pathways in polymer electrolyte membrane for enhanced conduction, Solid State Ionics 310 (2017), https://doi.org/10.1016/j.ssi.2017.08.013.
[266] P.E. Lokhande, A. Pakdel, H.M. Pathan, D. Kumar, D.V.N. Vo, A. Al-Gheethi, A. Sharma, S. Goel, P.P. Singh, B.K. Lee, Prospects of MXenes in energy storage applications, Chemosphere 297 (2022), https://doi.org/10.1016/j.chemosphere.2022.134225.
[267] R.K. Mishra, H.J. Maria, K. Joseph, S. Thomas, Basic structural and properties relationship of recyclable microfibrillar composite materials from immiscible plastics blends: an introduction. https://doi.org/10.1016/B978-0-08-101991-7.00001-7, 2017.
[268] S.V.S. Prasad, R.K. Mishra, S. Gupta, S.B. Prasad, S. Singh, Introduction, history, and origin of two dimensional (2D), Materials (2021) 1–9, https://doi.org/10.1007/978-981-16-3322-5_1.
[269] Y. Zhou, R. Li, Z. Lv, J. Liu, H. Zhou, C. Xu, Green hydrogen: a promising way to the carbon-free society, Chin. J. Chem. Eng. 43 (2022), https://doi.org/10.1016/j.cjche.2022.02.001.
[270] Q. Zhu, J. Li, P. Simon, B. Xu, Two-dimensional MXenes for electrochemical capacitor applications: progress, challenges and perspectives, Energy Storage Mater. 35 (2021), https://doi.org/10.1016/j.ensm.2020.11.035.
[271] M.K. Aslam, Y. Niu, M. Xu, MXenes for non-lithium-ion (Na, K, Ca, Mg, and Al) batteries and supercapacitors, Adv. Energy Mater. 11 (2021), https://doi.org/10.1002/aenm.202000681.
[272] C. Yang, H. Huang, H. He, L. Yang, Q. Jiang, W. Li, Recent advances in MXene-based nanoarchitectures as electrode materials for future energy generation and conversion applications, Coord. Chem. Rev. 435 (2021), https://doi.org/10.1016/j.ccr.2021.213806.
[273] M.R. Lukatskaya, S. Kota, Z. Lin, M.Q. Zhao, N. Shpigel, M.D. Levi, J. Halim, P. L. Taberna, M.W. Barsoum, P. Simon, Y. Gogotsi, Ultra-high-rate pseudocapacitive energy storage in two-dimensional transition metal carbides, Nat. Energy 6 (2017), https://doi.org/10.1038/nenergy.2017.105.
[274] P. Das, Z.S. Wu, MXene for energy storage: present status and future perspectives, JPhys Energy 2 (2020), https://doi.org/10.1088/2515-7655/ab9b1d.
[275] H. Shi, C.J. Zhang, P. Lu, Y. Dong, P. Wen, Z.S. Wu, Conducting and lithiophilic MXene/graphene framework for high-capacity, dendrite-free lithium-metal anodes, ACS Nano 13 (2019), https://doi.org/10.1021/acsnano.9b07710.
[276] Y. Xia, T.S. Mathis, M.-Q. Zhao, B. Anasori, A. Dang, Z. Zhou, H. Cho, Y. Gogotsi, S. Yang, Thickness-independent capacitance of vertically aligned liquid-crystalline MXenes, Nature 557 (2018) 409–412, https://doi.org/10.1038/s41586-018-0109-z.
[277] L. Yao, S. Ju, X. Yu, Rational surface engineering of MXene@N-doped hollow carbon dual-confined cobalt sulfides/selenides for advanced aluminum batteries, J Mater Chem A Mater 9 (2021), https://doi.org/10.1039/d1ta03465k.
[278] T.B. Sobyra, K. Matthews, T.S. Mathis, Y. Gogotsi, P. Fenter, *Operando* X-ray reflectivity reveals the dynamical response of Ti_3C_2 MXene film structure during electrochemical cycling, ACS Energy Lett. 7 (2022) 3612–3617, https://doi.org/10.1021/acsenergylett.2c01577.
[279] J. Zhou, X. Zha, X. Zhou, F. Chen, G. Gao, S. Wang, C. Shen, T. Chen, C. Zhi, P. Eklund, S. Du, J. Xue, W. Shi, Z. Chai, Q. Huang, Synthesis and electrochemical properties of two-dimensional hafnium carbide, ACS Nano 11 (2017) 3841–3850, https://doi.org/10.1021/acsnano.7b00030.
[280] X. Guo, H. Gao, S. Wang, G. Yang, X. Zhang, J. Zhang, H. Liu, G. Wang, MXene-based aerogel anchored with antimony single atoms and quantum dots for high-performance potassium-ion batteries, Nano Lett. 22 (2022) 1225–1232, https://doi.org/10.1021/acs.nanolett.1c04389.
[281] J. Zhu, X. Zhang, H. Gao, Y. Shao, Y. Liu, Y. Zhu, J. Zhang, L. Li, VS4 anchored on Ti3C2 MXene as a high-performance cathode material for magnesium ion battery, J. Power Sources 518 (2022) 230731, https://doi.org/10.1016/j.jpowsour.2021.230731.
[282] M. Ghidiu, M.R. Lukatskaya, M.Q. Zhao, Y. Gogotsi, M.W. Barsoum, Conductive two-dimensional titanium carbide “clay” with high volumetric capacitance, Nature 516 (2015), https://doi.org/10.1038/nature13970.
[283] J. Luo, X. Tao, J. Zhang, Y. Xia, H. Huang, L. Zhang, Y. Gan, C. Liang, W. Zhang, Sn4+ ion decorated highly conductive Ti3C2 MXene: promising lithium-ion anodes with enhanced volumetric capacity and cyclic performance, ACS Nano 10 (2016), https://doi.org/10.1021/acsnano.5b07333.
[284] Z. Ling, C.E. Ren, M.Q. Zhao, J. Yang, J.M. Giammarco, J. Qiu, M.W. Barsoum, Y. Gogotsi, Flexible and conductive MXene films and nanocomposites with high capacitance, Proc. Natl. Acad. Sci. U. S. A. 111 (2014), https://doi.org/10.1073/pnas.1414215111.
[285] M. Beidaghi, B. Anasori, Y. Gogotsi, M.W. Barsoum, Electrochemical properties of ordered, two-dimensional, double transition metals carbides (MXenes), ECS Meeting Abstracts MA2015-02 (2015), https://doi.org/10.1149/ma2015-02/9/557.
[286] S. Zheng, X. Shi, P. Das, Z.S. Wu, X. Bao, The road towards planar microbatteries and micro-supercapacitors: from 2D to 3D device geometries, Adv. Mater. 31 (2019), https://doi.org/10.1002/adma.201900583.
[287] N. Kurra, M. Alhabeb, K. Maleski, C.H. Wang, H.N. Alshareef, Y. Gogotsi, Bistacked titanium carbide (MXene) anodes for hybrid sodium-ion capacitors, ACS Energy Lett. 3 (2018), https://doi.org/10.1021/acsenergylett.8b01062.
[288] G.S. Gund, J.H. Park, R. Harpalsinh, M. Kota, J.H. Shin, T. il Kim, Y. Gogotsi, H. S. Park, MXene/polymer hybrid materials for flexible AC-filtering electrochemical capacitors, Joule 3 (2019), https://doi.org/10.1016/j.joule.2018.10.017.
[289] M.S. Jayalakshmy, R.K. Mishra, Applications of carbon-based nanofiller-incorporated rubber composites in the fields of tire engineering, flexible electronics and EMI shielding, in: Carbon-Based Nanofillers and Their Rubber Nanocomposites, Elsevier, 2019, pp. 441–472, https://doi.org/10.1016/B978-0-12-817342-8.00014-7.
[290] R.K. Mishra, A. Dutta, P. Mishra, S. Thomas, Recent progress in electromagnetic absorbing materials, in: Advanced Materials for Electromagnetic Shielding, 2018, https://doi.org/10.1002/9781119128625.ch7.
[291] R.K. Mishra, Progress in polymer nanocomposites for electromagnetic shielding application, in: Reza K. Haghi (Ed.), Modern Physical Chemistry: Engineering Models, Materials, and Methods with Applications, first ed., Apple Academic Press, New York, 2018, pp. 198–237.
[292] Y. Duan, X. Fang, Z. Zhang, R. Sun, J. Hong, F. Ruan, Q. Hu, Z. Xu, Lightweight, flexible rCEF@PPy/MXene for ultra-efficient EMI shielding felt with Joule heating performance, Mater. Lett. 341 (2023) 134297, https://doi.org/10.1016/j.matlet.2023.134297.
[293] X. Yang, J. Luo, H. Ren, Y. Xue, C. Yang, T. Yuan, Z. Yang, Y. Liu, H. Zhang, J. Yu, Simultaneously improving the EMI shielding performances and mechanical properties of CF/PEKK composites via MXene interfacial modification, J. Mater. Sci. Technol. 154 (2023) 202–209, https://doi.org/10.1016/j.jmst.2023.01.020.
[294] D. Huang, Y. Chen, L. Zhang, X. Sheng, Flexible thermoregulatory microcapsule/polyurethane-MXene composite films with multiple thermal management functionalities and excellent EMI shielding performance, J. Mater. Sci. Technol. 165 (2023) 27–38, https://doi.org/10.1016/j.jmst.2023.05.013.
[295] V.T. Nguyen, B.K. Min, Y. Yi, S.J. Kim, C.G. Choi, MXene(Ti3C2TX)/graphene/PDMS composites for multifunctional broadband electromagnetic interference shielding skins, Chem. Eng. J. 393 (2020), https://doi.org/10.1016/j.cej.2020.124608.
[296] R.K. Mishra, M.G. Thomas, J. Abraham, K. Joseph, S. Thomas, Electromagnetic interference shielding materials for aerospace application, in: Advanced Materials for Electromagnetic Shielding, Wiley, 2018, pp. 327–365, https://doi.org/10.1002/9781119128625.ch15.
[297] R.K. Mishra, A. Shaji, S. Thomas, Processing, rheology, barrier properties, and theoretical study of microfibrillar and nanofibrillar in situ composites. https://doi.org/10.1016/B978-0-08-101991-7.00010-8, 2017.
[298] R.K. Mishra, S. Loganathan, S. Thomas, In-situ microfibrillar/nanofibrillar single polymer composites: preparation, characterization, and application. https://doi.org/10.1016/B978-0-08-101991-7.00005-4, 2017.
[299] Y. Zhang, W. Wang, J. Xie, K. Dai, F. Zhang, Q. Zheng, Smart and flexible CNTs@MXene heterostructure-decorated cellulose films with excellent electrothermal/photothermal conversion and EMI shielding performances, Carbon N Y 200 (2022) 491–499, https://doi.org/10.1016/j.carbon.2022.08.040.
[300] X. Zheng, P. Wang, X. Zhang, Q. Hu, Z. Wang, W. Nie, L. Zou, C. Li, X. Han, Breathable, durable and bark-shaped MXene/textiles for high-performance wearable pressure sensors, EMI shielding and heat physiotherapy, Composer Part A Appl Sci Manuf 152 (2022) 106700, https://doi.org/10.1016/j.compositesa.2021.106700.
[301] Z. Sha, H. He, H. Ma, B. Hong, J. Lu, X. Fei, M. Zhu, All-in-one integrated flexible PE@PET/MXene films for high-performance electromagnetic shields with self-reinforced conductivity and mechanical properties, Carbon N Y 216 (2024) 118595, https://doi.org/10.1016/j.carbon.2023.118595.
[302] P. Dehghan, M. Simiari, M. Gholampour, M. Aghvami-Panah, A. Amirkiai, Tuning the electromagnetic interference shielding performance of polypropylene cellular nanocomposites: role of hybrid nanofillers of MXene and reduced graphene oxide, Polym. Test. 126 (2023) 108162, https://doi.org/10.1016/j.polymertesting.2023.108162.
[303] F. Jia, J. Dong, X. Dai, Y. Liu, H. Wang, Z. Lu, Robust, flexible, and stable CuNWs/MXene/ANFs hybrid film constructed by structural assemble strategy for efficient EMI shielding, Chem. Eng. J. 452 (2023) 139395, https://doi.org/10.1016/j.cej.2022.139395.
[304] H. Tan, J. Gou, X. Zhang, L. Ding, H. Wang, Sandwich-structured Ti3C2Tx-MXene/reduced-graphene-oxide composite membranes for high-performance electromagnetic interference and infrared shielding, J. Membr. Sci. 675 (2023) 121560, https://doi.org/10.1016/j.memsci.2023.121560.
[305] N. Duan, Z. Shi, J. Wang, C. Zhang, J. Xi, X. Yang, G. Wang, Multilayer Ti3C2Tx MXene/graphene oxide/carbon fiber fabric/thermoplastic polyurethane composite for improved mechanical and electromagnetic interference shielding performance, Colloids Surf. A Physicochem. Eng. Asp. 677 (2023) 132339, https://doi.org/10.1016/j.colsurfa.2023.132339.
[306] S. Feng, Z. Zhan, Y. Yi, Z. Zhou, C. Lu, Facile fabrication of MXene/cellulose fiber composite film with homogeneous and aligned structure via wet co-milling for enhancing electromagnetic interference shielding performance, Composer Part A Appl Sci Manuf 157 (2022) 106907, https://doi.org/10.1016/j.compositesa.2022.106907.
[307] Z. Wang, S. Wang, Z. Du, L. Yang, X. Cheng, H. Wang, Multifunctional wearable electronic textile based on fabric modified by MXene/Ag NWs for pressure sensing, EMI and personal thermal management, Compos. B Eng. 266 (2023) 110999, https://doi.org/10.1016/j.compositesb.2023.110999.
[308] Y. Hu, J. Chen, G. Yang, Y. Li, M. Dong, H. Zhang, E. Bilotti, J. Jiang, D. G. Papageorgiou, Highly conductive and mechanically robust MXene@CF core-shell composites for in-situ damage sensing and electromagnetic interference shielding, Compos. Sci. Technol. 246 (2024) 110356, https://doi.org/10.1016/j.compscitech.2023.110356.

[309] X. Yang, W. He, Q. Xu, H. Wang, H. Xing, J. Feng, X. Zhu, X. Li, J. Zhang, X. Zheng, Flexible and ultrathin GO@MXene sandwich-type multilayered film toward superior electromagnetic interference shielding in a wide gigahertz range of 3.95–18.0 GHz, J. Alloys Compd. 946 (2023) 169338, https://doi.org/10.1016/j.jallcom.2023.169338.
[310] G. Zhao, C. Sui, L. Miao, J. Li, L. Wen, G. Cheng, C. Zhao, W. Hao, Y. Sang, J. Li, Z. Zhang, Y. Zhao, F. Wang, R. Liu, X. He, C. Wang, Strong and continuous MXene/sodium alginate composite fibers prepared by immersion rotary jet spinning process with outstanding electromagnetic interference shielding performance, Chem. Eng. J. 469 (2023) 143983, https://doi.org/10.1016/j.cej.2023.143983.
[311] M.C. Vu, D. Mani, J.-B. Kim, T.-H. Jeong, S. Park, G. Murali, I. In, J.-C. Won, D. Losic, C.-S. Lim, S.-R. Kim, Hybrid shell of MXene and reduced graphene oxide assembled on PMMA bead core towards tunable thermoconductive and EMI shielding nanocomposites, Composer Part A Appl Sci Manuf 149 (2021) 106574, https://doi.org/10.1016/j.compositesa.2021.106574.
[312] Y. Li, K. Wu, M. Zhang, X. Yang, W. Feng, P. Wang, K. Li, Y. Zhan, Z. Zhou, Flexible MXene/Graphene oxide films with long-lasting electromagnetic interference shielding performance, Ceram. Int. 48 (2022) 37032–37038, https://doi.org/10.1016/j.ceramint.2022.08.275.
[313] Y. Zhang, Q. Gao, S. Zhang, X. Fan, J. Qin, X. Shi, G. Zhang, rGO/MXene sandwich-structured film at spunlace non-woven fabric substrate: application to EMI shielding and electrical heating, J. Colloid Interface Sci. 614 (2022) 194–204, https://doi.org/10.1016/j.jcis.2022.01.030.
[314] X.-A. Ye, S.-Y. Zhang, D.-Q. Zhao, L. Ding, K. Fang, X. Zhou, G.-G. Wang, Super-flexible and highly conductive H-Ti3C2Tx MXene composite films with 3D macro-assemblies for electromagnetic interference shielding, Composer Part A Appl Sci Manuf 176 (2024) 107866, https://doi.org/10.1016/j.compositesa.2023.107866.
[315] J. Xiong, R. Ding, Z. Liu, H. Zheng, P. Li, Z. Chen, Q. Yan, X. Zhao, F. Xue, Q. Peng, X. He, High-strength, super-tough, and durable nacre-inspired MXene/heterocyclic aramid nanocomposite films for electromagnetic interference shielding and thermal management, Chem. Eng. J. 474 (2023) 145972, https://doi.org/10.1016/j.cej.2023.145972.
[316] M. Xiang, R. Yang, H. Zhuang, J. Wu, C. Liu, Z. Yang, S. Dong, Electromagnetic interference shielding composites obtained from waste face masks, MXene and polyethylene terephthalate micro plastics, Journal of Hazardous Materials Advances 12 (2023) 100365, https://doi.org/10.1016/j.hazadv.2023.100365.
[317] H. Yue, Y. Ou, J. Wang, H. Wang, Z. Du, X. Du, X. Cheng, Ti3C2Tx MXene/delignified wood supported flame-retardant phase-change composites with superior solar-thermal conversion efficiency and highly electromagnetic interference shielding for efficient thermal management, Energy 286 (2024) 129441, https://doi.org/10.1016/j.energy.2023.129441.
[318] J. Liu, Y. Liu, M. Zou, W. Zhang, S. Peng, K. Liu, J. Hua, Electrostatic induced self-assembled MXene/EPOSS for high-performance electromagnetic interference shielding materials, Polym. Test. 126 (2023) 108142, https://doi.org/10.1016/j.polymertesting.2023.108142.
[319] L. Ran, L. Qiu, F. Sun, Z. Chen, L. Zhao, L. Yi, X. Ji, Multilayer assembly of strong and tough MXene/cellulose films for excellent electromagnetic shielding, J. Alloys Compd. 961 (2023) 171020, https://doi.org/10.1016/j.jallcom.2023.171020.
[320] K. Gong, Y. Peng, A. Liu, S. Qi, H. Qiu, Ultrathin carbon layer coated MXene/PBO nanofiber films for excellent electromagnetic interference shielding and thermal stability, Composer Part A Appl Sci Manuf 176 (2024) 107857, https://doi.org/10.1016/j.compositesa.2023.107857.
[321] Z. Cai, Y. Ma, M. Yun, M. Wang, Z. Tong, J. Suhr, L. Xiao, S. Jia, X. Chen, Multifunctional MXene/holey graphene films for electromagnetic interference shielding, Joule heating, and photothermal conversion, Compos. B Eng. 251 (2023) 110477, https://doi.org/10.1016/j.compositesb.2022.110477.
[322] I. Ihsanullah, M. Bilal, Potential of MXene-based membranes in water treatment and desalination: a critical review, Chemosphere 303 (2022) 135234, https://doi.org/10.1016/j.chemosphere.2022.135234.
[323] Raghvendra Kumar Mishra, 3 graphene-based fibers and their application in advanced composites system, in: Composite Materials for Industry, Electronics, and the Environment: Research and Applications, CRC Press, 2019, pp. 3–23.
[324] S. Yaragalla, R. Mishra, S. Thomas, N. Kalarikkal, H.J. Maria, Carbon-based nanofillers and their rubber nanocomposites. https://doi.org/10.1016/C2016-0-03648-3, 2018.
[325] H. Assad, I. Fatma, A. Kumar, S. Kaya, D.-V.N. Vo, A. Al-Gheethi, A. Sharma, An overview of MXene-Based nanomaterials and their potential applications towards hazardous pollutant adsorption, Chemosphere 298 (2022) 134221, https://doi.org/10.1016/j.chemosphere.2022.134221.
[326] Y.A.J. Al-Hamadani, B.-M. Jun, M. Yoon, N. Taheri-Qazvini, S.A. Snyder, M. Jang, J. Heo, Y. Yoon, Applications of MXene-based membranes in water purification: a review, Chemosphere 254 (2020) 126821, https://doi.org/10.1016/j.chemosphere.2020.126821.
[327] S.S. Ray, T.S.K. Sharma, R. Singh, A. Ratley, W.M. Choi, Y.-H. Ahn, D. Sangeetha, Y.-N. Kwon, Towards the next generation improved throughput MXene-based membrane for environmental applications: a holistic review, J. Environ. Chem. Eng. 11 (2023) 110243, https://doi.org/10.1016/j.jece.2023.110243.
[328] Q. Lin, Y. Liu, Z. Yang, Z. He, H. Wang, L. Zhang, M. Belle Marie Yap Ang, G. Zeng, Construction and application of two-dimensional MXene-based membranes for water treatment: a mini-review, Results in Engineering 15 (2022) 100494, https://doi.org/10.1016/j.rineng.2022.100494.
[329] J. Yang, S. Zhu, H. Zhang, Polycation-intercalated MXene membrane with enhanced permselective and anti-microbial properties, Nanomaterials 13 (2023) 2885, https://doi.org/10.3390/nano13212885.
[330] R. Akhter, S.S. Maktedar, MXenes: a comprehensive review of synthesis, properties, and progress in supercapacitor applications, Journal of Materiomics 9 (2023) 1196–1241, https://doi.org/10.1016/j.jmat.2023.08.011.
[331] A. Khosla, Sonu, H.T.A. Awan, K. Singh, Gaurav, R. Walvekar, Z. Zhao, A. Kaushik, M. Khalid, V. Chaudhary, Emergence of MXene and MXene–polymer hybrid membranes as future- environmental remediation strategies, Adv. Sci. 9 (2022), https://doi.org/10.1002/advs.202203527.
[332] A. Khosla, Sonu, H.T.A. Awan, K. Singh, Gaurav, R. Walvekar, Z. Zhao, A. Kaushik, M. Khalid, V. Chaudhary, Emergence of MXene and MXene–polymer hybrid membranes as future- environmental remediation strategies, Adv. Sci. 9 (2022) 2203527, https://doi.org/10.1002/advs.202203527.
[333] H. Kamyab, T. Khademi, S. Chelliapan, M. SaberiKamarposhti, S. Rezania, M. Yusuf, M. Farajnezhad, M. Abbas, B. Hun Jeon, Y. Ahn, The latest innovative avenues for the utilization of artificial Intelligence and big data analytics in water resource management, Results in Engineering 20 (2023) 101566, https://doi.org/10.1016/j.rineng.2023.101566.
[334] P. Baraneedharan, D. Shankari, A. Arulraj, P.J. Sephra, R.V. Mangalaraja, M. Khalid, Nanoengineering of MXene-based field-effect transistor gas sensors: advancements in next-generation electronic devices, J. Electrochem. Soc. 170 (2023) 107501, https://doi.org/10.1149/1945-7111/acfc2b.
[335] M.M. Tunesi, R.A. Soomro, X. Han, Q. Zhu, Y. Wei, B. Xu, Application of MXenes in environmental remediation technologies, Nano Converg 8 (2021) 5, https://doi.org/10.1186/s40580-021-00255-w.
[336] M. Khatami, S. Iravani, MXenes and MXene-based materials for the removal of water pollutants: challenges and opportunities, Comments Mod. Chem. 41 (2021) 213–248, https://doi.org/10.1080/02603594.2021.1922396.
[337] R. Liu, W. Li, High-Thermal-Stability and High-Thermal-Conductivity Ti3C2T x MXene/Poly(vinyl alcohol) (PVA) Composites, ACS Omega 3 (2018), https://doi.org/10.1021/acsomega.7b02001.
[338] Y. Zou, L. Fang, T. Chen, M. Sun, C. Lu, Z. Xu, Near-infrared light and solar light activated self-healing epoxy coating having enhanced properties using MXene flakes as multifunctional fillers, Polymers 10 (2018) 474, https://doi.org/10.3390/polym10050474.
[339] Y. Cao, Q. Deng, Z. Liu, D. Shen, T. Wang, Q. Huang, S. Du, N. Jiang, C. Te Lin, J. Yu, Enhanced thermal properties of poly(vinylidene fluoride) composites with ultrathin nanosheets of MXene, RSC Adv. 7 (2017), https://doi.org/10.1039/C7RA00184C.
[340] R. Kang, Z. Zhang, L. Guo, J. Cui, Y. Chen, X. Hou, B. Wang, C. Te Lin, N. Jiang, J. Yu, Enhanced thermal conductivity of epoxy composites filled with 2D transition metal carbides (MXenes) with ultralow loading, Sci. Rep. 9 (2019), https://doi.org/10.1038/s41598-019-45664-4.
[341] L. Ding, Y. Wei, L. Li, T. Zhang, H. Wang, J. Xue, L.-X. Ding, S. Wang, J. Caro, Y. Gogotsi, MXene molecular sieving membranes for highly efficient gas separation, Nat. Commun. 9 (2018) 155, https://doi.org/10.1038/s41467-017-02529-6.
[342] J. Shen, G. Liu, Y. Ji, Q. Liu, L. Cheng, K. Guan, M. Zhang, G. Liu, J. Xiong, J. Yang, W. Jin, 2D MXene nanofilms with tunable gas transport channels, Adv. Funct. Mater. 28 (2018), https://doi.org/10.1002/adfm.201801511.
[343] J. Shen, G. Liu, Y. Ji, Q. Liu, L. Cheng, K. Guan, M. Zhang, G. Liu, J. Xiong, J. Yang, W. Jin, 2D MXene nanofilms with tunable gas transport channels, Adv. Funct. Mater. 28 (2018), https://doi.org/10.1002/adfm.201801511.
[344] C.E. Ren, K.B. Hatzell, M. Alhabeb, Z. Ling, K.A. Mahmoud, Y. Gogotsi, Charge- and size-selective ion sieving through Ti $_3$ C $_2$ T $_x$ MXene membranes, J. Phys. Chem. Lett. 6 (2015) 4026–4031, https://doi.org/10.1021/acs.jpclett.5b01895.
[345] S. Mehdi Aghaei, A. Aasi, B. Panchapakesan, Experimental and theoretical advances in MXene-based gas sensors, ACS Omega 6 (2021), https://doi.org/10.1021/acsomega.0c05766.
[346] F. Da Silva Santos, L. Vitor da Silva, P.V.S. Campos, C. de Medeiros Strunkis, C.M. G. Ribeiro, M.O. Salles, Review—recent advances of electrochemical techniques in food, energy, environment, and forensic applications, ECS Sensors Plus 1 (2022), https://doi.org/10.1149/2754-2726/ac5cdf.
[347] A. Kausar, Polymer/MXene nanocomposite–a new age for advanced materials, Polymer-Plastics Technology and Materials 60 (2021), https://doi.org/10.1080/25740881.2021.1906901.
[348] S.Y. Hong, Y. Sun, J. Lee, M. Yifei, M. Wang, J. Do Nam, J. Suhr, 3D printing of free-standing Ti3C2Tx/PEO architecture for electromagnetic interference shielding, Polymer 236 (2021), https://doi.org/10.1016/j.polymer.2021.124312.
[349] X. Zhao, X.J. Zha, L.S. Tang, J.H. Pu, K. Ke, R.Y. Bao, Z. ying Liu, M.B. Yang, W. Yang, Self-assembled core-shell polydopamine@MXene with synergistic solar absorption capability for highly efficient solar-to-vapor generation, Nano Res. 13 (2020), https://doi.org/10.1007/s12274-019-2608-0.
[350] Y. Wu, P. Nie, J. Wang, H. Dou, X. Zhang, Few-layer MXenes delaminated via high-energy mechanical milling for enhanced sodium-ion batteries performance, ACS Appl. Mater. Interfaces 9 (2017), https://doi.org/10.1021/acsami.7b12155.
[351] T. Liu, X. Liu, N. Graham, W. Yu, K. Sun, Two-dimensional MXene incorporated graphene oxide composite membrane with enhanced water purification performance, J. Membr. Sci. 593 (2020), https://doi.org/10.1016/j.memsci.2019.117431.
[352] K.M. Kang, D.W. Kim, C.E. Ren, K.M. Cho, S.J. Kim, J.H. Choi, Y.T. Nam, Y. Gogotsi, H.T. Jung, Selective molecular separation on Ti3C2tx-graphene oxide membranes during pressure-driven filtration: comparison with graphene oxide and MXenes, ACS Appl. Mater. Interfaces 9 (2017), https://doi.org/10.1021/acsami.7b10932.
[353] D. Rana, T. Matsuura, Surface modifications for antifouling membranes, Chem. Rev. 110 (2010), https://doi.org/10.1021/cr800208y.

[354] J. Saththasivam, K. Wang, W. Yiming, Z. Liu, K.A. Mahmoud, A flexible Ti3C2Tx (MXene)/paper membrane for efficient oil/water separation, RSC Adv. 9 (2019), https://doi.org/10.1039/c9ra02129a.
[355] Y.Z. Tan, H. Wang, L. Han, M.B. Tanis-Kanbur, M.V. Pranav, J.W. Chew, Photothermal-enhanced and fouling-resistant membrane for solar-assisted membrane distillation, J. Membr. Sci. 565 (2018), https://doi.org/10.1016/j.memsci.2018.08.032.
[356] L. Zhao, K. Wang, W. Wei, L. Wang, W. Han, High-performance flexible sensing devices based on polyaniline/MXene nanocomposites, InfoMat 1 (2019), https://doi.org/10.1002/inf2.12032.
[357] L. Ding, Y. Wei, Y. Wang, H. Chen, J. Caro, H. Wang, A two-dimensional lamellar membrane: MXene nanosheet Stacks, Angew. Chem. Int. Ed. 56 (2017), https://doi.org/10.1002/anie.201609306.
[358] R. Han, P. Wu, High-performance graphene oxide nanofiltration membrane with continuous nanochannels prepared by the in situ oxidation of MXene, J Mater Chem A Mater 7 (2019), https://doi.org/10.1039/c9ta00137a.
[359] Z. Xu, Y. Sun, Y. Zhuang, W. Jing, H. Ye, Z. Cui, Assembly of 2D MXene nanosheets and TiO2 nanoparticles for fabricating mesoporous TiO2-MXene membranes, J. Membr. Sci. 564 (2018), https://doi.org/10.1016/j.memsci.2018.03.077.
[360] Y. Gao, H. Chen, A. Zhou, Z. Li, F. Liu, Q. Hu, L. Wang, Novel hierarchical TiO2/ C nanocomposite with enhanced photocatalytic performance, Nano 10 (2015), https://doi.org/10.1142/S1793292015500642.
[361] L. Hao, H. Zhang, X. Wu, J. Zhang, J. Wang, Y. Li, Novel thin-film nanocomposite membranes filled with multi-functional Ti3C2Tx nanosheets for task-specific solvent transport, Composer Part A Appl Sci Manuf 100 (2017), https://doi.org/10.1016/j.compositesa.2017.05.003.
[362] L. Xu, Y. Wang, S.A.A. Shah, H. Zameer, Y.A. Solangi, G. Das Walasai, Z.A. Siyal, Economic viability and environmental efficiency analysis of hydrogen production processes for the decarbonization of energy systems, Processes 7 (2019), https://doi.org/10.3390/pr7080494.
[363] I.H. Sajid, M.Z. Iqbal, S. Rizwan, Recent advances in the role of MXene based hybrid architectures as electrocatalysts for water splitting, RSC Adv. 14 (2024), https://doi.org/10.1039/d3ra06725d.
[364] C. Li, J.B. Baek, Recent advances in noble metal (Pt, Ru, and Ir)-Based electrocatalysts for efficient hydrogen evolution reaction, ACS Omega 5 (2020), https://doi.org/10.1021/acsomega.9b03550.
[365] Y. Li, L. Zhou, S. Guo, Noble metal-free electrocatalytic materials for water splitting in alkaline electrolyte, Inside Energy 3 (2021), https://doi.org/10.1016/j.enchem.2021.100053.
[366] H. Wu, C. Feng, L. Zhang, J. Zhang, D.P. Wilkinson, Non-noble metal electrocatalysts for the hydrogen evolution reaction in water electrolysis, Electrochem. Energy Rev. 4 (2021), https://doi.org/10.1007/s41918-020-00086-z.
[367] J. Peng, X. Chen, W.J. Ong, X. Zhao, N. Li, Surface and heterointerface engineering of 2D MXenes and their nanocomposites: insights into electro- and photocatalysis, Chem 5 (2019), https://doi.org/10.1016/j.chempr.2018.08.037.
[368] T. Su, Z.D. Hood, M. Naguib, L. Bai, S. Luo, C.M. Rouleau, I.N. Ivanov, H. Ji, Z. Qin, Z. Wu, 2D/2D heterojunction of Ti 3 C 2/g-C 3 N 4 nanosheets for enhanced photocatalytic hydrogen evolution, Nanoscale 11 (2019), https://doi.org/10.1039/c9nr00168a.
[369] M. Naguib, M. Kurtoglu, V. Presser, J. Lu, J. Niu, M. Heon, L. Hultman, Y. Gogotsi, M.W. Barsoum, Two-dimensional nanocrystals produced by exfoliation of Ti 3AlC 2, Adv. Mater. 23 (2011), https://doi.org/10.1002/adma.201102306.
[370] N.A. Mohamed, J. Safaei, A.F. Ismail, M.F. Mohamad Noh, N.A. Arzaee, N. N. Mansor, M.A. Ibrahim, N.A. Ludin, J.S. Sagu, M.A. Mat Teridi, Fabrication of exfoliated graphitic carbon nitride, (g-C3N4) thin film by methanolic dispersion, J. Alloys Compd. 818 (2020), https://doi.org/10.1016/j.jallcom.2019.152916.
[371] J. Sui, X. Chen, Y. Li, W. Peng, F. Zhang, X. Fan, MXene derivatives: synthesis and applications in energy convention and storage, RSC Adv. 11 (2021), https://doi.org/10.1039/d0ra10018h.
[372] Y. Li, Z. Jin, L. Zhang, K. Fan, Controllable design of Zn-Ni-P on g-C3N4 for efficient photocatalytic hydrogen production, Cuihua Xuebao/Chinese Journal of Catalysis 40 (2019), https://doi.org/10.1016/S1872-2067(18)63173-0.
[373] P. Kuang, J. Low, B. Cheng, J. Yu, J. Fan, MXene-based photocatalysts, J. Mater. Sci. Technol. 56 (2020), https://doi.org/10.1016/j.jmst.2020.02.037.
[374] Z. Guo, J. Zhou, L. Zhu, Z. Sun, MXene: a promising photocatalyst for water splitting, J Mater Chem A Mater 4 (2016), https://doi.org/10.1039/c6ta04414j.
[375] K. Takanabe, Photocatalytic water splitting: quantitative approaches toward photocatalyst by design, ACS Catal. 7 (2017), https://doi.org/10.1021/acscatal.7b02662.
[376] A. Kudo, Y. Miseki, Heterogeneous photocatalyst materials for water splitting, Chem. Soc. Rev. 38 (2009), https://doi.org/10.1039/b800489g.
[377] Á. Morales-García, M. Mayans-Llorach, F. Viñes, F. Illas, Thickness biased capture of CO2 on carbide MXenes, Phys. Chem. Chem. Phys. 21 (2019), https://doi.org/10.1039/c9cp04833b.
[378] J. Chen, Q. Huang, H. Huang, L. Mao, M. Liu, X. Zhang, Y. Wei, Recent progress and advances in the environmental applications of MXene related materials, Nanoscale 12 (2020), https://doi.org/10.1039/c9nr08542d.
[379] S. Bai, M. Yang, J. Jiang, X. He, J. Zou, Z. Xiong, G. Liao, S. Liu, Recent advances of MXenes as electrocatalysts for hydrogen evolution reaction, NPJ 2D Mater Appl 5 (2021), https://doi.org/10.1038/s41699-021-00259-4.
[380] R. Bhardwaj, A. Hazra, MXene-based gas sensors, J Mater Chem C Mater 9 (2021) 15735–15754, https://doi.org/10.1039/D1TC04085E.
[381] I. Navitski, A. Ramanaviciute, S. Ramanavicius, M. Pogorielov, A. Ramanavicius, MXene-based chemo-sensors and other sensing devices, Nanomaterials 14 (2024), https://doi.org/10.3390/nano14050447.
[382] R. Liu, M. Miao, Y. Li, J. Zhang, S. Cao, X. Feng, Ultrathin biomimetic polymeric Ti 3 C 2 T x MXene composite films for electromagnetic interference shielding, ACS Appl. Mater. Interfaces 10 (2018), https://doi.org/10.1021/acsami.8b18347.
[383] C. Jin, Z. Bai, MXene-based textile sensors for wearable applications, ACS Sens. 7 (2022), https://doi.org/10.1021/acssensors.2c00097.
[384] K. Nabeela, N.B. Sumina, MXenes and their composites as piezoresistive sensors, in: MXenes and Their Composites: Synthesis, Properties and Potential Applications, 2021, https://doi.org/10.1016/B978-0-12-823361-0.00011-3.
[385] N. Noriega, M. Shekhirev, C.E. Shuck, J. Salvage, A. VahidMohammadi, M. K. Dymond, J. Lacey, S. Sandeman, Y. Gogotsi, B.A. Patel, Pristine Ti $_3$ C $_2$ T $_x$ MXene enables flexible and transparent electrochemical sensors, ACS Appl. Mater. Interfaces (2024), https://doi.org/10.1021/acsami.3c14842.
[386] S. Hideshima, Y. Ogata, D. Takimoto, Y. Gogotsi, W. Sugimoto, Vertically aligned MXene bioelectrode prepared by freeze-drying assisted electrophoretic deposition for sensitive electrochemical protein detection, Biosens. Bioelectron. 250 (2024) 116036, https://doi.org/10.1016/j.bios.2024.116036.

2024-04-26

Exploring transformative and multifunctional potential of MXenes in 2D materials for next-generation technology

Mishra, Raghvendra Kumar

Elsevier

Mishra RK, Sarkar J, Verma K, et al., (2024) Exploring transformative and multifunctional potential of MXenes in 2D materials for next-generation technology. Open Ceramics, Volume 18, June 2024, Article number 100596

https://doi.org/10.1016/j.oceram.2024.100596